UNIVERSITÀ
POLITECNICA
DELLE MARCHE

DEPARTMENT OF ENGINEERING

Master's Degree in Biomedical Engineering

Dynamic analysis of different levels of constraint in Total Knee Arthroplasty during Gait and Squat: a Finite Element study

Relator:

Prof. Marco Mandolini

Candidate:

Rachele Saldari

Supervisor:

Prof. Bernardo Innocenti

Academic Year 2021-2022

A zia Manuela:
le tue parole vivono nel mio cuore.

I. Contents

II. List of figures

III. List of tables

Abstract

Total Knee Arthroplasty (TKA) is a successful orthopaedic surgical procedure performed to restore physiological functionality in pathological knee, but implant failures and patient dissatisfaction during activities still persist. Several TKA implants with different levels of constraint are currently available on the orthopaedic market, and just some of them have been compared to evaluate how each design can affect the knee biomechanics during dynamic activities. Thus, a more comprehensive biomechanical study among them could be helpful for the surgeon to better understand TKA performance thus facilitating the decision-making process and also to meet the necessity of a more scientific rationale for post-TKA activities. Basing on a previously validated knee model, the purpose of this study is to compare the knee biomechanics effect due to five common prosthetic implants (Mobile Bearing (MB) Cruciate Retain (CR) and Ultra-Congruent (UC), Fixed Bearing (FB) CR, Posterior Stabilized (PS) and Condylar Constrained Knee (CCK)) characterized by different levels of constraint, simulating gait and squat. By means of Finite Element Analysis (FEA), these designs have been incorporated in the virtual model of the lower leg, with patellar component and patellar tendon included, and consequently analysed in terms of polyethylene stress and tibial bone stress, tibiofemoral and patellofemoral kinematics, and kinetics.

The outcomes have been compared among the models, showing that UC design shows the best kinematics and kinetics performance with respect to the other implants, and that TF contact stress changes with the difference in design constraint. Congruency and mobility are design factors that can rise the insert stress, while the addition of constraint in CCK reduces the stress with respect to PS, which moreover generated the highest stress values. Thus, the higher the constraint level, the lower the stress on the insert. It has been observed that through the squat simulation it is possible to offer a better overview of the TKA performance with respect to gait.

Future developments could integrate this analysis considering other designs, modelling patient-specific variations and simulating other activities.

Sommario

L'intervento di protesi totale al ginocchio (TKA) è una procedura ortopedica di successo eseguita per ripristinare le funzioni fisiologiche nel ginocchio patologico, ma ancora oggi perdurano sia il fallimento dell'impianto protesico che l'insoddisfazione dei pazienti nel compimento di attività motorie. Nel mercato ortopedico sono attualmente disponibili numerosi impianti di TKA caratterizzati da livelli differenti di vincolo e solamente alcune tipologie sono state messe a confronto per valutare come influenzino la biomeccanica del ginocchio durante le attività dinamiche. Pertanto, uno studio biomeccanico approfondito sugli effetti dei vari design potrebbe risultare utile sia per il chirurgo al fine di comprendere meglio le prestazioni delle TKA facilitando così il processo decisionale, sia per la necessità di un opportuno fondamento scientifico riguardo le possibili attività praticabili dopo l'intervento. Sulla base di un modello di ginocchio precedentemente validato, lo scopo di questo progetto di tesi è quello di comparare l'effetto sulla biomeccanica del ginocchio dovuto a cinque impianti protesici comuni (a piatto mobile (MB) con conservazione del crociato posteriore (CR) standard e Ultra-Congruente (UC), a piatto fisso (FB) CR, postero-stabilizzato (PS) e semi-vincolato (CCK)) caratterizzati da livelli diversi di vincolo, simulando le attività di cammino e squat. Mediante l'Analisi a Elementi Finiti (FEA), questi design sono stati incorporati nei modelli virtuali della parte inferiore della gamba, includendo la protesi rotulea e il tendine rotuleo, e conseguentemente analizzati in termini di stress sull'inserto in polietilene e sulla tibia, di cinematica e cinetica tibio-femorale e femoro-rotulea. I risultati sono stati confrontati tra i modelli, rivelando che il design UC presenta il miglior comportamento sia rispetto alla cinematica che alla cinetica rispetto alle altre protesi, e che lo stress tibio-femorale varia in base alla differenza di vincolo del design protesico. Congruenza e mobilità sono fattori di design che possono innalzare i valori di stress nell'inserto, mentre nella CCK l'aggiunta del vincolo riduce lo stress rispetto alla PS, la quale genera inoltre i valori maggiori di stress. Dunque, maggiore è il livello di vincolo, minore lo stress sull'inserto.

Da questo studio è emerso infine che tramite la simulazione dello squat è possibile avere un quadro più completo degli effetti delle protesi rispetto al cammino. Sviluppi futuri potrebbero integrare questa analisi considerando altri design, modellando le strutture in base alle variazioni specifiche del paziente, e simulando altre attività motorie.

1 Introduction

Total knee arthroplasty (TKA) is the gold standard treatment for patients with primary osteoporosis, as it can relief pain and restore normal knee joint functionality and kinematics [1]. TKA is recognized as a highly successful and reproducible treatment, with more than 600,000 surgeries performed each year in the USA [2] and that number is expected to increase exponentially over the next decades [3]. The most common age group for total knee replacements remains from 65 to 84 years [4] and the increasing size of the aging population will only further test the longevity and durability of TKA [5]. TKA procedure involves the reconstruction of damaged joints accomplished through the resection of abnormal articular surfaces of the knee and their substitution using metal and polyethylene components [6]. Over time, the collaboration between surgeons and engineers has been crucial to allow improvement and continuous development in the design of the prosthesis. Interestingly, the progress in technologies and the use of new materials let researchers try again old-fashioned techniques from the past in order to be improved. Every different concept of the design tries to answer to special needs as the reach of the highest range of motion (ROM), the reduction of pain and debris, articular geometry, the type of fixation, the modularity of augments and stems, the types of constraints, knee kinematic and of course costs [7]. The main goal to achieve during the design and realization of a prosthesis is to guarantee the highest survival rate to avoid as much as possible revision surgeries [8]. The knee prosthetic implant has a survival rate of 85% with 10 to 25 years of follow-up [1], [9]. Although the success of TKA is well documented, implant failures and patient dissatisfaction during activities still persist [10] in a limited number of patients [11] (indeed a patient satisfaction about 80–90% after 1-5 years has been reported [1]), due to difficulties or joint pain during motion [3], [11], other than the loss of proprioception [12]. Instability and limited ROM are listed as key limiting factors to normal function even in patients with a well-functioning TKA, and both relate intimately to the kinematics of the knee joint [13].

Patient outcomes in TKA surgery can be affected by implant design, alignment, or patient-related anatomical factors [3]. Concerning the first one, in order to best meet each individual's demand, several solutions for TKA implant design with different levels of constraint are currently available on the orthopaedic market [2]. Their differences mostly rely on the tibial insert design, which choice is strictly related to the decision of the orthopaedist to resect or retain the posterior cruciate ligament (PCL) [14] based on the patient condition; so, it is identified a first distinction between Cruciate retaining (CR) and Posterior stabilized (PS) design. Good clinical outcomes and a knee kinematics close to the native knee derive post-CR implantation [6], but it depends on one of the primary stabilizers of the joint: the PCL [15]. If PCL flexion contracture or laxity occur, CR adoption is not the suggested one because of the challenging ligament balancing, thus PS design have been introduced to reduce this problem, replacing the soft tissue function with the post-cam mechanism [16]. But even PS presents a disadvantage related to the risk of polyethylene wear [15], thereby other kind of inserts have been designed and produced. Starting from the PS it has been realized the Condylar Constrained Knee (CCK), which presents a wider post and a deeper femoral cam aiming to provide more stability in patients with insufficiency in the collateral ligaments [5]. Another considered design factor which has an impact on the level of constraint includes the rotation of the tibial insert with respect to the tibial tray, resulting in the implementation of both Fixed Bearing (FB) and Mobile Bearing (MB) options [14] and in particular the last one has been thought to allow a more physiological motion of the implant [16]. For what concerns MB version, it can be found in the standard and in the Ultra-Congruent (UC) version, characterized by a high anterior wall and a deep-dished plate which increases the implant conformity and theoretically reduces the contact stress peaks on the bone-implant interface [15]. Of growing interest in the orthopaedic research field is to compare the available designs in terms of knee joint kinematics and contact mechanics during daily activities [17]. Indeed, several studies have compared TKA designs basing on in vivo, in vitro and in silico methods, performed during daily activities or simulating them [18]. In literature some researchers have taken into consideration just the PS and CR design to

evaluate the PCL resection or conservation effect [19] or PS and CCK to assess the changes deriving from an increment of constraint [5]; others have focused on the difference in the insert bearing, thus on the FB and MB design [20]; other studies have compared FB CR and MB CR UC to assess the possible benefits of a higher insert conformity and mobility [21]; finally some numerical studies have compared more than two different designs and, up to now, the maximum amount is four different designs, including the most constrained hinged prostheses [10]. In the current scenario where the orthopaedic surgeon must choose among numerous typologies of insert and also select the other components to assemble the overall implant, no absolute guidelines are available to select the best matching solution for each patient. A potential reason for this, nonetheless the increasement of the research interest and the development of TKA, lies in the limited amount of clinical and biomechanical evidence-based justifications on the effects of the different design features characterizing the various available products [2]. Thus, a more complete biomechanical study among them could be helpful for the surgeon to better understand the TKA performance thus facilitating the decision-making process and also to meet the necessity of a more scientific rationale for post-TKA activities. In this background, the present study tries to fill some gaps in the literature. Starting from a previously validated knee model and published paper which has biomechanically compared four implant designs in different static configurations [6], in this study the addition of a further insert design and the simulation of two dynamic activities which are the gait cycle and the squat have been performed, also including patellar resurfacing and the patellar tendon. Regarding this, an accurate knowledge of knee joint motion during activities such as walking and squat, would provide indeed a more deepen and needed insight into the biomechanical mechanisms underlying patient outcomes subsequent to TKA surgery [11]. Therefore, the purpose of this study is to compare the effect of five common prosthetic implants (MB CR and UC, FB CR, PS and CCK,) on the knee biomechanics during gait and squat simulations. The same manufacturer and boundary conditions have been considered, in order to obtain outcomes that are influenced only by the design features. The simulations have been

carried out by means of Finite Element Analysis (FEA), which is a numerical technique widely spread in orthopaedic biomechanics research, that allows modelling of complex geometry such as the knee joint [22] and that is very useful for the process of implant design and preoperative testing [23]. The outcomes of the present work have been discussed in terms of polyethylene stress and tibial bone stress, tibiofemoral (TF) and patellofemoral (PF) kinematics and kinetics.

1.1 The native knee joint

Since the early years of orthopaedics, it is a cornerstone that anatomy follows function. Anatomy of the knee joint is variable among the patients and the only constant is its complex function, which is the result of the three joints by which the knee is composed: medial tibio-femoral (TF), lateral TF and patello-femoral (PF) joint. All of these articulations are enclosed within a single articular capsule that contains synovial fluid [24]. Besides, the included bones are femur, tibia, patella, and fibula while the soft tissue contains several ligaments, tendons, muscles, and joint capsule (Figure 1.1) [25]. Given the complex anatomical architecture involved in the interplay for knee functioning and the variety of the possible movement patterns, it is crucial to describe in detail both its anatomy and biomechanics.

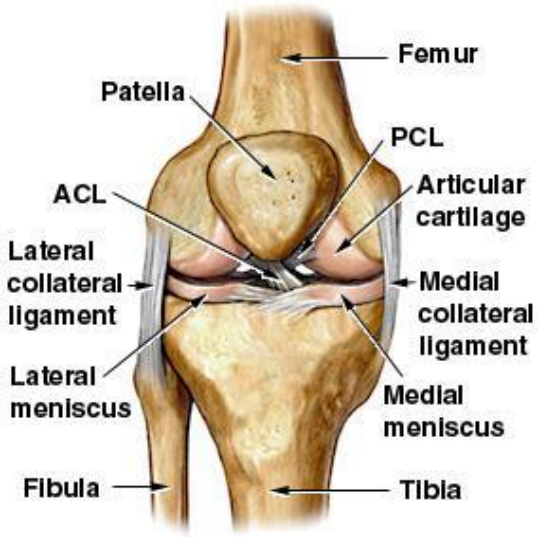

Figure 1.1. Anatomy of the native knee.

1.1.1 Anatomy

The knee joint is the largest joint and one of the most complex one within the human body. It is located between the two longest lever arms of the skeleton which are the hip and the ankle, factor that, generating high moments, contributes to the knee vulnerability to injury.

The knee joint could be considered as composed by three joints, related to three separated articular surfaces [9]:

1. The medial TF joint corresponding to the articulation between the medial femoral condyle and medial tibial surface.
2. The lateral TF joint corresponding to the articulation between the lateral femoral condyle and lateral tibial surface; these two articulations support most of the body weight.
3. The PF joint corresponding to the articulation between the femoral trochlear groove and the patella, articulation which creates a frictionless transfer of the forces generated after the contraction of the quadriceps muscle [24].

The knee is composed of four bones: femur (thigh bone), tibia (shin bone), patella (kneecap) and fibula (calf bone). The femur is the longest and strongest bone in the human body and extends from the hip to the knee. The distal femoral epiphysis is constituted by a double condyle, lateral and medial, which makes up the TF joint together with the proximal aspect of the tibia [26]. These condyles are separated posteriorly by the intercondylar notch, which contains the attachment areas of the anterior and posterior cruciate ligaments, while they are connected anteriorly by the femoral trochlear groove, which is a smooth shallow articular depression guiding the patella in the PF articulation [27]. The condyles differ from their shape and location, with the medial one being elliptically shaped, more distally located and with a large posterior offset, whereas the lateral one being ball-shaped, distally less round and with a smaller posterior offset (Figure 1.2).

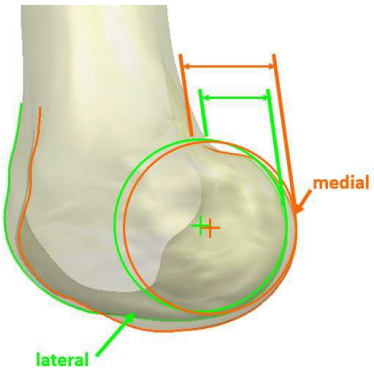

Figure 1.2. Medial and lateral femoral condyles.

Moreover, each condyle presents a convex eminence, named medial and lateral epicondyles, where the ligaments and tendons insert [26]. There are two long bones located in the lower leg: the tibia and the fibula. The tibia, also called shin bone, is the second largest and strongest bone of the human body. The tibia is found on the medial side of the leg and extends from the knee joint to the ankle. The proximal extremity of the tibia is a bearing surface composed of two plateaus, the medial and lateral tibial condyles, that are separated by an intercondylar eminence, including the medial and lateral tibial spines. The superior part of each tibial condyle consists of an oval articular surface covered by hyaline cartilage which houses the corresponding femoral condyle [26]. In the coronal plane, both tibial plateaus are concave whereas in the sagittal plane, only the medial one is concave, the lateral one being convex (Figure 1.3). This asymmetry increases the mobility of the knee joint in the lateral side. Moreover, the medial plateau presents a larger and thicker articular surface compared to the lateral one.

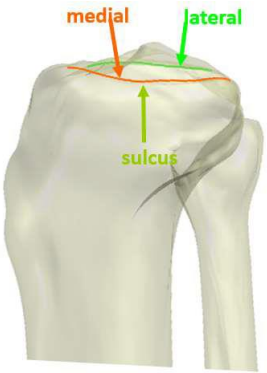

Figure 1.3. Medial and lateral tibial plateaus.

Connected to the lateral tibia in the proximal and distal extremity, there is the fibula. It is smaller and much thinner and represents an important attachment site for muscles. The two bones work together to stabilize the ankle and provide support to the muscles of the lower leg [27]. The patella is a hard triangular-shaped bone located in the intercondylar notch and embedded in the tendon of the quadriceps femoris muscle above, and the patella tendon below. The posterior surface of the patella can include up to seven facets covered by cartilage, with three on the medial and lateral surfaces articulating respectively with the medial and lateral femoral condyles [26]. From full-knee extension to approximately 20° of flexion, the patella stands superior to the trochlear groove. With 25° of flexion, the patella becomes engaged in the trochlear groove, and the patella should be fully engaged in the trochlea at about 40° flexion [27]. The patella plays a fundamental biomechanical role in transmitting tensile forces generated by the quadriceps to the patellar tendon (PT) and tibia, and by increasing the lever arm length of the extensor-mechanism throughout knee flexion [28]. It also protects the distal aspect of the femur from trauma, and the quadriceps from frictional wear, besides it also decreases the amount of sagittal TF shear stress placed on the knee joint. This kneecap presents a layer of cartilage in the articular surface, so that the resulting pulley can function with minimal friction (Figure 1.4). A layer of cartilage is also present on all the articular surfaces of the femur and tibia guaranteeing smooth and almost frictionless sliding and providing shock absorption [26].

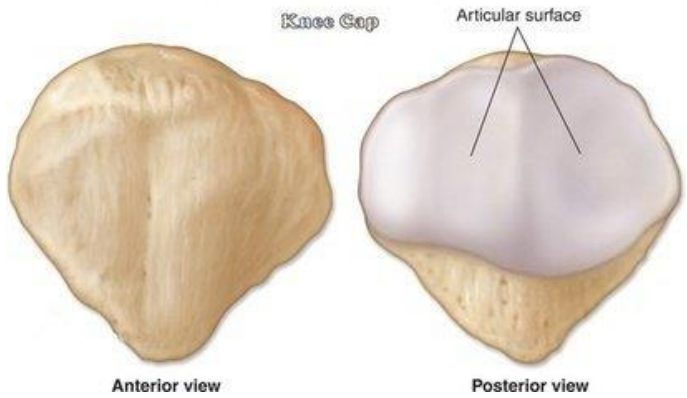

Figure 1.4. Patellar bone and cartilage on the articular surface.

Two semilunar cartilages called menisci are located between each femoral condyle and the underlying tibial plateau to enable the restoration of congruence between the bones extremities and to provide damping effects [29]. As well as the cartilage, in the soft tissue category an important part is represented by ligaments and tendons that together with the muscles keep support the knee and control its stability [26], [24]. The ligaments involved in the TF joint are the anterior cruciate ligament (ACL), posterior cruciate ligament (PCL), medial collateral ligament (MCL) and lateral collateral ligament (LCL) (Figure 1.5), while the ones involved in the PF joint are the PT, the medial PF ligament (MPFL) and the lateral retinaculum [24]. For what concerns the collateral ligaments, they both provide medio-lateral stability prohibiting the knee from moving side to side; LCL main function is to resist to varus forces, whereas MCL one to valgus forces. The LCL originates from the lateral epicondyle of the femur and attaches on the fibula head; it is shorter than the MCL making it less prone to injuries. The MCL originates from the medial epicondyle of the femur and inserts into the medial aspect of the proximal tibia. When the cruciate ligaments are torn, the LCL and MCL act as secondary restraints to the anterior and posterior tibial translation [26], [24]. Regarding the cruciate ligaments, they are located in the intercondylar region inside the knee joint and are classified according to their site of attachment to the tibia in ACL and PCL. In detail, the ACL is attached to the posterior aspect of the medial surface of the lateral femoral condyle and then, running inferiorly and crossing with PCL, it attaches anteriorly to the tibia. The PCL instead attaches to the anterior part of the lateral surface of the medial condyle of the femur and inserts distally on the posterior surface of the tibia. They contribute to the stability and prevents the anterior-posterior displacement of the knee joint: the ACL limits excessive frontal displacement of the tibia relative to the femur and the PCL the same but in the opposite direction. This is fundamental since excessive displacements would necessitate the generation of greater muscular force to retain balance [27]. Moreover, both cruciate ligaments guide kinematics during passive motion, limit and their sensory endings imply the important proprioceptive function [26], [27].

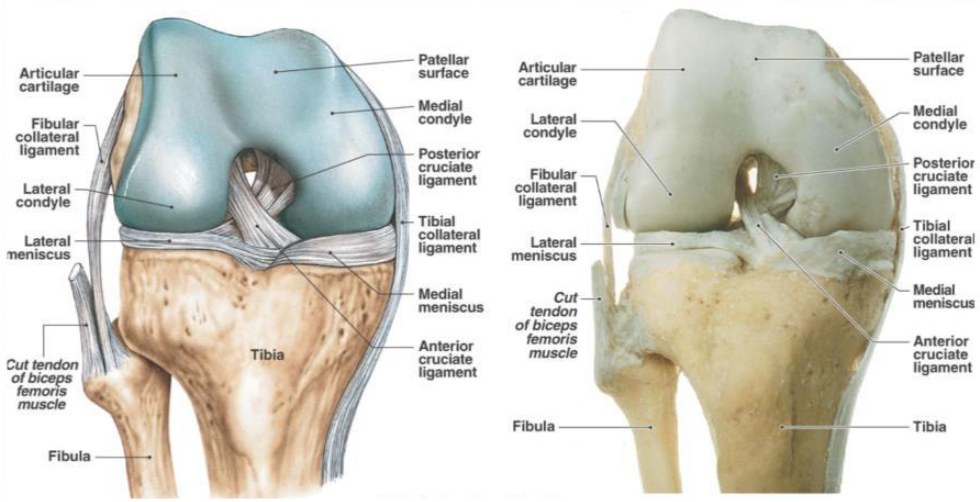

Figure 1.5. Anterior view of a flexed knee.

Taking into consideration the patella, the MPFL is one of its most important static stabilizers especially in the knee in extension and several studies have shown that it is the primary restraint to lateral patellar translation between 0 and 30° of knee flexion [27]. PT represents the connection between two bones which are the patellar one and the tibial tubercle but, since it is the extension of the quadriceps muscle, it is referred to as tendon (Figure 1.6). It enables the transmission of high tensile loads from the quadriceps muscle to the tibial bone and keeps the patella close to a constant distance from the tibia [27], [30].

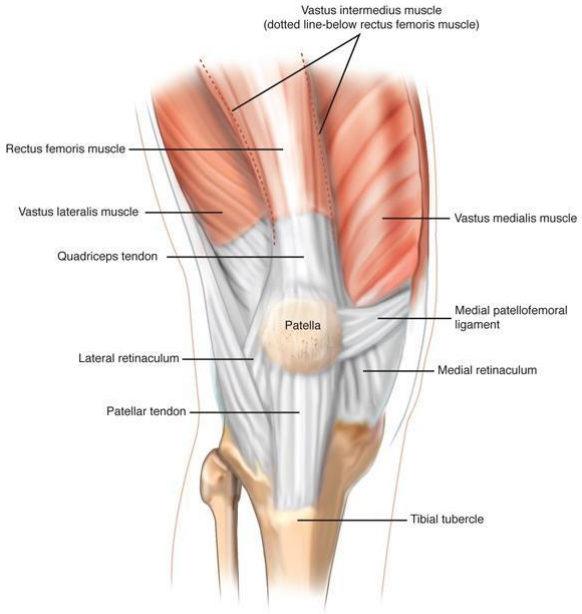

Figure 1.6. Knee anatomy from the frontal aspect, focus on PT and MPFL.

The two groups of muscles acting on the knee joint are the knee extensors (quadriceps femoris) and flexors (hamstrings). The quadriceps femoris, reported in Figure 1.7, is the strongest muscle in the human body and extends along the anterior compartment of the femur. It is composed of four sections: vastus medialis, vastus lateralis, vastus intermedius, and rectus femoris. They join each other above the patella forming the quadriceps femoris tendon, ending with the beginning of PT [27]. The contraction of this group of muscles allows the extension of the leg at the knee joint and have therefore a crucial role in activities such as walking, squatting, running, and jumping.

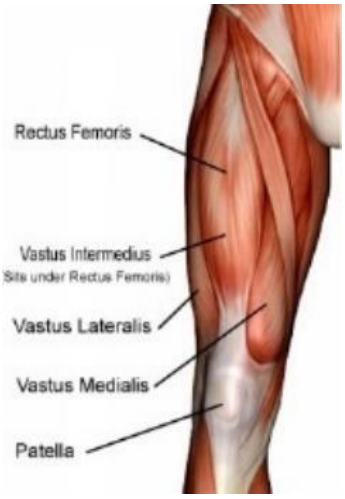

Figure 1.7. Quadriceps femoris muscles.

The hamstrings constitute a group of three muscles that are antagonists to the quadriceps, extending along the posterior surface of the femur. They are distinguished in medial hamstrings, that are the semitendinosus and semimembranosus, and in lateral hamstring, that is the biceps femoris. They are mostly bi-articulate since they flex the knee and extend the hip [27].

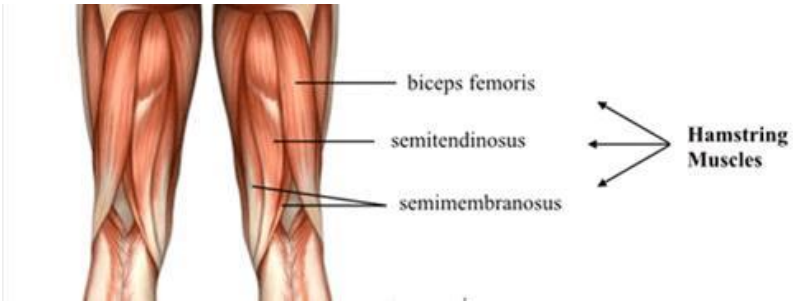

Figure 1.8. Hamstrings muscles.

1.1.2 Biomechanics

In biomechanics, kinematics describes the motion of multi-link systems, such as the human skeleton, without reference to the causes of motion, while kinetics is the study of the relationship between the motion of bodies and its causes. Understanding joint kinematics is very important in order to make better diagnoses of some pathologies, providing a quantitative evaluation of the treatment and improve the development of prosthetic devices [26]. Highly complex biomechanics underpins the knee joint behaviour and its ability to withstand intense mechanical loading [27]. The knee is very important for orthostatic posture because it ensures stability during walking, being like a biomechanical junction during the movement of the leg. This joint offers a wide range of motion and high resistance to external stress, thanks to passive stabilizers (ligaments, only loaded in tension) and active stabilizers (muscle and tendons, only acting under tension). Loads are transmitted by a combination of tensile force in the ligaments and muscles and of compressive force between the articular surfaces of the bones [26]. Correct joint kinematics is fundamental to protect articular functionality, since an alteration may change the transmission of physiological loads and in turn overload can be a consequence that may lead to degenerative arthrosis. In the TF joint the distal extremity of the femur and the proximal extremity of the tibial slide on each other to set up a six-degrees-of-freedom movement system: three rotations and three translations along a set of perpendicular axes, as shown in Figure 1.9.

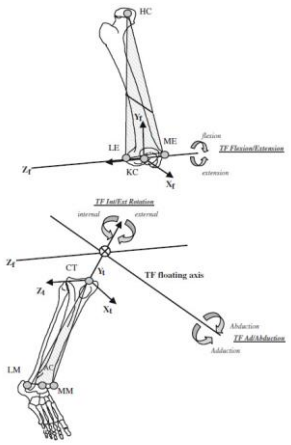

Figure 1.9. The Grood-Suntay coordinate system used to describe the 3D kinematics [31].

The axis where internal-external (IE) rotation and superior-inferior translation occur is the tibial mechanical axis; the axis where flexion-extension (FE) and medio-lateral (ML) translation are defined is the femoral trans-epicondylar axis and the one where varus-valgus rotation and antero-posterior (AP) translation refer to is the floating axis obtained by means of cross-product between the previous two axes. The axes have been defined by reliable and surgically relevant bony markers [32]. The mechanical axis of the overall leg (or load-bearing axis) corresponds to the line extending from the center of the femoral head to the center of the ankle joint and it is crucial for the propagation of the forces. The anatomical axis of the femur and of the tibia are determined as their mid-diaphyseal lines. About the femur, there is an angle of 6° between the mechanical and anatomical axis, while the mechanical and anatomical axis of the tibia coincide. In a healthy knee the mechanical axes of femur and tibia are aligned [33]. The abovementioned three translations are significantly restricted by the fibrous capsule, ligaments, and muscles. Concerning the rotations, the FE, which is the rotation around the sagittal plane, represents the primary motion of the TF joint and it has the greatest range, while the varus-valgus and the IE rotation around the frontal and transverse plane are more restricted. The range of motion from full extension to full flexion is from -15° to 140°, but it's important to ponder that this range changes in relation to the activity. For instance, during walking the FE angle ranges from -3°/0 ° to 57/65 °, during descending stairs from -5° to about 90 °, during ascending stairs from -5° to 80° and during cycling the flexion can reach until 110°.

However, in general, the knee can flex up to 130° in the case of an active flexion and up to 160° in a passive flexion [34]. During this motion (that happens for instance during gait and squat), the so called "screw-home" mechanism occurs: in the course of the last 30° of extension the tibia externally rotates up to 20°, while during the first 30° of flexion the tibia internally rotates up to 20° with a medial pivoting allowed by the geometry of the articulation (the medial tibial plateau is slightly concave) [27], [34], [35], [36]. This mechanism is not only necessary to achieve the full extension of the knee but also responsible for the locking of the knee attributed to ligaments, which guarantee maximal stability [26], [27].

Furthermore, the tibial plateau slopes posteriorly approximatively 7°/10°, which helps bend or flex the femoral condyles on the tibia. Besides this, another peculiarity of knee flexion is the combined movement of rolling backward and sliding forward of the femoral condyles over the tibial plate, commonly called femoral roll-back, enabling a wide rotation on the sagittal plane (Figure 1.10) [26][36]. This happens since in the sagittal plane the femoral condyles outlines are longer than the dimension of the tibial plateau, thus with this movements' combination, the femoral posterior dislocation off the shorter tibial plateau is overcome and a flexion up to 130° can be achieved. In this situation the ACL is in tension and prevents further posterior displacement of the femur relative to the tibia. More in detail, from the maximum extension, the condyles begin to roll between 0° and 10°/15° of flexion and then slide until 130°. Due to the high asymmetry of the condyles, sliding starts from the medial condyle and then to the external one during rolling [34].

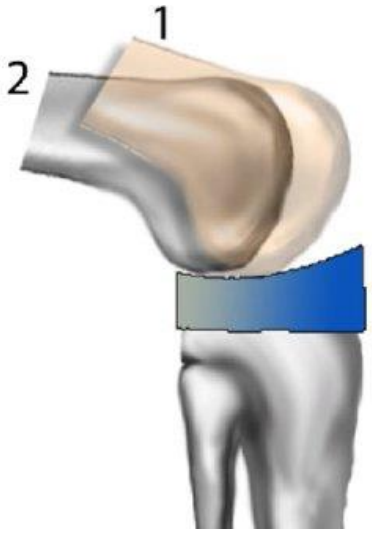

Figure 1.10. Flexed knee femoral rollback.

Lastly, flexion is also associated with motion in the frontal plane, the ab-adductions due to the different curvature of the condyles. These passive movements proportionally increase with knee flexion up to 30°, involving only a few degrees, because then are limited by the soft tissue surroundings [26].

The patella articulates with the lateral femoral ridge as it approaches full extension, then it glides into the femoral trochlear groove at full flexion [27] with an overall caudal patellar movement of about 7 cm, giving rise to a "sliding" articulation. Contact areas of the patella and trochlea are not uniform and vary according to the range of motion. At full TF joint extension, the PF joint contact occurs at the distal end of the patella and, as flexion increases, the contact area spreads across the width of the patella and moves proximally. The PF engagement occurs at around 30°of flexion and the maximum contact between femur and patella is at 45°of flexion. The increase of PF contact area with knee flexion is a functional mechanism that controls and dissipate the stress magnitude by propagating the ever-increasing load on PF joint (due to the backwards shift of the body's center of gravity during flexion) over a larger area, thus maintaining physiological contact stress values [34]. Moreover, patellar position during flexion allows a change in the AP direction of the PT force, as it can be seen in Figure 1.11.

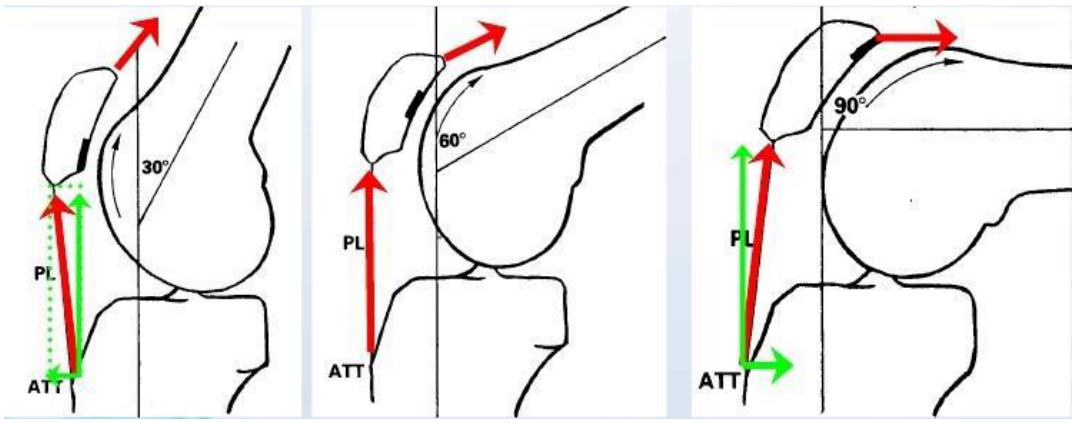

Figure 1.11. Patellar movement during 30°, 60° and 90° of flexion. "ATT": tibial attachment of patellar ligament. PL: patellar ligament.

There is an anatomical factor that affects the PF kinematics: in the frontal plane the extended PF joint shows a resultant lateral force acting on the patella stemming from the lines of action of the PT and the quadriceps; this is often referred to as the Q-angle effect (Figure 1.12). It is approximately equal to 13° (with a Standard Deviation of 4.5°) in males and 18° in females (due to the wider pelvis) in the extended knee, while in the flexed knee is about 8°.

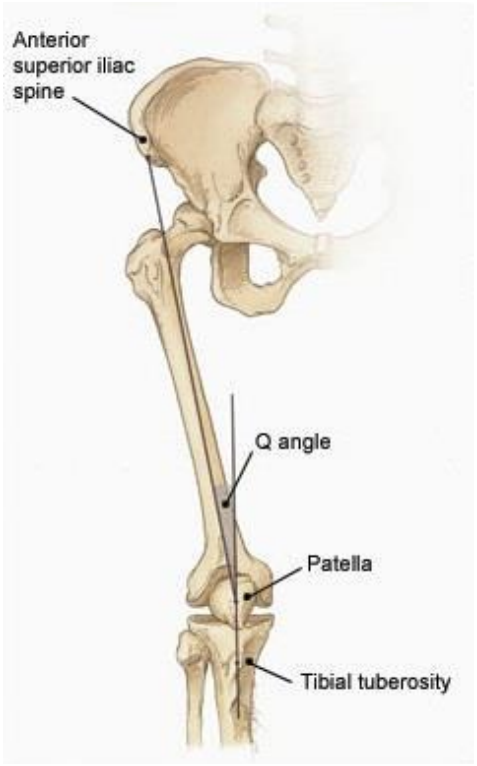

Figure 1.12. Q-angle effect representation.

This effect tends to subluxate the patella laterally by increasing lateral force, translation and rotation, but there is a passive restraining force to provide stability which is exerted for the 60% by MPFL, for 13% by medial patello-meniscal ligament and for 10% by lateral retinaculum (Figure 1.13) [34].

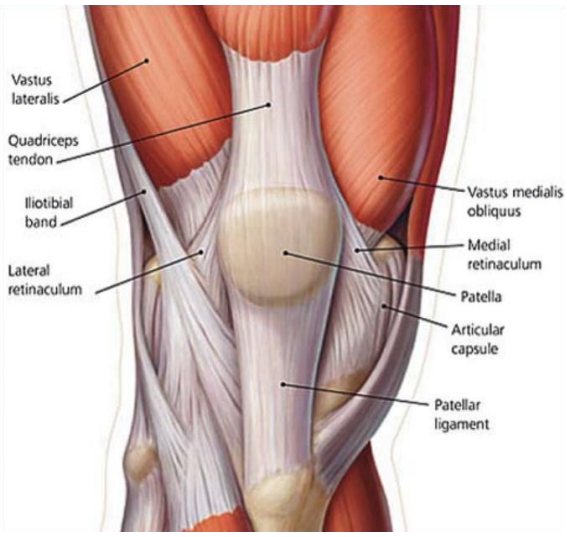

Figure 1.13. Soft tissue around PF joint [37].

Another aspect that is worth mentioning is the position of the patella with respect to the tibial plateau. The patellar height can be evaluated by means of the Blackburne-Peel index (Figure 1.14) [38]: if this index falls in a certain normal range it enables the better compromise in terms of contact area and force, while if it is higher ("patella alta" condition) or lower ("patella baha" condition), high contact pressure and force are generated, with the risk of anterior knee pain [39].

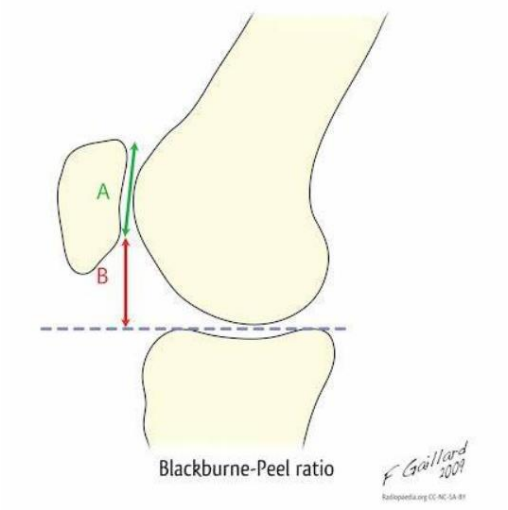

Figure 1.14. Blackburne-Peel ratio [39].

1.1.3 Pathologies

The main pathologies that affect the knee, resulting in degenerative and harmful conditions for its structures are:

- Osteoarthritis (OA): it is a painful chronic joint disease and a common cause of disability in people over 65 years [26], [27], [40], related to a complex interplay of genetic, metabolic, biochemical, and biomechanical factors. It affects the whole joint, in particular it degrades the articular cartilage (as it is displayed in Figure 1.15) whose presence in a healthy knee prevents pain (since it is not innervated). As a result, bone comes directly into contact with bone that, being rather vascularized, provokes painful condition [26]. It is also related to the formation of osteophytes, ligamentous laxity, weakening of periarticular muscles, thickening of the joint capsule, subchondral bone changes and meniscal damage [40], [41]. The wearing out of the cartilage has the

consequence of narrowing of the joint space, with the development of bony spurs and erosions in the bone ends and inducing changes in the tensile behaviour of the ligaments and tendons [26], [27]. All these elements cause an unequal distribution of loading; the disproportionate loading increment in one knee compartment with respect to the other is supposed to be one factor responsible for accelerated joint degeneration [27].

- Rheumatoid arthritis (RA): it is an auto-immune inflammatory arthritis that can occur at any age (with women being more prone) and impacts the joint tissue, entailing the deterioration of cartilage (as shown in Figure 1.15), but also of other structures and sometimes organs.
- Avascular necrosis (AVN): it is defined as bone cellular death because of an insufficient blood supply inside the joint and it involves articular cartilage loss. The bones thus risk collapse, with associated pain and joint function loss.
- Post-traumatic arthritis: it is a disease that degenerate following an injury to the cartilage or to the ligaments, leading to unstable joint and it is a substantial issue in young and active patients [26].

Figure 1.15. Normal knee representation on the left, OA in the center, RA on the right.

Joint replacement with an implant is often the treatment used as a last resort for knee arthritis [40] and it is explained in detail in the next chapter.

1.2 Total knee arthroplasty

TKA is an orthopaedic surgical procedure performed to replace the articular surfaces of the knee with prosthetic parts, restoring normal function in patients suffering from degenerative and rheumatologic knee joint disease, as well as from certain knee joint fractures [42]. It is a well-described treatment option for OA patients who have failed conservative treatment measures, that provides pain relief improving the functional status of the patient [9]. A representation of TKA components can be appreciated in Figure 1.16.

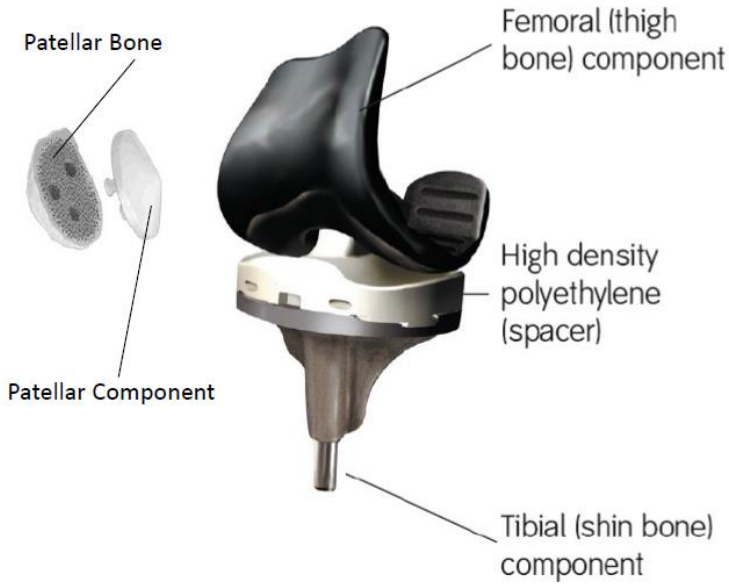

Figure 1.16. TKA components.

The knee prosthesis is made up of 3 main parts:

1. the femoral component: it replaces the distal part of the femur. In many cases, the implant follows an asymmetric design to better reflect the asymmetrical geometry of the native femoral condyles. Furthermore, nowadays the designs are characterized by a smooth deep groove with a short, narrow notch that improves the patellar tracking and stability, avoiding possible patella dislocation [26]. It is made up of strong polished metal; Cobalt-Chrome (CoCr) is commonly utilized.

2. the tibial insert: it is used to fill the gap between the distal femur and the proximal tibia, which has been originated after the removal of menisci. The insert has an important role as a damper, allowing a smooth gliding surface, absorbing shocks, and preventing luxation. The Ultra-High Molecular Weight Polyethylene (UHMWPE) material is usually used to build the insert; it is characterized by excellent mechanical properties, such as resistance to impact, abrasion, breaking, yielding, fatigue, as well as elasticity, low coefficients of friction, chemical inertness, and biocompatibility [43].
3. the tibial component: it has a flat plate and a short stabilizer stem that is fitted into the center of the tibial bone. The tibial component is made up of metal, commonly Cobalt-Chrome, or Titanium alloy.

In addition, some researchers recommend resurfacing the patella during knee arthroplasty, whereas many surgeons prefer to implant the patellar component only in selected cases [26]. The patellar component (Figure 1.17) is made in UHMWPE and always cemented.

Figure 1.17. Resurfacing patella illustration.

The goal of knee replacement is to achieve normal function and kinematics. For most of the patients, TKA procedure enable them to return to simple activities such as walking or climbing stairs and leads to an improved quality of life with less pain and more mobility. Nevertheless, both orthopaedic surgeons and patients continue to seek a better functional outcome [36], thus a cooperation between engineers and orthopaedic surgeons is fundamental to analyse and upgrade the existing prostheses designs or to eventually design new ones.

Currently, several TKA designs with different characteristics are available on the market and have been proposed and developed in order to provide a suitable solution for each knee joint condition and to satisfy the patients' demand [2]. The level of deterioration of the joint is the reference aspect that drives the choice of the design by the surgeon, but also the surgeon's experience and the economic budget can tailor the prosthesis selection process [44]. In the following section, the typologies of prosthesis design that have been analysed in the present study are described.

1.2.1 Prostheses design

One of the most important factors for a TKA is the level of constraint that the design typology introduces for the purpose of driving the stability of the joint by limiting or permitting specific degrees of motion. Many design choices are available as manufacturers produce a range of implant designs [14]. All the TKA designs that have been taken into consideration in this study are illustrated in Figure 1.18 and explained afterwards.

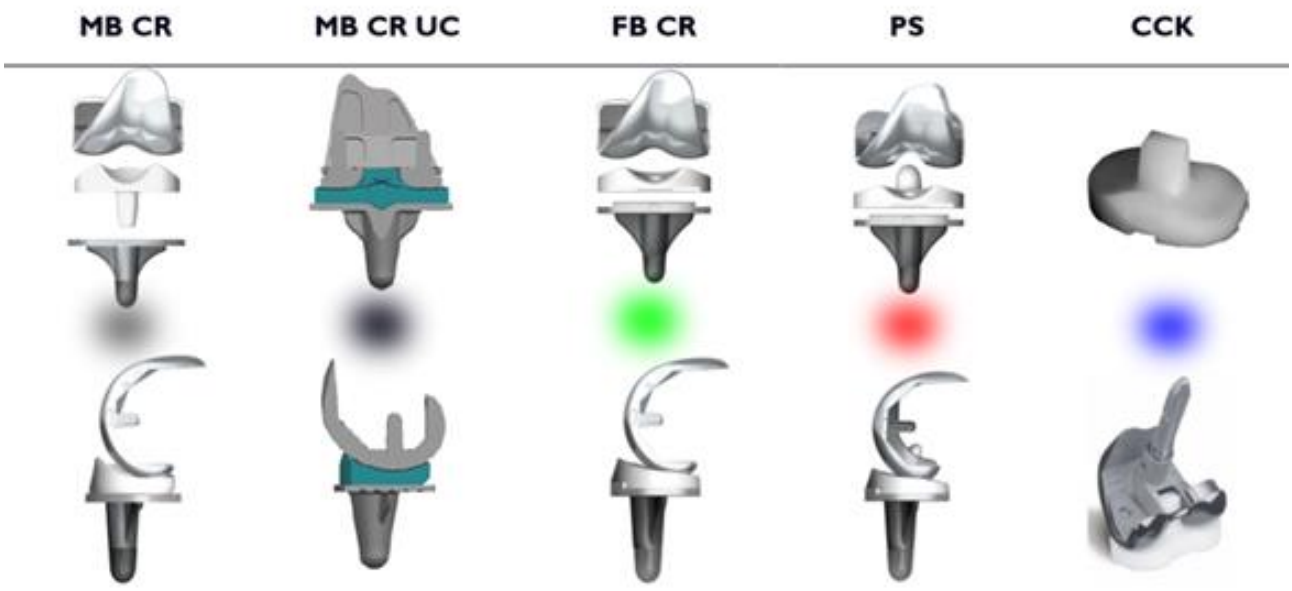

Figure 1.18. TKA designs from the less (left) to the most constrained (right).

Before proceeding with the implant application in an OA patient, the ACL is always removed. Then, the following step for the surgeon is to decide whether to retain or resect the PCL, basing on its health. So, based on this evaluation, a first selection in the design can be made.

If the PCL condition is accepted as healthy by the surgeon, the CR design can be designated. In the CR tibial component, a groove is present in the posterior part, to leave the necessary space to the preserved PCL. This design is categorized as non-constrained implants as the femoral component and tibial insert are not linked together by any constraint and rely on the patient's ligaments to ensure the knee stability [blevins2015]. CR designs, conserving the PCL which is one of the primary stabilizers of the knee [15]), can result in a closer native knee kinematics [comparison of long term], reducing patellar complications and shear forces [21]. Moreover, this implant design allows the patient to feel the joint since the cruciate has sensory endings related to the proprioception. Despite these advantages, there is also a drawback: in general, when the surgeon cuts the femoral and tibial bones in the extended and flexed position of a correctly aligned knee, the resulting gaps must guarantee the isometry between the collateral ligaments but in case of PCL retention this additional structure makes this procedure more complex. Indeed, in the CR the ligament balancing is very challenging, especially in cases of PCL laxity, knee deformities or flexion contracture [21], [45]. Alternatively, if the choice falls on the excision of a too weak or injured PCL, the PS design is the option, solving then the ligament balancing issue of the previous implant [15]. Regarding this, the cruciate stability function is replaced by a post-cam system integrated in the prosthesis which, adding a constraint, is classified as a semi-constrained design [14].

In detail, the tibial insert exhibits a rounded spine on the surface (called post) that during flexion articulates and engages with a transverse metal box (called cam) incorporated in the femoral component. This interaction promotes the femoral roll-back present in the native knee thus increasing the range of flexion and prevents the abnormal backward movement of the tibia during flexion movement [46], [47], [48].

Although this design has proved useful and easier technique with respect to the CR, it implies excessive bone cut and carries post-cam-related complications resulting in high stress on the insert and risk of wear where the post-cam mechanism operates, or of post breakage [48], [21]. The correct analysis of the post-cam interface is fundamental to avoid the risk of luxation, so it is useful checking for the post-cam contact force and area during different activities.

Another implant that involves the post-cam is the CCK: it is a semi-constrained prosthesis but, with respect to PS, it adds a constraint in the articulation, being characterized by a wider post with rectangular shape that more conformingly fits in the overlying deeper box. This shape can reduce IE rotation and ML displacements (also FE and AP displacements during high flexion), also improving the stability on varus-valgus direction [49], [50]. Mainly used in revision surgery, where CCK is often recommended to be coupled with hinged mechanism, in primary arthroplasty can be a valid choice when the soft tissue alone cannot provide enough stability to the knee [50].

Concerning the CR, in this study three sub-typologies have been included: FB, MB, (MB) UC. The first presents the insert in a rigidly fixed position upon the tibial metal component, constraining the insert rotation. Instead in the second version the tibial platform is free to IE rotate in relation to the fixed tibial component, and a higher articular conformity is achieved; this mobility feature was indeed developed for a more physiological motion and to correct small tibial rotational misalignment, therefore minimizing loads and polyethylene wear [21]. Beyond this, the MB CR are less forgiven for ligament balancing with respect to FB CR since the additional degree of motion makes the knee more subjected to instability, with a consequent risk of luxation and spin-out of the insert from its position on the tibial component.

Actually, relatively high rate of MB mechanical complications such as loosening of the femoral component, tibiofemoral dislocation in high flexion and insert breakage have been described [51], [36].

With the purpose of further increasing the implant congruency, thus reducing stress peaks on the bone-implant interface thanks to the availability of a larger articular contact area, the third typology has been produced. UC has an insert with deep dished plate and high anterior wall [15], and it has been found to stabilize the knee in AP direction even in patient with PCL deficiency [21].

In general, among this variety of design, the more loosening the ligaments, the more constraints the prostheses should provide to the joint.

2 State of the art

The TKA implants that have been considered in this work are characterized by different levels of constraint therefore differently affect the interactions between the bones and the implant [52]. In fact, it has been demonstrated that the implant design has significant effects on its performance, thus the distinct designs can fulfil the knee replacement giving different implications [53], [54], [55], [56].

Intending to achieve a clearer overview of the TKA design effects, previous studies have examined kinematics or wear often focusing on a single implant typology and at short term follow-up [56], [57]. In addition, Bourdon et al. 2021 [14] have suggested that implant design affects kinematics and wear also at long-term follow-up. Some studies use in vitro analysis to test the implants and to measure kinematics and contact mechanics such as Arnout et al. 2015 [58] which performed dynamic analysis on eight PS prostheses belonging to different orthopaedic companies. All these studies agree on the concept that for accomplishing a functional replacement of the knee joint, the design of TKA should be able to guarantee stability, function like a physiological knee for a long period of time, trying to avoid complications and the necessity of revision [56], [57]. Alongside the enrichment of the implant designs range by manufacturers, it has also grown the need and the interest of surgeons and engineers in investigating the kinematic and kinetic outcomes deriving from the variety of geometries and mechanisms of the available prostheses [57].

In this background several researchers have focused the attention on the comparative examination of a couple of prostheses or more, which are different in the constraint's level, by using various methods.

Concerning this, literature research covering the last twenty years has been run and the most significant papers that consider two TKA designs or more have been selected, inspected, and accordingly arranged in two tables.

The first one, Table 1, collects the information regarding those studies that utilize in vivo or in vitro techniques, while the second one, Table 2, contains studies based on numerical approach.

Table 1. In vitro and in vivo studies about different TKA designs.

Author	Implant number	Design	Manufacturer	Analysis	Outcomes
Stukenborg-Colsman et al. 2002 [59]	3	FB SD, FB HC (high conformity), MB	Stryker	In vitro	Contact area, contact stress
Most et al. 2003 [60]	2	PS, CR	Zimmer	In vitro	Joint kinematics
Victor et al. 2005 [61]	2	CR, PS	Smith&Nephew	in vivo	Joint kinematics
Sharma et al. 2007 [62]	2	High flexion FB CR, High flexion FB PS	Zimmer	In vivo	Joint kinematics
Harato et al. 2008 [63]	2	PS, CR	Smith&Nephew	In vivo	Functional score, range of motion, radiographs, postoperative complications
Shiramizu et al. 2009 [64]	6	FB PS, MB PS, FB CR	Zimmer, Depuy, Smith & Nephew, Biomet	In vitro	contact area and pressure
Kolisek et al. 2009 [65]	2	CR, PS	Stryker	In vivo	Functional score, range of motion, radiographs
Urwin et al. 2014 [66]	2	FB, MB	Depuy	In vivo	Joint kinematics and kinetics
Riaz et al. 2017 [67]	2	FB CR, MB CR	Depuy	In vivo	Functional score, range of motion
Puah et al. 2018 [68]	5	PS, CCK	Zimmer, Depuy, Smith & Nephew	In vivo	Functional score, range of motion
Lee et al. 2020 [69]	2	PS, UC	Stryker, B. Braun	In vivo	Functional score, range of motion
Gray et al. 2020 [11]	3	PS, CR, Medial Stabilized	Medacta International	In vivo	Joint kinematics
Bourdon et al. 2021 [14]	3	PS, CR	Depuy, Smith&Nephew	In vivo	Contact area and joint kinematics
Castellarin et al. 2022 [70]	3	MB CR SD, MB CR AD, MB CR UC	Adler Ortho	In vitro	Joint kinematics

In Table 1 there are studies that have compared different designs by means of disparate methods. In particular, there are in vitro methods which use robotic manipulators and motion capture systems on cadaveric knee with TKA in order to measure the kinematic outcomes [60], [70], but also pressure and contact values by means of pressure sensors [59], [64]. The remaining studies in the Table 1 are based on in vivo randomized-control trials and meta-analyses [71] that use fluoroscopic image acquisition to measure kinematic range of motion with different years of follow-up such as Victor et al. 2005 [61], Sharma et al. 2008 [62], Urwin et al. 2014 [66], Bourdon et al. 2021 [14], and in some cases also perform clinical evaluation usually coupled with qualitative questionnaire for the patients to record functional scores like in Kolisek et al. 2009 [65], Riaz et al. 2017 [67], Puah et al. 2018 [68], Lee et al. 2020 [69]. Some of these studies take into analysis just PS and CR designs to verify the differences in their performance and to understand the effect of PCL resection in the first case and retainment in the second one, but without demonstrating superiority in patient satisfaction, pain, complications and in implant performance [60], [61], [65], [11], as it is also reported in Song et al. 2019 [72]. Instead, in Harato et al. 2008 [63], PS display statistically significant improvements in range of motion when compared with the CR group, with equivalent clinical knee scores and survivorship. Also Bourdon et al. 2021 [14] have shown that, at long term follow-up, there were differences in kinematics and wear resistance between CR and PS implants; indeed PS was found to be superior to CR for posterior rollback and lift-off risk and exhibited better wear resistance. Several studies have investigated prostheses with different bearing modality, FB and MB [59], [64], [66], [67], and in Castellarin et al. 2022 [70] also the MB CR UC version is inserted in the comparison. More in detail, Stukenborg-Colsman et al. 2002 [59] have found that FB modality results in higher contact stress peaks with respect to MB case and Shiramizu et al. 2009 [64] have observed wider contact areas in the MB. Instead in Urwin et Al. 2014 [66] there was no difference in AP direction in knee kinematics of the MB group when compared to the FB group. Riaz et al. 2017 [67] have failed to elicit an objectively demonstrable clinical difference between the MB and FB implanted knees, and radiological benefits of the MB about wear have been not evident at a

minimum ten-year follow-up. Additionally, the comparison of PS and CCK carried out by Puah et al. 2018 [68] have shown that the use of a CCK in primary knee arthroplasty produces similar ROM and functional scores at six-months and two-years of follow-up, with no functional impairment or benefit over a PS. Furthermore, from the Table 1 it can be noted that in some cases the considered prostheses are not produced by the same manufacturer, thus their analysis results could be subjected to differences related to the company's choices regarding the geometry or materials [64], [68], [69], [14]. In the same table also the outcomes typology of the relative studies has been inserted.

Since the complexity of knee joint kinematics has always challenged and fascinated the scientific community, the researchers have explored other tools to better understand the behaviour of different implant designs. In this context, the FEA has made its way in the orthopaedic field and become one of the most reliable virtual simulation tools for evaluating wear, crack propagation, fatigue, and other mechanical parameters, being also used in many types of preoperative testing [23]. FEA represents indeed a valid alternative to in vivo or in vitro assessments, since it is able to provide analogous results to them, while maintaining lower cost in comparison [28]. It is a numerical technique widely spread in orthopaedic biomechanics research, that allows the modelling of complex geometry such as the knee joint, the application of systems of loads and the prediction and measurement of local parameters such as internal stress and displacement [22]. This method is largely used to detect abnormal forces which can be the cause of TKA complications and failure for the patient, by affecting joint stability and implant integrity.

In this scenario, several works have applied FEA to virtually simulate different everyday life conditions or activities on prosthetic knee joint models to better understand the effects of one or the other design, supporting the surgeon on the most suitable choice to improve patient satisfaction and to reduce the incidence of TKA revision.

The most relevant studies that have performed numerical analysis in the last 20 years have been collected from literature and organized in Table 2.

Table 2. Numerical studies about different TKA designs.

Author	Implant number	Design	Manufacturer	Software	Activity	Outcomes	Patella included
Zelle et al. 2009 [19]	3	CR High flexion, PS High flexion, CR	Depuy	FE program Marc	Squat	Insert stress, TF kinematics	Yes
Innocenti et al. 2011 [73]	4	FB PS, high flexion FB PS, MB CR, hinged design	Smith&Nephew	LifeMOD/ KneeSIM	Squat	PF and TF contact force	Yes
Pianigiani et al. 2012 [74]	4	FB PS, high flexion FB PS, MB CR, hinged design	Smith&Nephew	LifeMOD/ KneeSIM	Squat	TF kinematics	Yes
Srinivas et al. 2013 [20]	2	FB and MB	Not specified – same company	LS-DYNA	Gait cycle	Insert stress	No
Pianigiani et al. 2015 [5]	2	PS, CCK	Smith&Nephew	LifeMOD/ KneeSIM	Gait, step ascent, step descent, squat	Post-cam contact force	Yes
Pianigiani et al. 2015 [75]	2	PS, CCK	Not specified- Same company	Abaqus	Gait, Squat	TF Kinematics and kinetics	No
Pianigiani et al. 2016 [10]	4	FB PS, FB high flexion PS, MB CR, hinged design	Smith&Nephew	LifeMOD/ KneeSIM	Squat	TF and PF Kinematics and kinetics	Yes
Castellarin et al. 2018 [53]	2	MB CR SD and MB CR AD	Adler Ortho	Abaqus	Gait, Squat	TKA kinematics and bone stress	Yes
Innocenti 2019 [21]	2	FB CR and MB CR UC	Link	Abaqus	Gait, Squat	TKA kinematics and kinetics	No
Shu et al. 2021 [76]	4	FB CR, MB CR, PS, Medial Pivot	Adler Ortho	Abaqus	Gait	TF kinematics and kinetics (insert pressure)	Yes
Castellarin et al. 2023 [6]	4	PS, CCK, MB CR and UC	Adler Ortho	Abaqus	3 static configurations	Bone and insert stress, contact mechanics	No

Even with numerical methods some researchers have taken into analysis just PS and CR designs such as Zelle et al. 2009 [19] which have found that the amount of femoral roll-back produced by the CR high-flexion design (design which provides for a larger range of motion) was inferior compared to the PS high-flexion design. Other studies compared PS and CCK implants; Pianigiani et al. 2015 [5] have reported that CCK design has shown only slightly higher contact force in the posterior surface of the post-cam, as compared to a conventional PS design. In another paper Pianigiani et al. 2015 [75] have built a CCK starting from a PS model, showing that the CCK limits the IE rotation and increases the AP translation, more evident for high demanding tasks such squatting, thus it could induce earlier wear compared to the PS. Srinivas et al. 2013 [20] have instead investigated about the stress induced by different bearing designs: they have found out no significant differences in the maximal stresses in the superior surface of the MB and FB inserts, while on the inferior surface the peak stresses were higher in the MB one, thus deducing that MB designs may be associated with higher overall insert stresses and wear than the FB ones. In the examination of two prosthesis designs, Castellarin et al. 2018 [53] have compared a couple of MB CR but one with a symmetric insert and the other with an asymmetric one; they finally have assessed that TKA kinematics was similar for the two designs, although the asymmetric solution has shown less bone stress, thus avoiding lift-off and pain. Innocenti 2019 [21] has demonstrated that in case of PCL deficiency the MB CR UC has been able to guarantee proper knee stability and kinematic while the FB CR, with lower congruency and in the same situation, has not been able to stabilize the joint, since has induced irregular kinematic pattern and component dislocation. Other surgeons and engineers have directed their attention on groups of more than two implant designs [76], [6], some of them also including the most constrained hinged designs [73], [74], [10]. In particular, Innocenti et al. 2011 [73] have investigated the sensitivity of the PF and TF contact forces to patient-related anatomical factors, and component position in the different implant types and they have shown that PF contact forces are mostly affected by patella height, by an anterior tibial component translation and by patellar component tilt, whereas TF contact forces by the anterior displacement of the insertion points of

the MCL with respect to the reference position. Starting from this sensitivity study, Pianigiani et al. 2012 [74] focused on TF kinematics outcomes, finding that it can be altered by changes in implant positioning and collateral ligaments insertion, irrespective of the different design. Following the same research line, Pianigiani et al. 2016 [10] have studied the same prostheses but involving kinetics analysis, trying to give a possible explanation the common paradox in which even if kinematics remains close to the physiological range of motion, the patient may still complain about pain and functional limitations; their results have shown that contact forces are more heavily affected by malconfigurations than kinematics, thus highlighting that the study of the kinetics is necessary to understand the overall biomechanical TKA effects. Shu et al. 2021 [76], after their four implants comparison, have found out that MB CR designs has exhibited the smallest contact pressures while PS greatest ones, with respect to FB CR and to a medial-pivot design (it presents high conformity to the medial side).

For what concerns the simulation performed on the FEA models and as reported in Table 2, some studies simulated the gait cycle [20], [76], other ones the more high-demanding activity of squat [19], [73], [74], [10], some papers have included both the abovementioned simulations [5], [75], [53], [21], one of which involving step ascending-descending tasks [5], and finally one study has simulated three static common configurations of the knee [6]. For what concerns the presence of the patella or patellar component in the models and of the PF in the analysis, some works have not involved them [20], [75], [21], [6].

Nonetheless the existence of abovementioned research and the increasing interest in the discrimination of which design performs the best, together with the willingness to support the surgeon in the selection process towards the most suitable implant for each single patient condition, still no absolute guidelines exist to spot the best match [70]. Moreover, up to now, the maximum number of implant designs considered by FEA studies is limited to four.

There is no outright consensus in the available literature on how to select the most appropriate solution for each case and this issue could be related to the lack of complete clinical and biomechanical evidence-based directives describing the effects of the various current options of TKA designs [77].

Besides, parallel to the aging of the population and with the improvement of the quality of life, there is the growing need for developing a more detailed scientific rationale about TKA performances during both daily and high-demanding activities [78]. With such implant variety in fact, it follows that is important for surgeons and engineers to provide a needed insight into the available geometries' biomechanical mechanisms and their kinematic profiles [57], also to let the market improve and to increase patient possibilities and satisfaction in performing motor tasks [11].

3 Materials and Methods

In this chapter the geometries, materials, constraints, interactions, loading, mesh, regions of interest (ROI), output and dynamic FEA settings are examined.

3.1 Geometry

The finite element model developed for this study is based on a previously validated knee finite element model [79], which geometry is composed of a left leg of medium size obtained from computer tomography (CT) scans, containing tibia and femur bones (Figure 3.1) which have been then partitioned into cortical and cancellous sections.

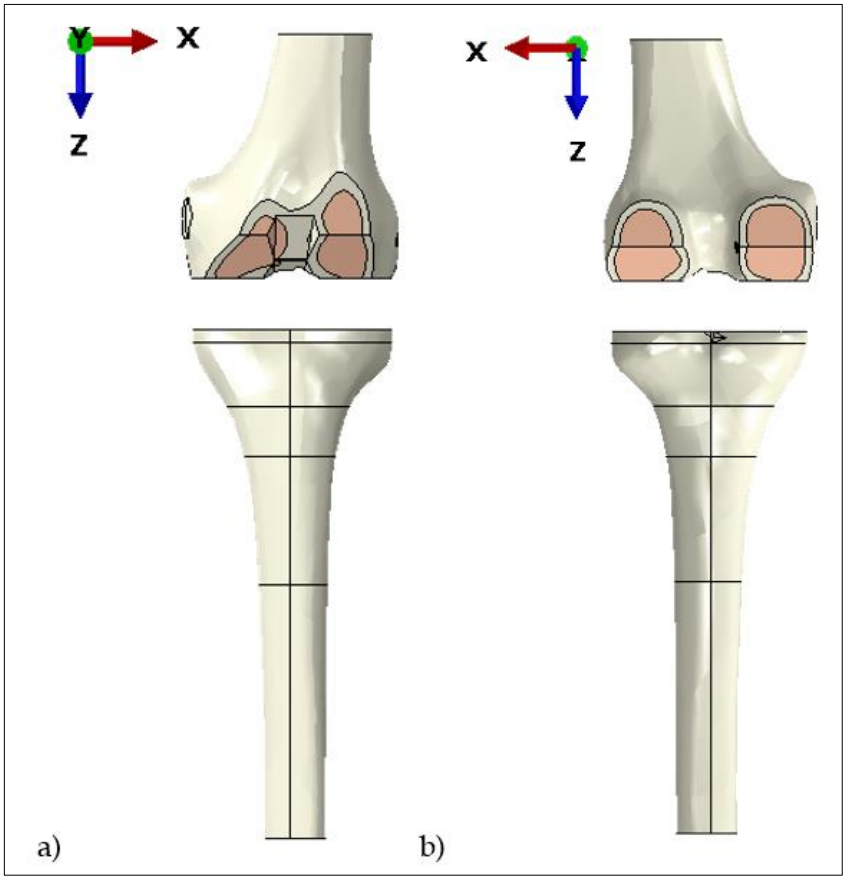

Figure 3.1. Model of femur and tibia of a left leg: a) anterior view; b) posterior view.

The included prosthesis designs, depicted in Figure 3.2 and Figure 3.3, are:

- FB PS
- FB CCK
- GESUS FB CR
- GENUS MB CR
- GENUS MB CR UC

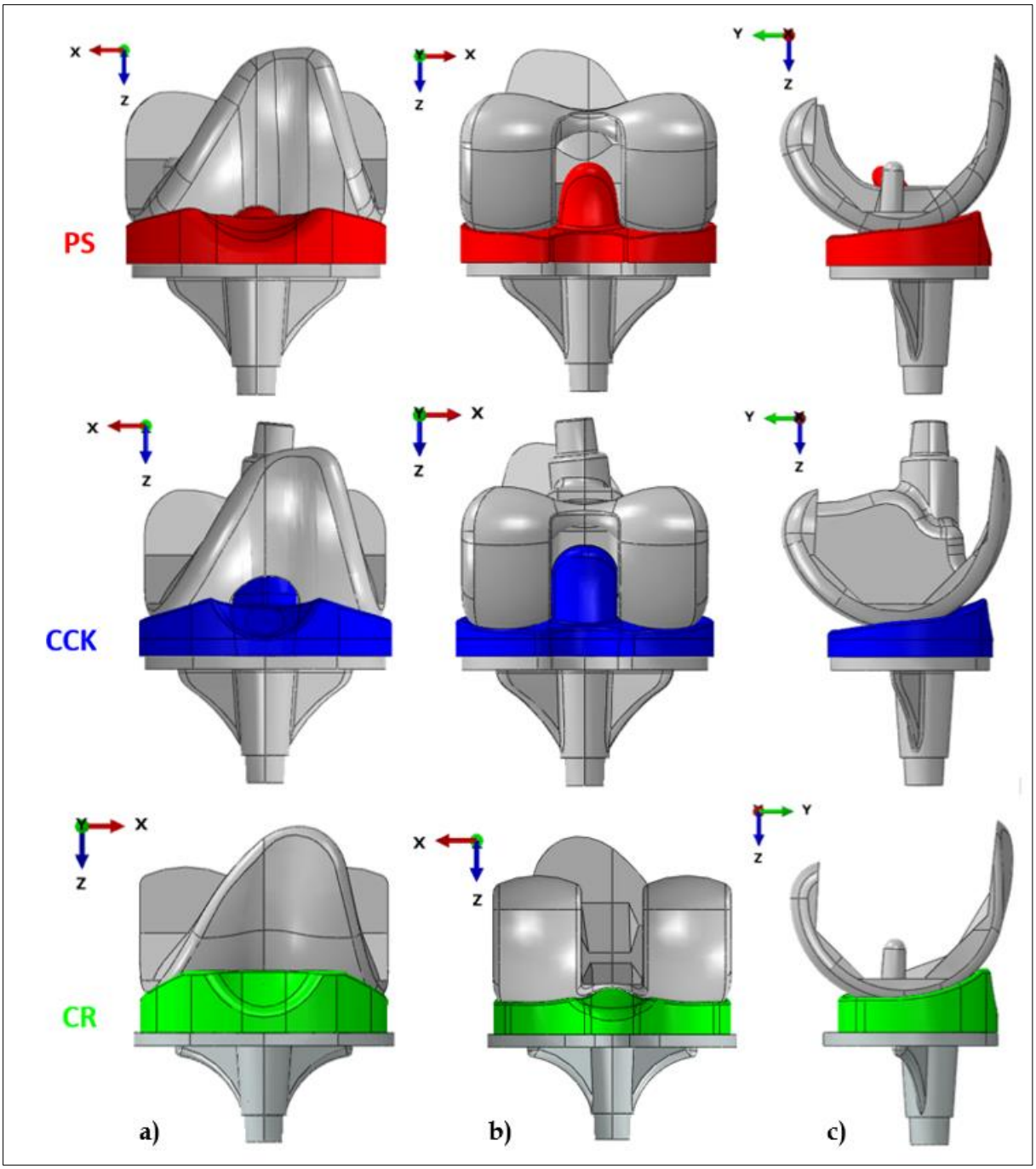

Figure 3.2. FB TKA models of PS, CCK and CR: a) frontal view, b) posterior view, c) medial view.

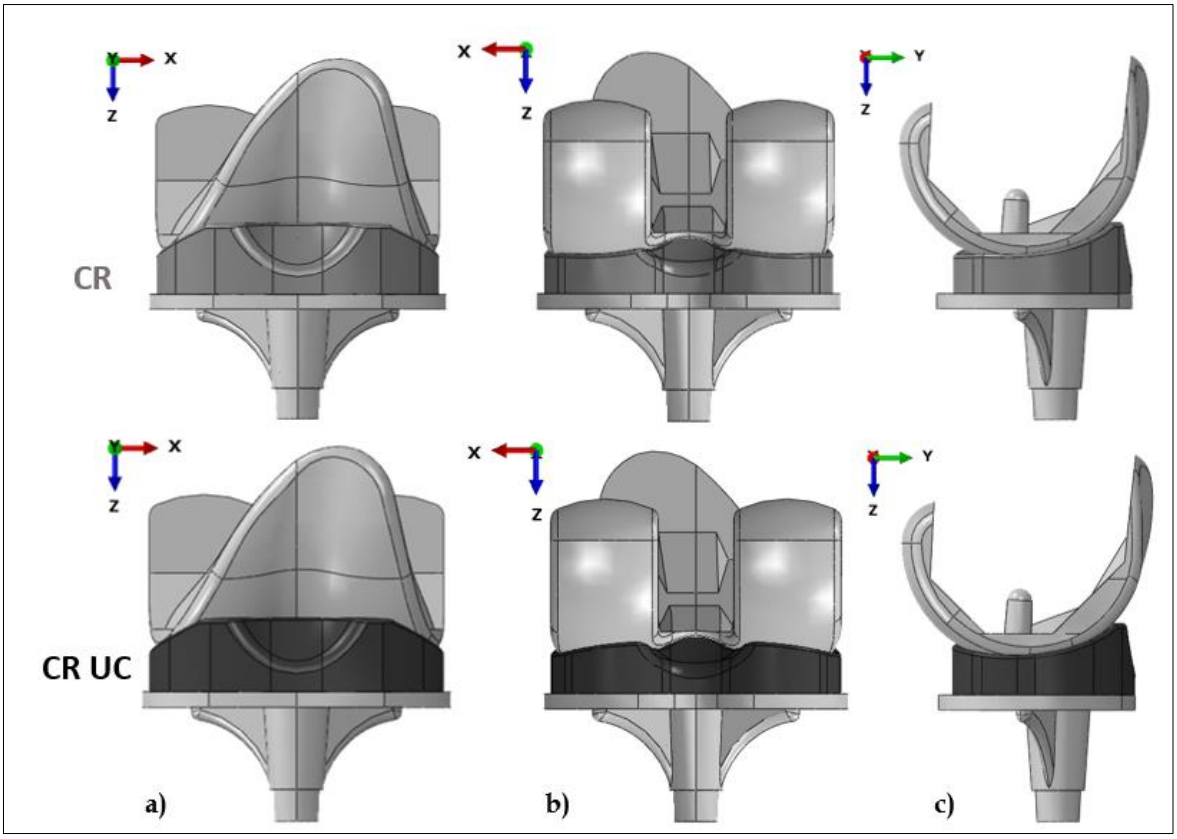

Figure 3.3. MB TKA models of CR standard and CR UC: a) frontal view, b) posterior view, c) medial view.

The CAD files of the implant components (femoral component, tibial insert, tibial tray and cemented resurfacing patella), all being left sides, were provided by the company Adler Ortho (Cormano, Milan, Italy) and virtually implanted on the knee model by following the related surgical instructions, using the press-fit fixation approach, and following the correct mechanical alignment of the knee [80].

All the femoral components and tibial inserts are of size 6, while the tibial components are of size 5. Among all the models just the tibial insert differs in the shape, and in the FB PS and CCK the tibial tray stems are longer and larger with respect to the other implants. In all the models intended for the squat simulation, the patellar component and the PT have been incorporated.

The fully assembled models for gait simulations with FB and MB prostheses can be appreciated respectively in Figure 3.4 and in Figure 3.5.

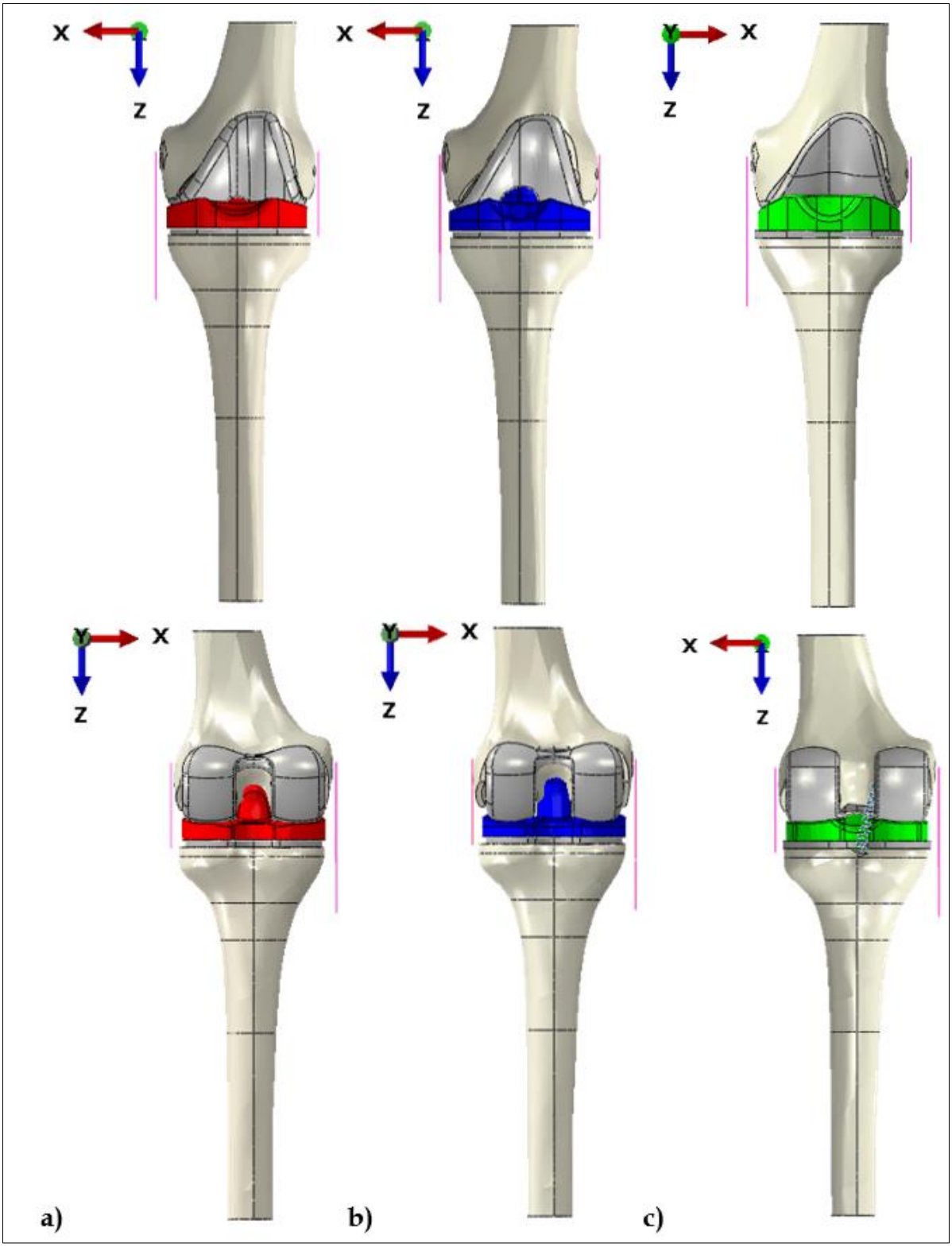

Figure 3.4. Full knee models for gait simulation of a) FB PS b) FB CCK c) FB CR, in the frontal view (up) and in the posterior view (bottom).

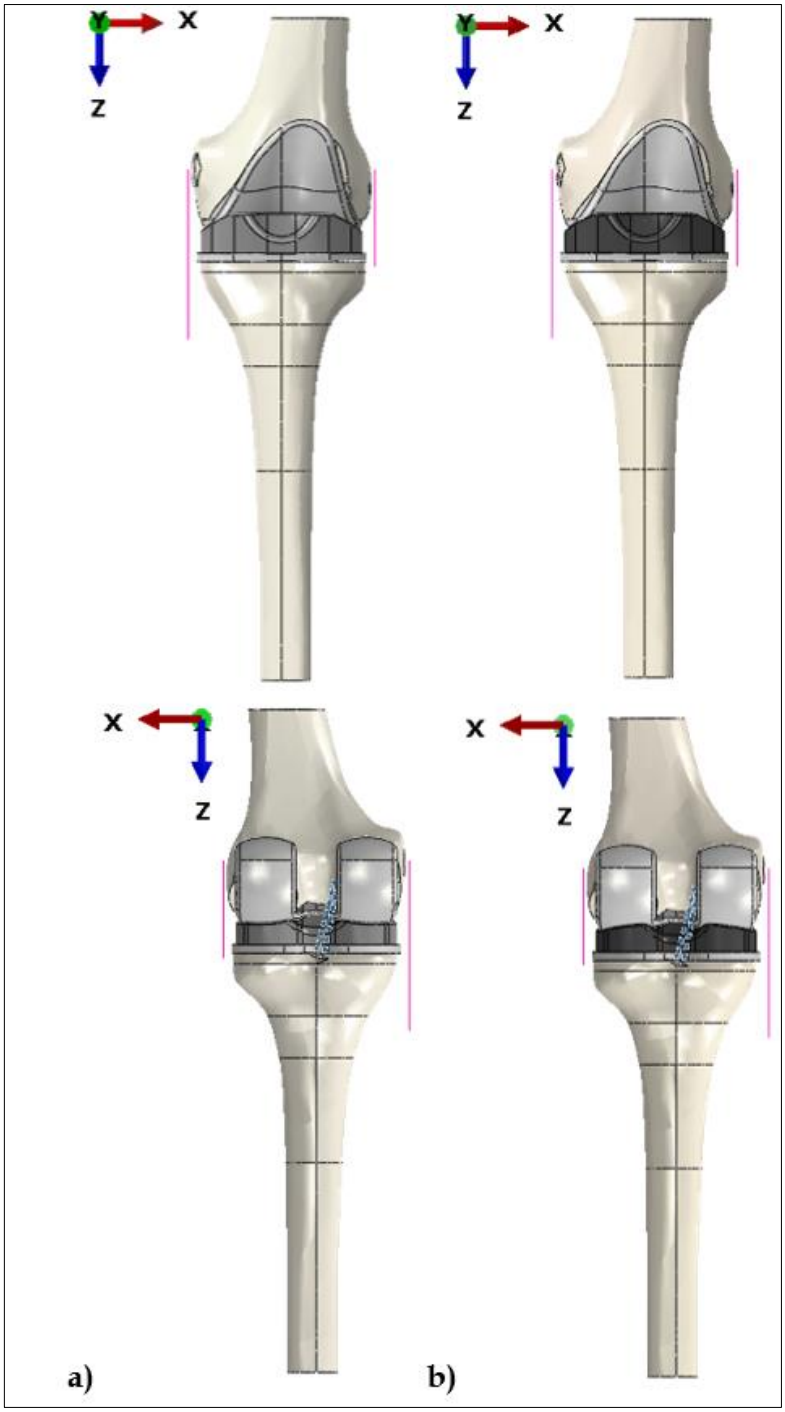

Figure 3.5. Full knee models for gait simulation of a) MB CR and b) MB CR UC, in the frontal view (up) and in the posterior view (bottom).

Regarding the models for the squat simulation, the GENUS cemented resurfacing patella implant of size 30 mm has been positioned with a physiological height with respect to the knee joint line; in particular, the Blackburne-peel ratio method has been used [39], considering as normal height a ratio value between 0.8 and 1.0.

Furthermore, a skin shell on the anterior surface of the patellar component has been defined simulating the physiological cortical bone of the patella in contact with the patellar component. In Figure 3.6 an example for the complete model of TKA with patellar component used for the squat simulations is illustrated.

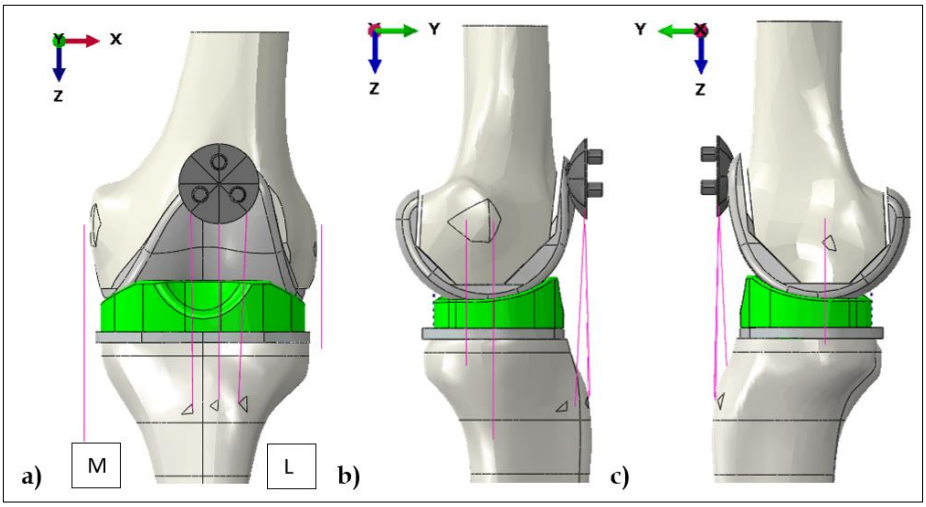

Figure 3.6. Focus on patella resurfacing and PT: a) frontal view (M is the medial side, L the lateral side), b) medial view, c) lateral view.

For what concerns ligaments, LCL and MCL have been modelled as pre-strained beams with a specific cross section. The MCL is constituted by two beams (anterior (aMCL) and posterior (pMCL)), while LCL by one beam [80], [53], as it can be seen in Figure 3.7. Their insertion points in the bones were defined according to the literature [81].

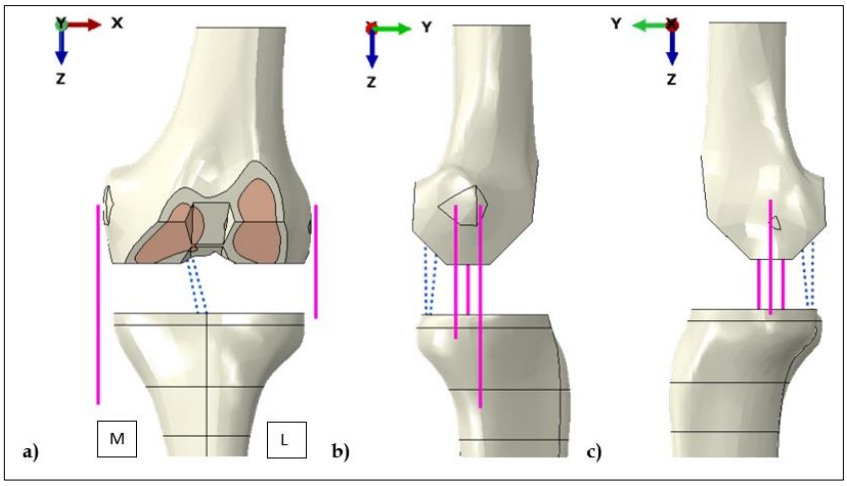

Figure 3.7. Detail of collateral ligaments: a) frontal view (M is the medial side, L the lateral side), b) medial view, c) lateral view.

The PCL has been incorporated in the CR models (FB CR, MB CR and MB CR UC) as composed by two axial connector wires (Figure 3.8), anterior (aPCL) and posterior (pPCL), which follow a force-strain behaviour model taken from literature and depicted in Figure 3.9Figure 3.9 [82].

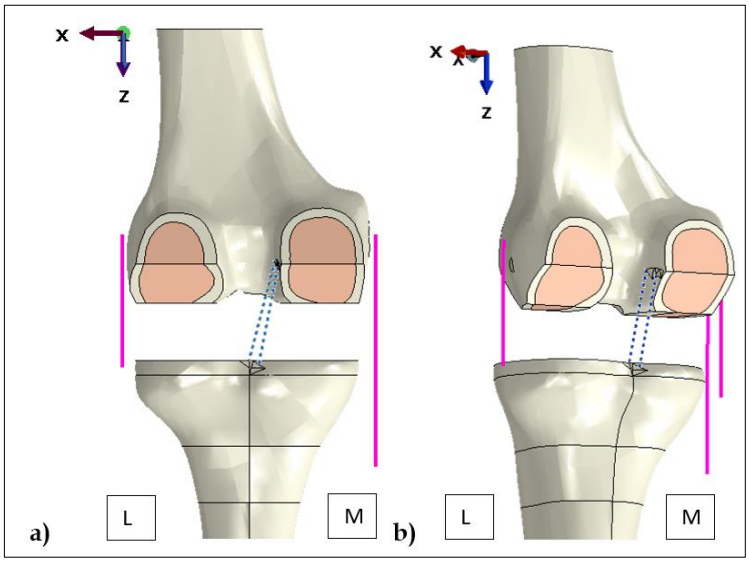

Figure 3.8. Detail of PCL modelled as axial connectors (dashed wires): a) posterior view, b) lateral-posterior view. M is the medial side, L the lateral side.

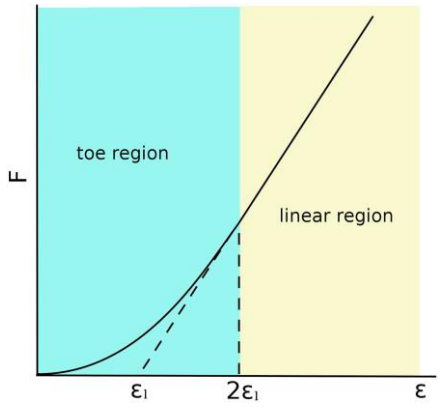

Figure 3.9. Force–strain behaviour of a generic ligament; $2\varepsilon_1$ is the threshold strain, which indicates the change from the toe to the linear regions.

The PT has been modelled by means of three beams connecting the inferior part of the patellar component to the proximal part of the tibia, by using the same approach of the collateral ligaments and by defining the insertion points following the literature [83], [84], [85]. PT beams can be appreciated in Figure 3.6.

3.2 Material models and properties

The materials have been defined and assigned to the corresponding parts through literature research [21], [86], [80], [79], [87], [88]. For all the considered materials, the property of linear elasticity has been optioned. The properties used to model all the materials are summarized in Table 3, in which ε_r represents the pre-strain of the ligaments and, for the cortical bone, E_3 represents the axial direction.

Table 3.Material properties of the knee model.

Material	Material model	Young's modulus (MPa)	Poisson's ratio	Shear Modulus (MPa)	Density (t/mm^3)	ε_r
Cortical bone	Transversely isotropic	E1 = 11,500 E2 = 11,500 E3 = 17,000	v23 = 0.31 v13 = 0.31 v12 = 0.51	G_{23} = 4,400 G_{13} = 4,400 G_{12} = 3,800	1.85E^{-09}	
Cancellous bone	Elastic isotropic	2,130	0.31		2.90E^{-10}	
CoCr	Elastic isotropic	240,000	0.30		1.00E^{-08}	
UHMWPE	Elastic isotropic	0.685	0.40		9.70E^{-10}	
LCL	Elastic isotropic	228	0.45		3.10E^{-10}	0.05
MCL	Elastic isotropic	220	0.45		3.10E^{-10}	0.04
PCL	Elastic isotropic	177	0.45		3.10E^{-10}	
PT	Elastic isotropic	169	0.45		1.67E^{-09}	

3.2.1 Bones

The cortical bone has been considered linear transversely isotropic (with the principal axis corresponding to the anatomical axis of the bone) whereas the cancellous bone was considered linear elastic isotropic. Femur and tibia are partitioned into cortical and cancellous bone, while the patellar skin that covers the patellar component is made of cortical bone. The density of cortical and cancellous bone has been inserted in the bone material property (Table 3) [89].

3.2.2 Soft tissues

The LCL and MCL have been considered isotropic. Their pre-strain has been obtained by specifying the expansion coefficients and a temperature variation, following previous studies [79], [90], [53],[82]. The PCL material properties have been assigned to the modelled axial connectors aPCL and pPCL and the PT material properties have been assigned to the three PT beams (Table 3).

3.2.3 Total knee prostheses

All the TKA implant materials have been assumed as homogeneous and isotropic [21]. The femoral component and the tibial tray are made of CoCr. The tibial insert and the resurfacing patella are constituted of UHMWPE.

3.3 Constraints

The tie constraint has been applied between the lower cut surface of the femur and the internal surface of the femoral component. An anatomical landmark has been defined in the center of rotation of the femur, such as in the middle of the femoral condyles on the trans-epicondylar axis [32]. This reference point has been constrained with a continuum distributing coupling to the internal surface of the femoral component.

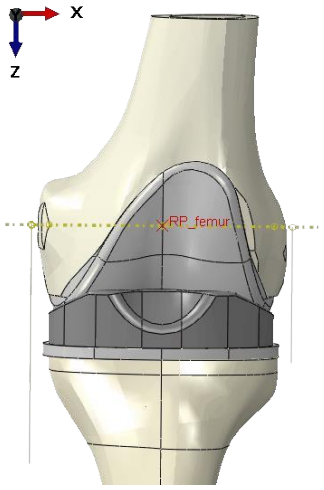

Figure 3.10. Detail of the reference point (RP) of the femur at the condyles center on the trans-epicondylar axis.

In case of squat simulation, other two reference points have been defined: one on the medial side of the patellar component being the point of MPFL action, which has been coupled (continuum distributing) with the medial surface of the patella, and one on the superior part of the patellar component as the quadriceps contribution, which has been coupled (continuum distributing) with the superior surface of the patella (Figure 3.11).

For the MCL and LCL, continuum distributing coupling constraints are applied between each ligament insertion points and the relative surface in the lateral or medial epicondyle surface (Figure 3.11), which has been previously partitioned. Same methodology has been used to kinematically couple the aPCL and pPCL insertion points to the posterior part of the medial epicondyle and to the posterior proximal part of the tibia, by constraining just the translations in the three directions.

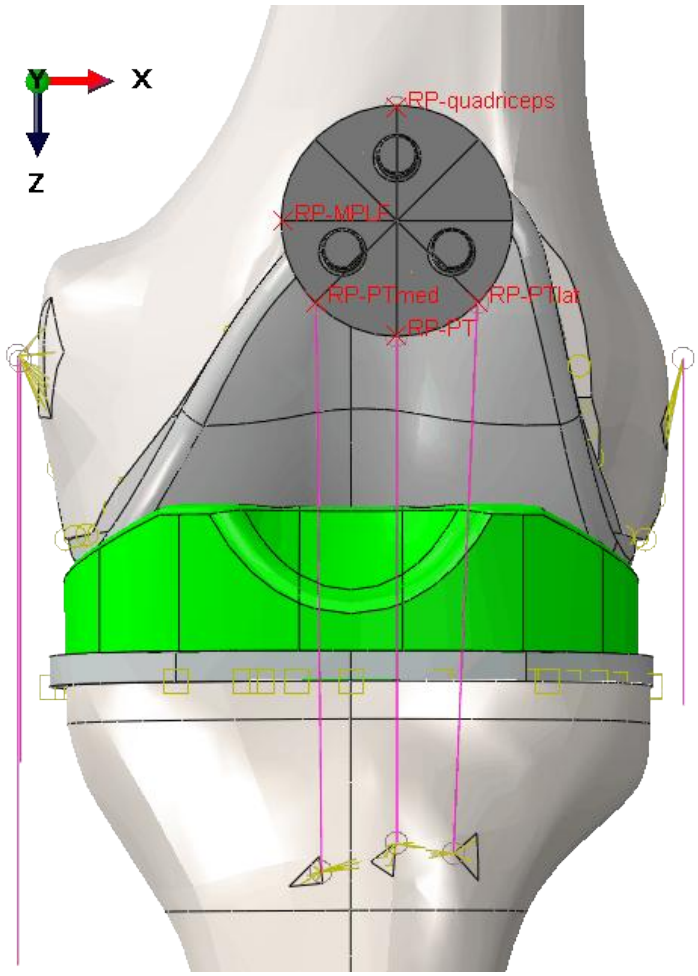

Figure 3.11. Focus on reference point (RP) for MPLF, quadriceps and PT (medial PTmed, central PT, lateral PTlat) attachments.

Regarding the three beams that compose the PT, their inferior ends have been attached to the tibia anterior proximal surface after partitioning it to obtain the physiological insertion area of PT (Figure 3.11). About the PT superior ends, three control points on each beam (as a node region) end have been connected to a reference point in the inferior surface of the patellar component through a continuum distributing coupling (Figure 3.12) and then the three reference points have been in turn kinematically coupled in terms of both translations and rotations with the inferior surface of the patella.

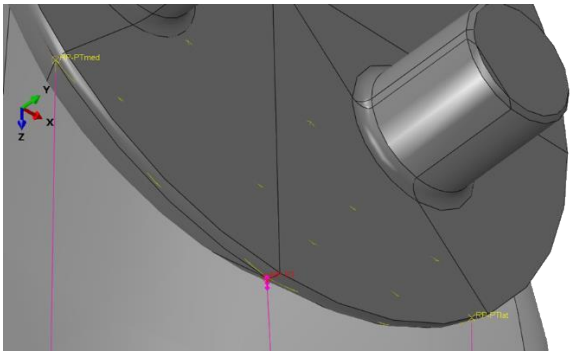

Figure 3.12. Focus on the PT attachment on the patella through a coupling (three nodes region-reference point).

A tie constraint between the tibial insert and the tibial tray has been applied to the fixed-bearing models of FB PS and FB CCK. To obtain the FB CR model, the same tie constraint has been used on the MB CR model, fixing the tibial platform rotation on the tibial tray (Figure 3.13). For the mobile bearing models, a reference point of rotation that coincides with the center of the insert peg, has been coupled with continuum distributing to the lateral surfaces of the peg.

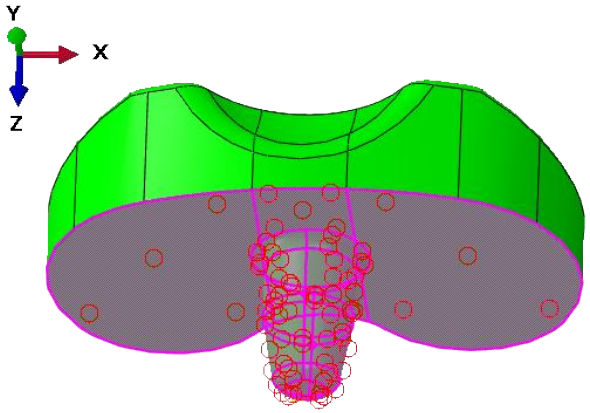

Figure 3.13. Focus on posterior surface on FB CR insert, fixed on the tibial tray.

3.4 Interactions

According to previous studies, the frictional behaviour using general contact with the penalty contact method has been used. A coefficient of friction of 0.04 has been considered for the interaction between the prosthetic components [79] which are: the femoral component and the tibial insert, the femoral and the patellar component, the tibial insert, and the tibial component.

To consider the cement layer of Polymethyl Methacrylate (PMMA) that is present in the interface between tibial bone and tibial tray, a surface-to-surface interaction with penalty contact between their surfaces has been defined, with a friction coefficient of 0.4, as previously adopted in literature [91].

3.5 Boundary conditions

In all the models, the distal extremity of the tibia has been fixed with an encastre (Figure 3.14) [86]. Regarding the femur, in the squat simulation any degree of motion (IE rotation, varus-valgus rotation, AP translation, ML translation, inferior-superior translation) has been allowed except to the FE rotation, to maintain the appropriate flexion angle.

In the gait cycle simulations, also the IE rotation has been superimposed according to the loading inputs. For the mobile bearing models, the insert rotation about the longitudinal axis has been left free. All the collateral ligaments attachment points on the tibia have been distally fixed [21].

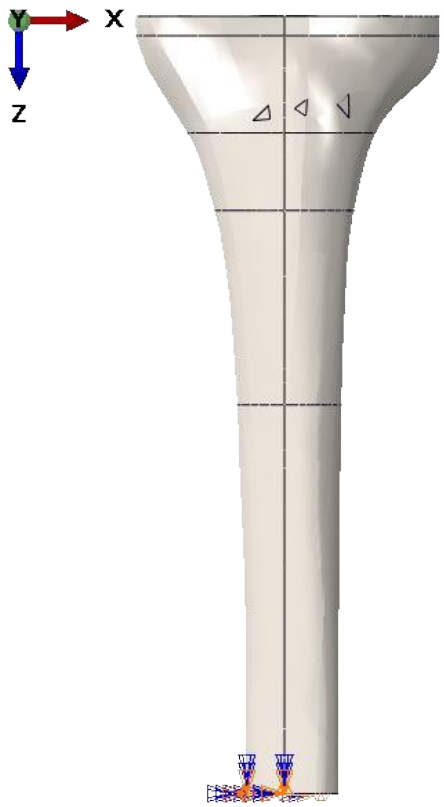

Figure 3.14. Tibia inferior surface fixed with encastre.

3.6 Loadings

The Gait cycle has been dynamically simulated with a cycle duration of 1s by means of input data relative to the kinematics (FE angle and IE angle) and the kinetics (AP force and Axial force), following the standard ISO-14243-1 [75].

For the Squat cycle, a 10s dynamic loaded movement up to 120° has been considered in terms of femur FE angle, Axial force, AP force and patellar ML force, Axial force, AP force input data. The Gait Loads have been imposed on the center of rotation of the femur, following a previous study [86]. For the squat the loads have been properly applied on the center of rotation of the femur, on the quadriceps insertion on the proximal surface of the patella and on the insertion point of the MPFL [74].

3.7 Mesh settings

All the parts of the models have been meshed using linear tetrahedral elements, with the element sizes chosen accordingly to each part. For the gait models the element size of each part was between 1.5 and 5 (Figure 3.15).

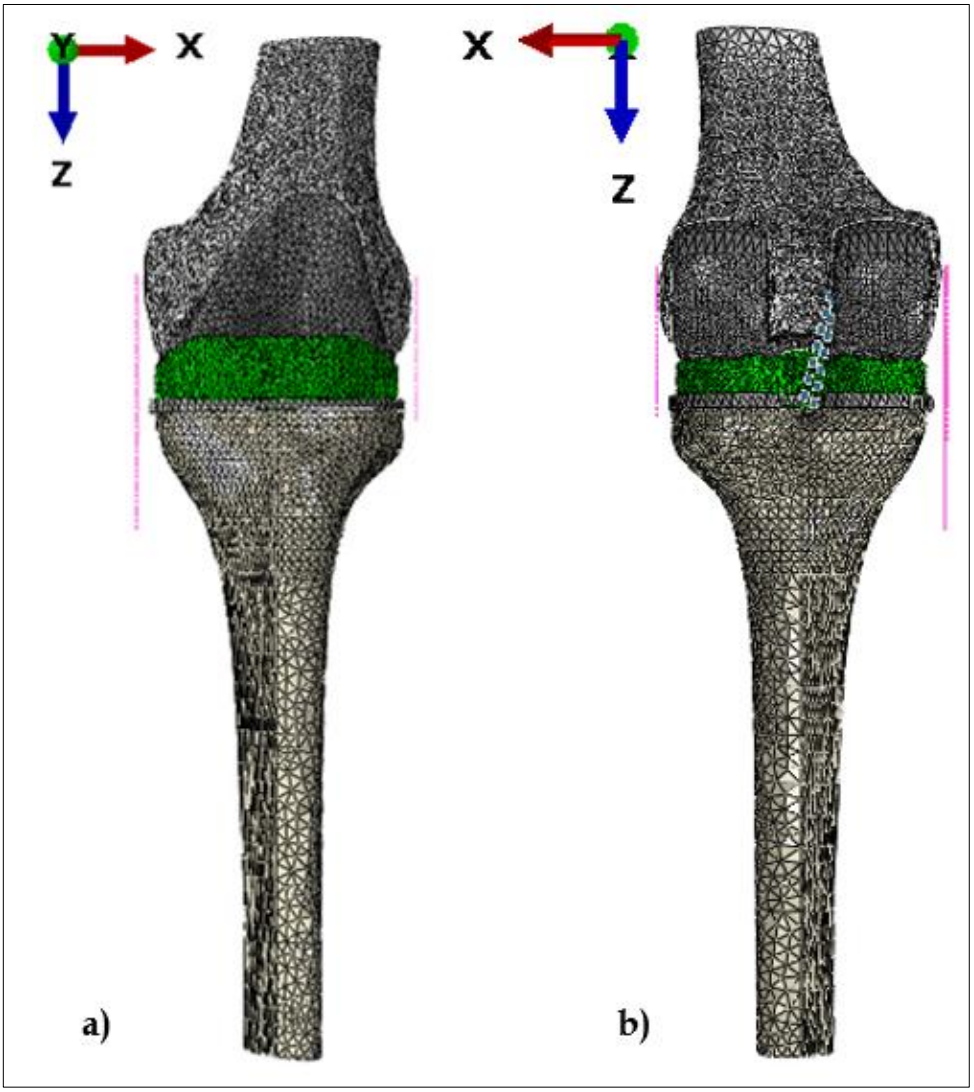

Figure 3.15. Mesh of a full knee for gait simulation: a) frontal view; b) posterior view.

For the squat models the mesh size of the femur and of the tibia have been increased with respect to the gait settings to speed-up the simulations (Figure 3.16); the femur mesh element size ranges between 5 and 30 (from proximal to distal part), while the tibia between 3.3 to 25 (from proximal to distal part).

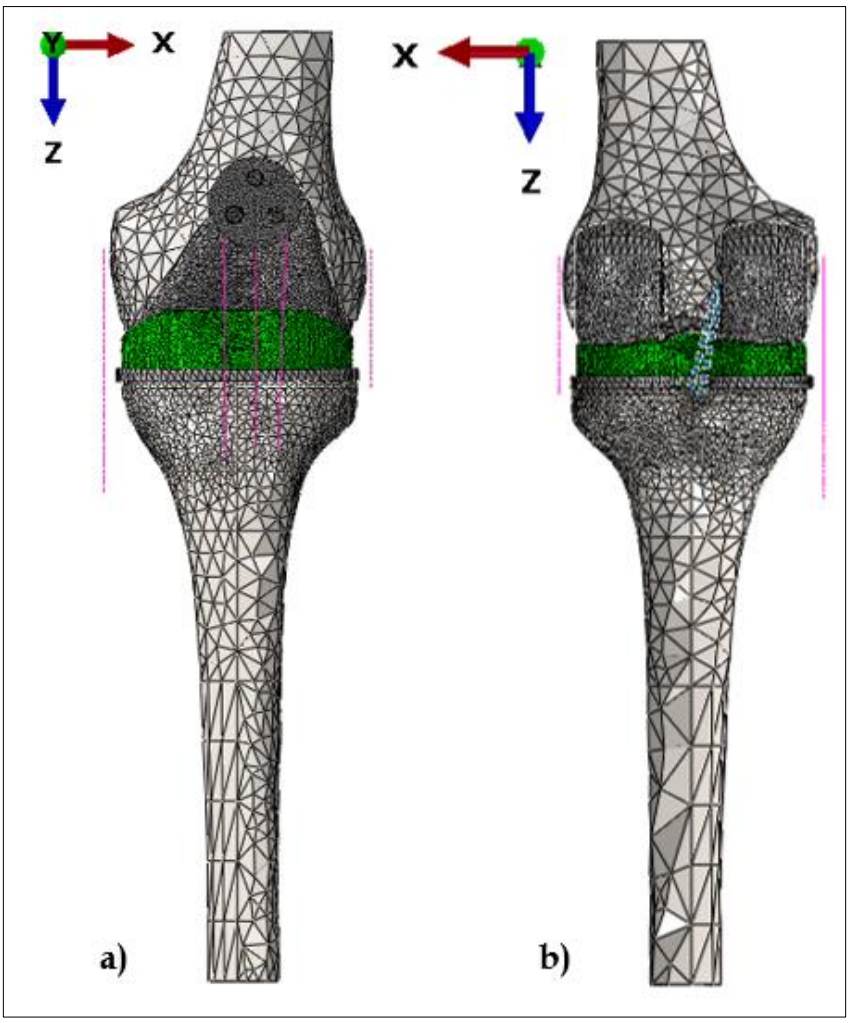

Figure 3.16. Mesh of a full knee for squat simulation: a) frontal view; b) posterior view.

3.8 Regions of interest and outputs

Four regions of interest (ROI) were defined to study the tibial bone stress (Figure 3.17):

- The medial and lateral proximal zones: two regions close to the tibial tray with a thickness of 5mm.
- The medial and lateral distal zones: two regions 30mm from the tibial cut surface with a thickness of 20mm.

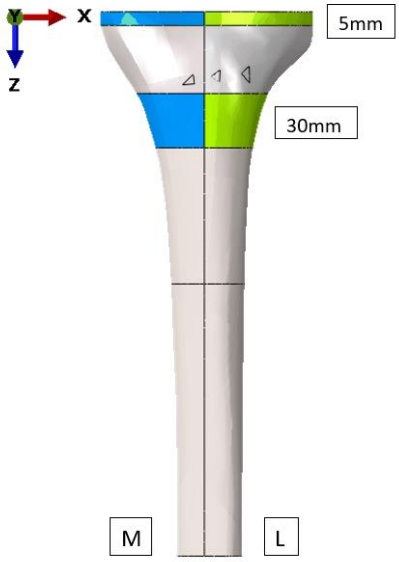

Figure 3.17. Proximal and distal tibial ROI.

Other ROIs have been attributed to the tibial inserts. Specifically, all the inserts have been divided into three parts: medial, lateral, and middle ones (Figure 3.18).

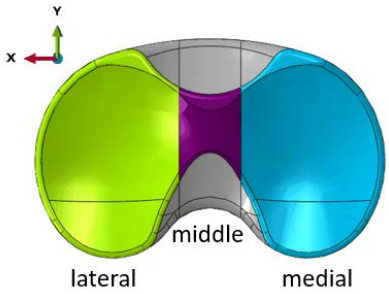

Figure 3.18. ROI on the insert.

About the evaluation of stress in the post-cam systems, from the CCK the medial, lateral, and posterior surfaces of the post have been considered (Figure 3.19), while from the FB PS just the posterior surface of the post. The patellar posterior surface is another ROI for deriving PF contact outcomes.

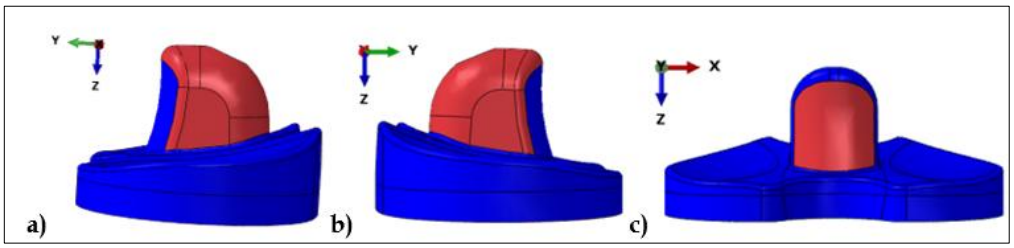

Figure 3.19. ROI on CCK post: a) medial, b) lateral and c) posterior surface.

The TF kinematics have been investigated in terms of femoral AP translation and IE angle, whereas the PF kinematics in terms of ML translation and angle around ML axis. The tibial insert IE rotation angles in MB CR and MB CR UC have been extracted and compared with the femoral IE angle. For all the models, the average von Mises stress in the cortical tibial bone has been investigated in all the proximal and distal ROI of the tibia.

Medial and lateral contact areas, contact forces, contact pressures, contact point and von Mises stresses have been extrapolated from the insert ROI, and they were then compared among the five models for the two simulated activities.

3.9 Dynamic Finite Element Analysis

Dynamic FEA has been performed on a total of ten models: five for the simulation of the gait cycle, five for the squat (one for each TKA design). Each model intended for the gait simulation contains the virtual geometry of femur, tibia, femoral component, tibial insert, tibial tray, and relative ligaments.

The models for the squat are equal to the gait ones, but with the addition of patellar component and patellar tendon, further including the quadriceps and MPFL contributions into the applied system of loads.

The PCL has been incorporated in the CR implants (FB CR, MB CR, MB CR UC).

ABAQUS/ Explicit version 2019 (Dassault Systèmes, Vélizy- Villacoublay, France) has been used to perform all the dynamic finite element simulations. The problem has been divided in two steps: the initial one in which all the initial conditions such as the boundary conditions have been included and the first step in which the loads, displacement and angle variations system have been considered.

The period has been set to 1.1 for gait and 10 for squat and automatic time incrementation has been chosen. Since Abaqus does not have a default system unit, the three chosen base units for length/mass/time are: [mm/t/s]. Thus, all the material properties, loads, displacements and angles have been defined using this system unit.

The mass scaling, that is used to scale the mass of the entire model at the beginning of each step, has been initially set to 10^{-3}, obtaining a relatively fast simulation and in order to check eventual convergence error; when the convergence has been fully reached, the outputs have then been checked.

Whether the trends presented several oscillations, the mass scaling was reduced, and the simulation run again. This process has been iterated for each model until the achievement of acceptable smooth curves and also affordable computational time. In some cases, such as the one depicted in Figure 3.20, the further reduction of mass scaling produced an increasement in the oscillations, therefore the previous choice has been kept for the data analysis.

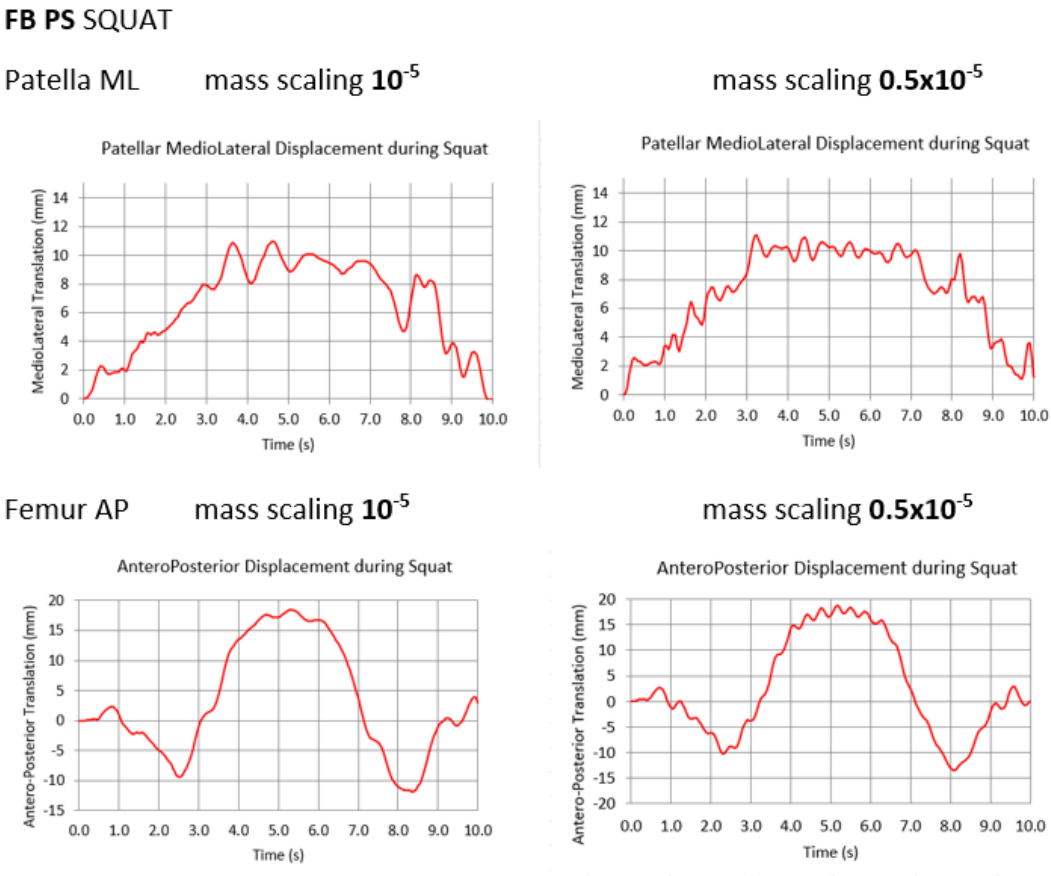

Figure 3.20. FB PS model outcomes during squat; the final choice for the mass scaling has been 10^{-5}.

In the Table 4 below, the chosen mass scaling for each model is reported. As it can be seen from the figure, the computational time increases with the reduction of the mass scaling value.

Table 4. Mass scaling values.

	PS	CCK	FB CR	MB CR	MB CR UC
Gait	10^{-6}	10^{-6}	10^{-6}	10^{-6}	10^{-6}
Squat	10^{-5}	10^{-6}	10^{-6}	10^{-6}	$0.5*10^{-5}$

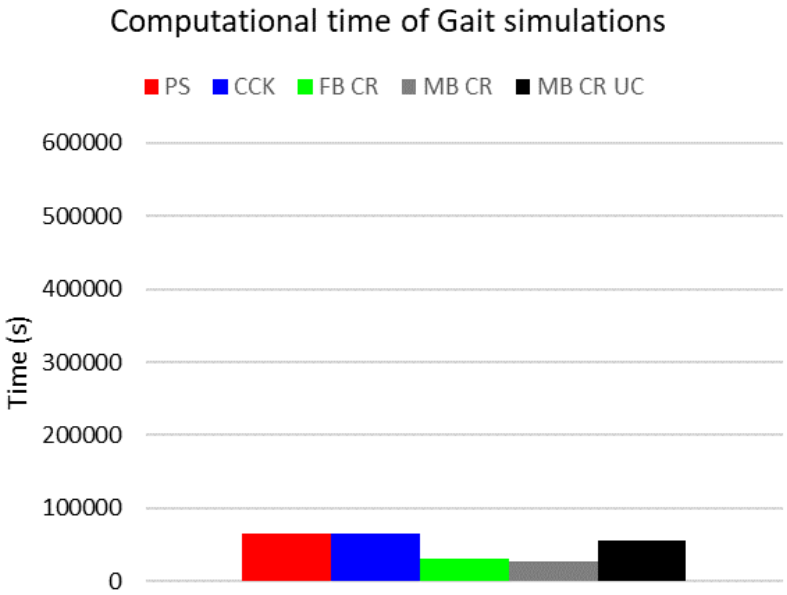

Figure 3.21. Computational time during Gait simulations

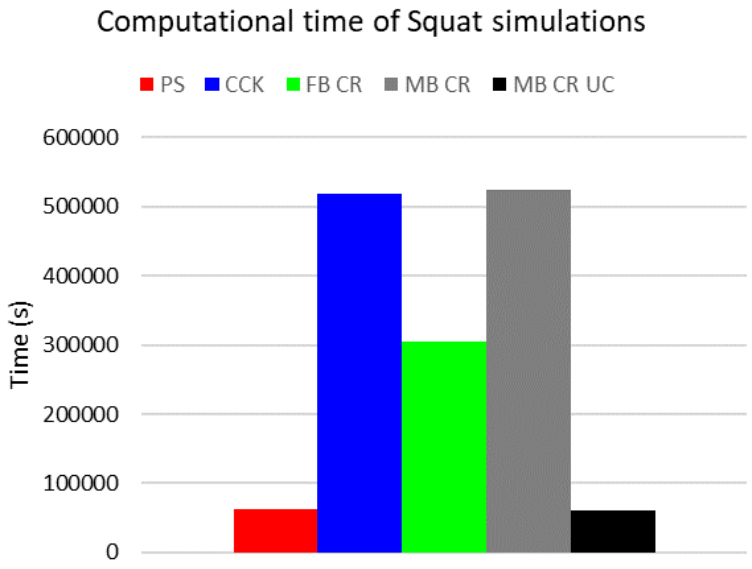

Figure 3.22. Computational time during Squat simulations.

4 Results and Discussion

The performance of TKA can be affected by implant design, other than alignment or patient-related anatomical factors. By considering the same manufacturer and equal boundary conditions, a FEA has been performed on five common implant designs during gait and squat simulations, in order to evaluate and compare the effects of different levels of constraint on knee biomechanics. For this perspective, the outcomes are accordingly discussed in terms of TF and PF kinematics and kinetics and of insert stress and tibial bone stress.

4.1 Gait simulation results

The outcomes of the gait cycle simulations are here reported and discussed. In some cases, apart from the graphs of the amplitudes that vary during the cycle, average or maximum values are collected in histograms and discriminated basing on the stance phase (from 0% to 70% of the cycle) and swing phase (from 70% to 100% of the cycle).

4.1.1 Antero-Posterior displacement of the femur

All the designs induce AP ranges that are acceptable for the physiological range of motion during gait being around 10-15mm (Figure 4.1, Figure 4.2). PS and CCK designs show similar trends of AP displacement, but CCK induces greater femur translations during both stance and swing phase, as we can also see from the range histogram. The higher posterior translation of PS and CCK could reflect the roll-back motion given by the post-cam mechanism [86]. FB CR and MB CR have similar trend; their ranges are almost one half of PS one and one third of CCK one.

These results indicate that in PS and CCK the resection of the PCL, which is noted to have a stabilizing function in terms of posterior translation, causes higher femur AP displacement [25], [1], and that CCK increases the sagittal femoral displacement as previously observed in literature [75]. MB CR UC, resulting in a smooth AP trend, limits almost completely femur AP displacement, thanks to the combination of the retention of the PCL and the inherent congruency of its design conformation that through a high anterior wall and a deep-dished plate guarantees a good stability during the walking cycle, without the guidance need of a post-cam system [15], [1]. Therefore, the PCL presence and increased conformity of the insert stabilize the femoral displacement.

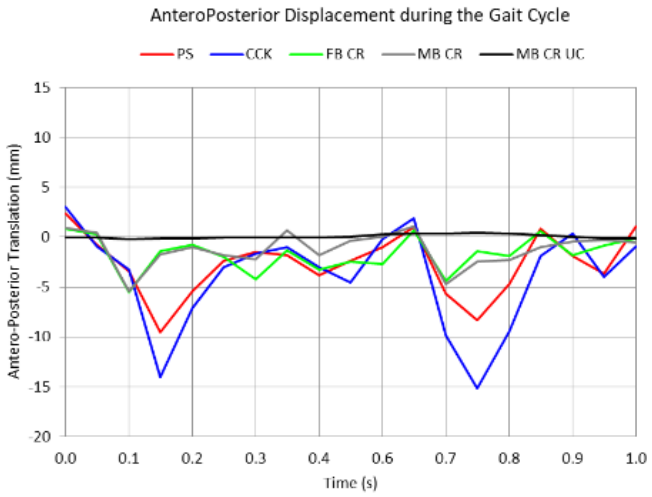

Figure 4.1. AP displacement of the femur during gait.

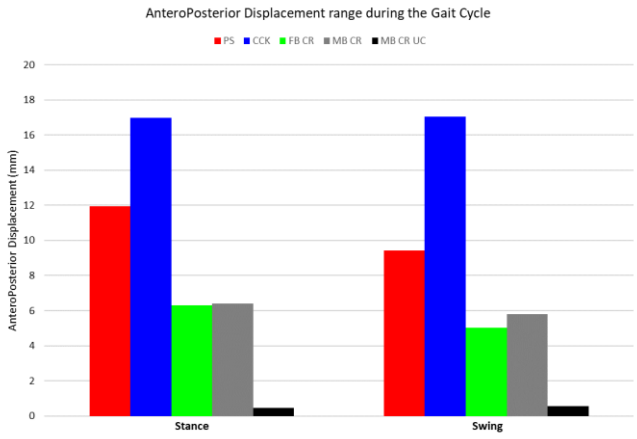

Figure 4.2. AP femoral displacement range during gait.

4.1.2 Internal-External rotation of the femur

The results of the five models show similar IE rotation ranges and patterns (Figure 4.3); the only difference is found in the swing phase in the FB CR where the femur internal rotation seems to be slightly limited.

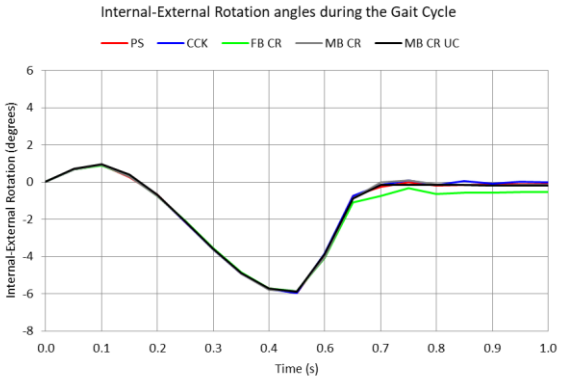

Figure 4.3. IE rotation angles of the femur during gait.

4.1.3 Internal-External rotation of Mobile Bearing inserts

The MB CR UC insert faithfully follows the IE rotation of the femur, in fact if we put them in the same graph they coincide. The MB CR insert instead seems to follow the femur IE rotation just for a while, then at the beginning of the swing (about 0.7s) there is an extra internal rotation of 5° followed by an external one to return to the initial position at the end of the cycle. This rise of the trend could be due to the lower congruency of the MB CR insert, which intrinsic mobility at the beginning of the swing would not allow to precisely follow the femur rotation.

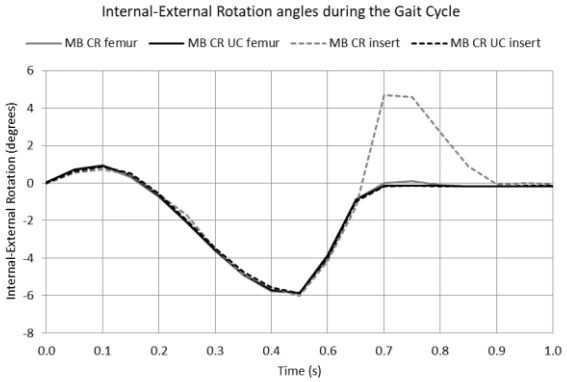

Figure 4.4. IE rotation angles of Mobile Bearing inserts (dashed lines) superimposed on femoral ones (solid lines) during gait.

4.1.4 Average von Mises Stress on the insert

4.1.4.1 Medial and Lateral surfaces

The stance phase is characterized by higher von Mises (VM) stress values if compared to the swing phase and greater values are then found on the medial (M) side of the insert rather than on the lateral (L) one for all the prostheses (Figure 4.5, Figure 4.6, Figure 4.7). PS and CCK have similar average values and reach the highest peaks during stance. MB CR UC has the highest average stress not only during stance but also during swing, phase in which in the other cases the stress decreases more.

MB TKA designs, with their increased implant conformity, theoretically were thought to offer the advantage of minimizing contact stress on the insert and therefore wear [53], but this is not observed here, as in previous research [20].

The MB CR with respect to its FB version shows similar VM stress pattern but slightly higher average, and it presents peaks of 0.87 MPa in the M side and 0.56 MPa in the L side at 0.7s that seem to be in correspondence of the extra internal rotation of the insert at the beginning of swing.

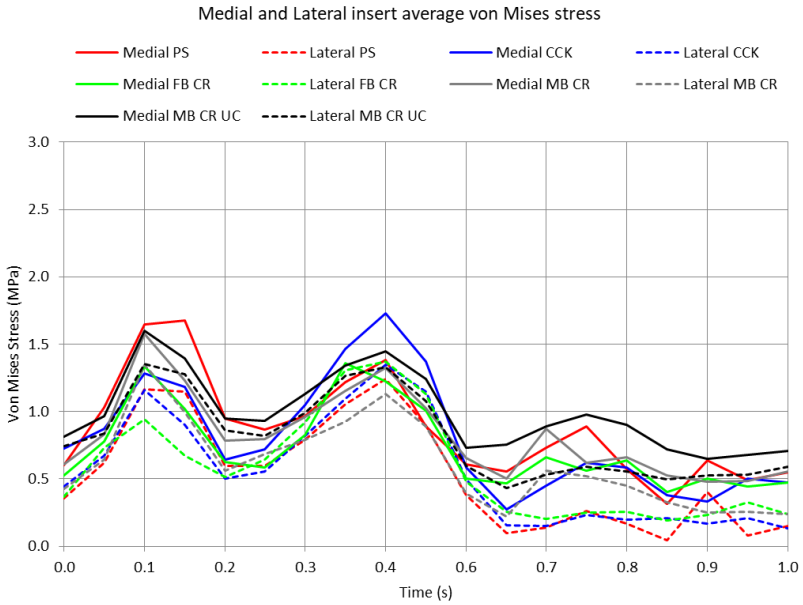

Figure 4.5. Medial and lateral insert average von Mises stress during gait.

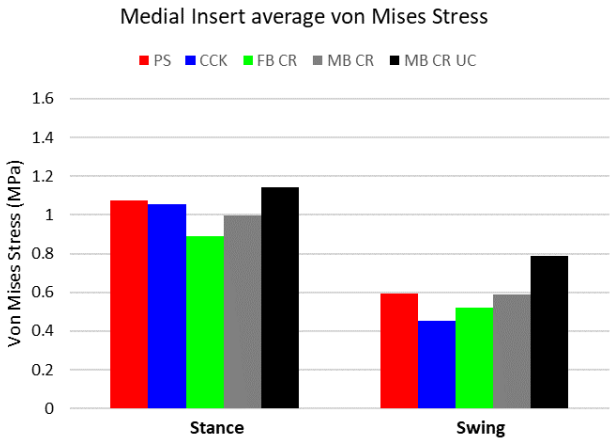

Figure 4.6. Average von Mises stress on the insert medial surface during gait.

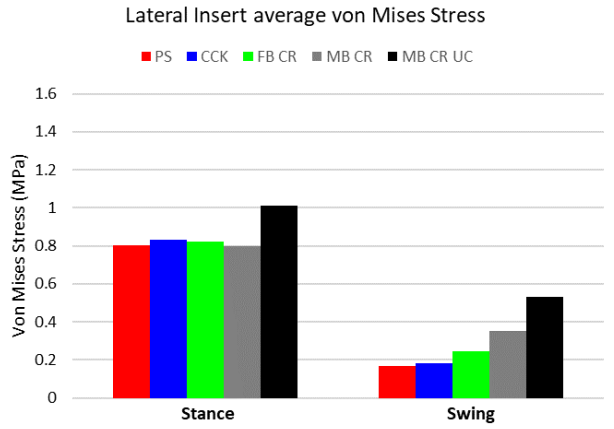

Figure 4.7. Average von Mises stress on the insert lateral surface during gait.

4.1.4.2 Middle surface

PS shows the lowest VM stress values along the cycle that are further reduced during swing. CCK exhibit instead a sudden high peak of 2.56MPa (even higher of the stress analysed in the M and L sides of the insert) during stance (between 0.4-0.5s), that could lead to post wear and lift-off. The two MB cases present higher average values both in stance and swing phase with respect to the other designs, almost doubling the FB CR stress values; in particular, the UC design exhibits the greatest average values.

The increase of congruency and mobility of the insert lead to higher values of stress in all the insert parts; the wider post of CCK induces abrupt peak of stress in the middle part of the insert (Figure 4.8, Figure 4.9).

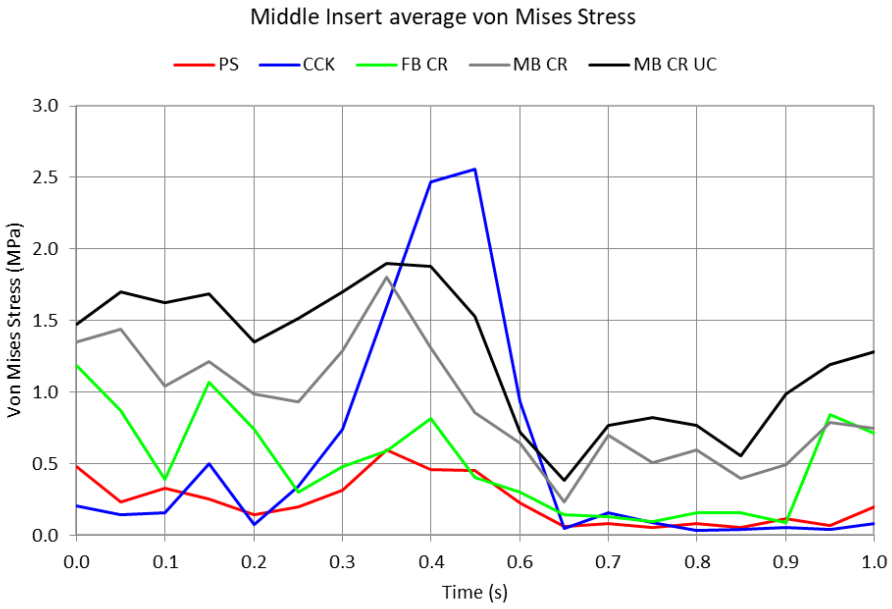

Figure 4.8. Average von Mises stress on insert middle surface during gait.

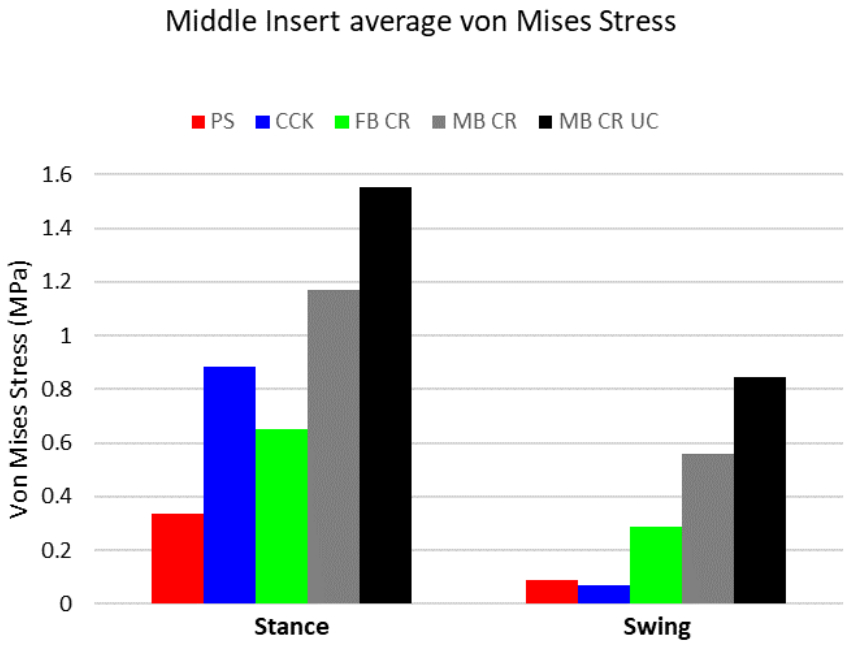

Figure 4.9. Average von Mises stress average on the insert middle surface during gait.

4.1.5 Average von Mises Stress on the tibial bone

4.1.5.1 Proximal region of 5mm

Similar trends for all the cases with higher values during stance and in M. About the CR designs, FB and MB CR present the highest peaks; at the beginning of stance in the M zone FB reaches 4.5MPa and MB 4.1MPa, while in the L zone they have almost the same peak values (respectively 3.95MPa and 3.9MPa) (Figure 4.10). However, during the rest of the walking MB seems to reduce the stress in both tibial distal zones. Instead, MB CR UC reduces the initial peak (in the M part 2.9MPa, in the L 2.8MPa) and then shows a similar behaviour to MB. FB CR has greatest average during stance both in M and L (average higher than 2MPa). PS and CCK shows almost the same trend and averages (Figure 4.11, Figure 4.12), but CCK exhibit slightly higher peaks (in M during stance CCK presents a peak higher thank PS peak of about 1 MPa).

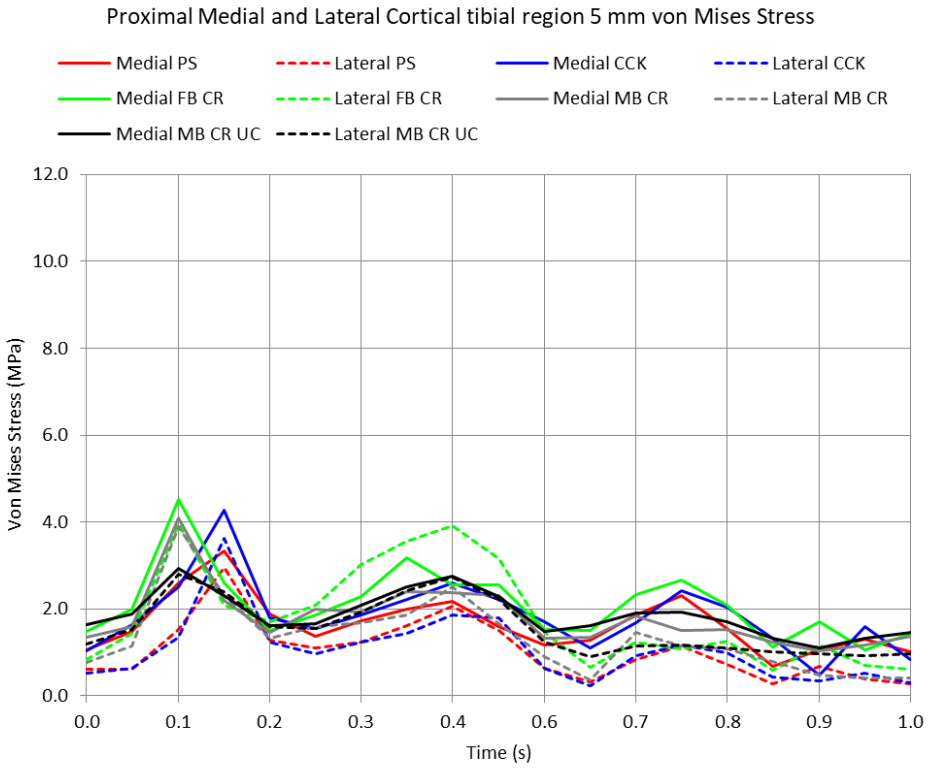

Figure 4.10. Average von Mises Stress on tibial proximal region during gait.

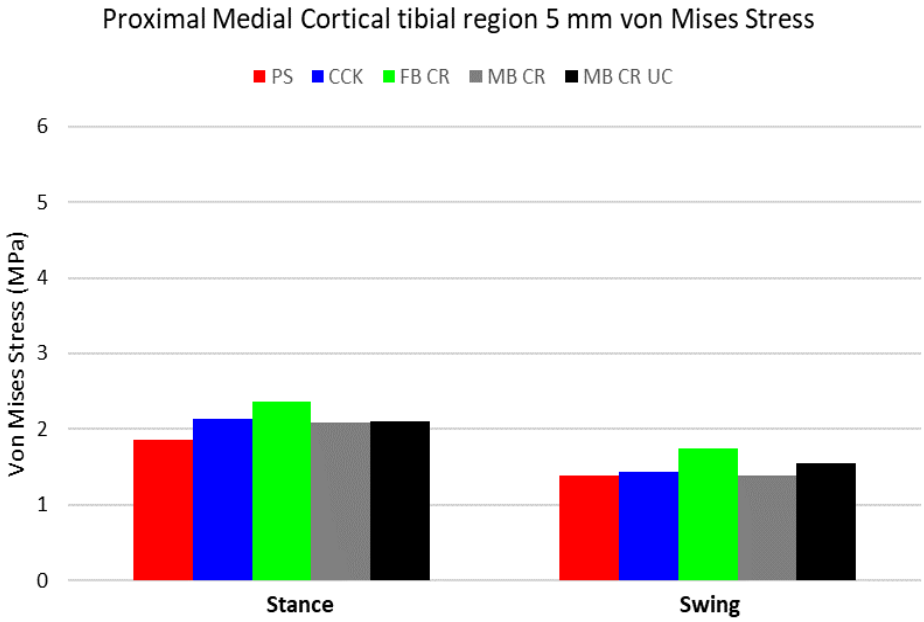

Figure 4.11. Average von Mises stress average of medial proximal tibial region during gait.

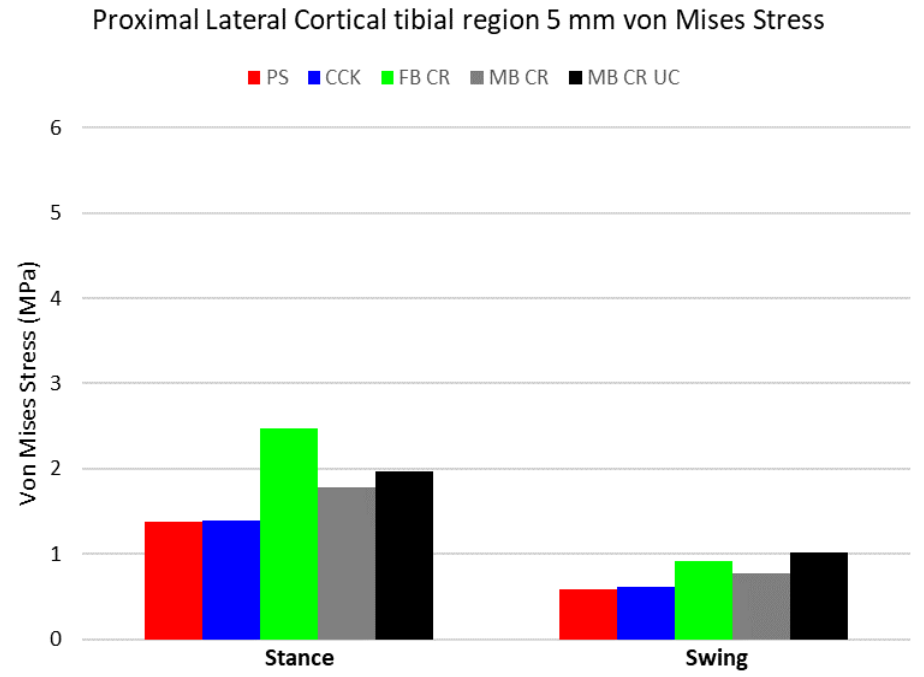

Figure 4.12. Average von Mises stress average of lateral proximal tibial region during gait.

4.1.5.2 Distal region of 30mm

Similar trends to the 5mm ones, but the values are almost the double. About the CR designs indeed, FB and MB present the highest peaks; at the beginning of stance in the M zone FB reaches 10.6MPa and MB 10.19MPa, while in the L zone the same peak values (respectively 8.8MPa and 8.7MPa). However, during the rest of the walking also in this ROI MB seems to reduce the stress in both tibial distal zones. Instead, MB CR UC reduces the initial peak (in the M part 6.36MPa, in the L 5.11MPa) and then shows a similar behaviour to MB (Figure 4.13), as in the 5mm ROI. FB CR has in general always the greatest average stress values among all designs also in the distal zones, while the MB and MB CR UC configuration, which are less constrained, in average lower the stress with respect to FB CR along the tibial bone. Then, PS and CCK show also here similar averages, slightly higher for CCK during stance (Figure 4.14, Figure 4.15), since it exhibits a peak at the beginning of the stance higher than PS (difference of about 1.7MPa in M and 1.2MPa in L).

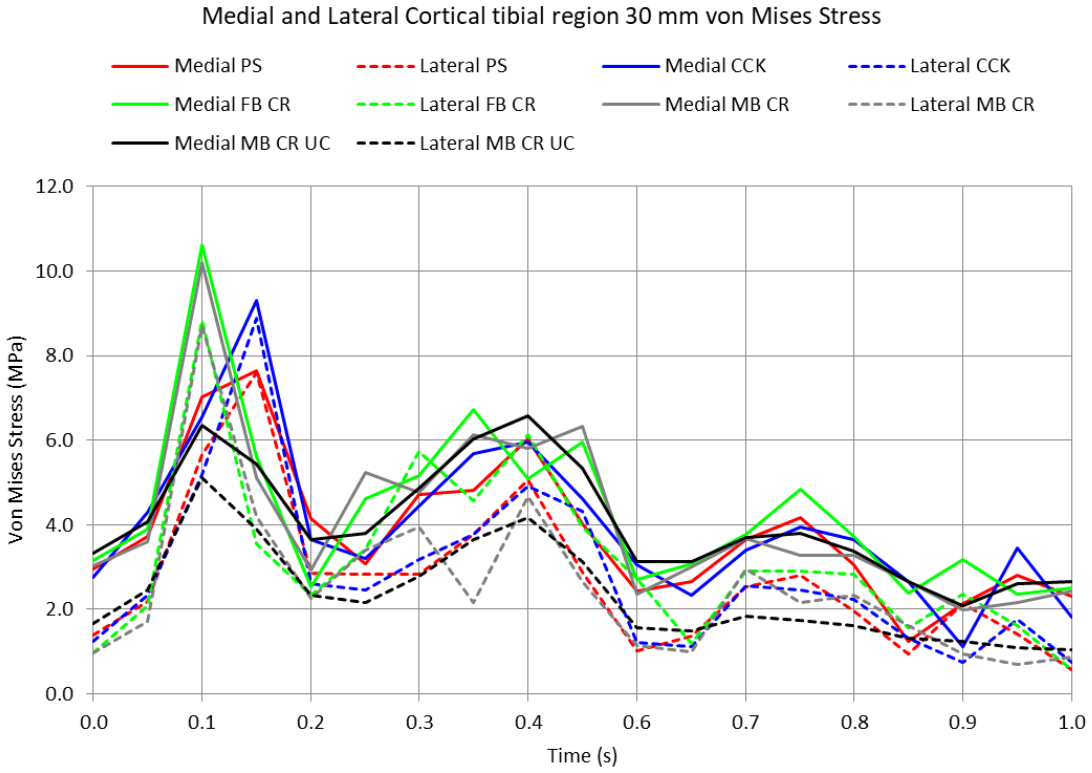

Figure 4.13. Average von Mises stress on tibial distal region during gait.

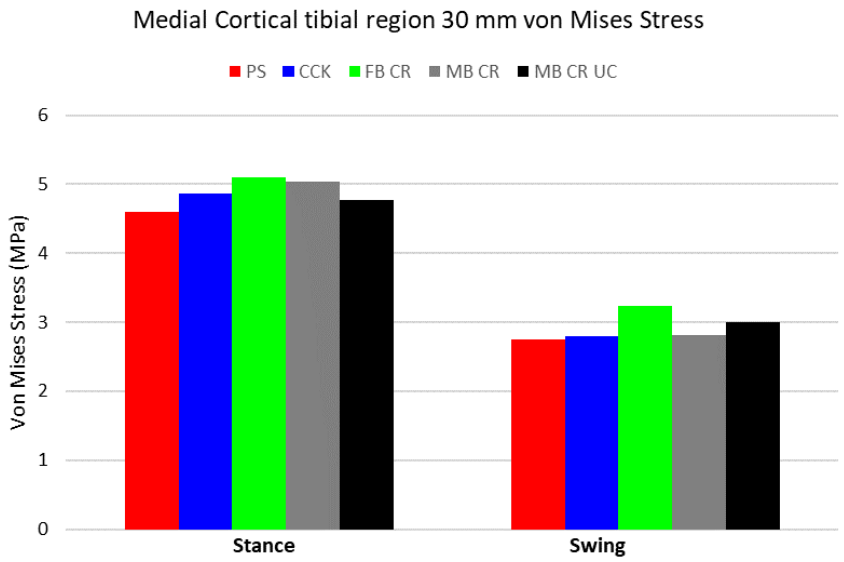

Figure 4.14. Average von Mises stress average of medial distal tibial region during gait.

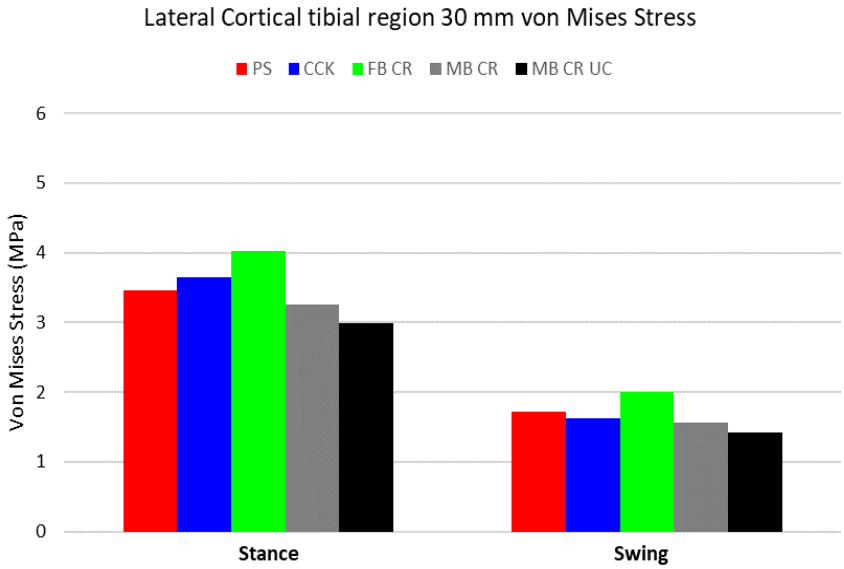

Figure 4.15. Average von Mises stress average of lateral distal tibial region during gait.

The distribution of the VM stress on the different zones of the tibia (proximal, distal) is relatively homogeneous between the models, apart from an initial rise of the stress at the beginning of the stance. This stress peak that rises at the beginning of the stance and that could aggravate OA patient's condition, seems to be related to the design differences. FB and MB CR show similar peaks, higher than the post-cam designs and UC.

Between the post-cam systems, CCK increases the stress value, as found in literature [75], [5].

In the CR, the mobility of MB insert is not able to decrease the peak induced by the FB CR, while the congruency of UC allows a drop, showing moreover the lowest peaks among all the designs. In the rest of the walking cycle, PS and CCK present almost the same behaviour, while among the CR, MB and UC slightly decrease the stress with respect to the FB in both considered tibial ROI [6].

FB CR has lower values of stress on the insert, but higher on tibia regions with respect to MB e UC which presenting more conformity are able to reduce the stress [92], [6].

4.1.6 Contact Area on the insert

4.1.6.1 Medial and Lateral surfaces

Contact area (CA) values higher in M than in L, in stance than in swing (Figure 4.16, Figure 4.17, Figure 4.18). MB CR UC has always the highest CA values, almost approaching 800mm^2 with averages always higher than 500mm^2. Indeed, the surface of the UC insert is designed to have a maximal contact between the femoral component and the insert, and its CA averages are twice as high as MB ones.

MB CR and FB CR trend are similar in the M side, while in the L side MB CR shows higher values than FB CR, thus it is more congruent thanks to the reduction in constraint [21], [53], [6]. The post-cam designs show the lower values of CA with respect to CR [76], [6]with CCK being the less compliant.

The most symmetric designs in terms of CA among M and L parts, seem to be MB CR UC and CCK; the FB CR shows very different higher values of CA in M part with respect to the L part, and this asymmetry seems to be recovered by the mobility of MB CR [76].

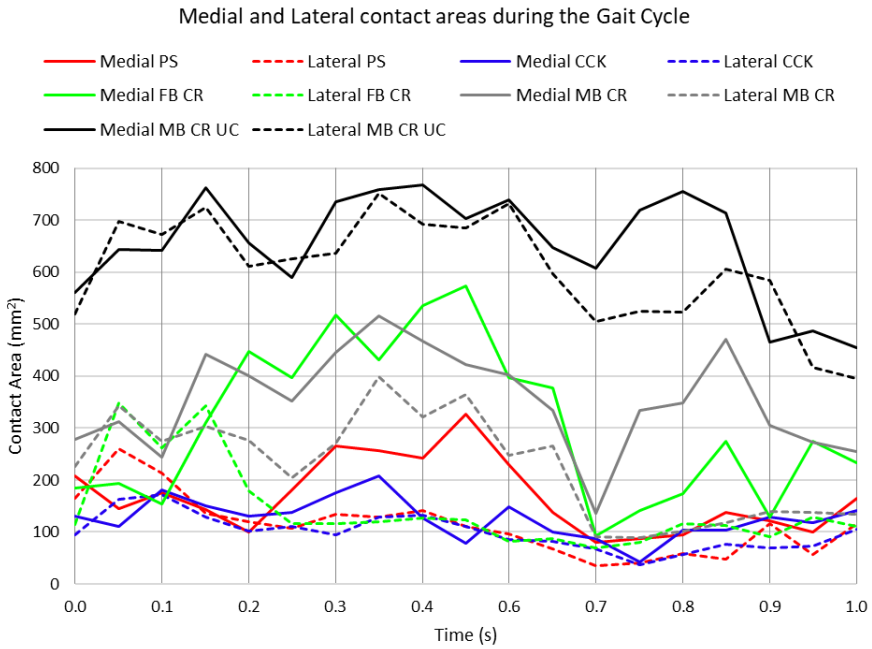

Figure 4.16. Medial and Lateral insert CA during gait.

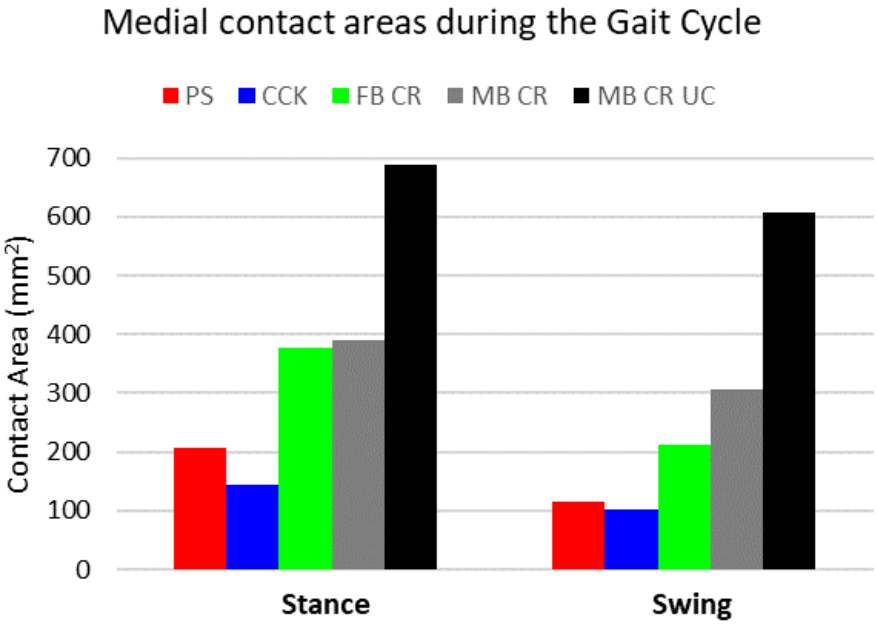

Figure 4.17. Medial insert CA average during gait.

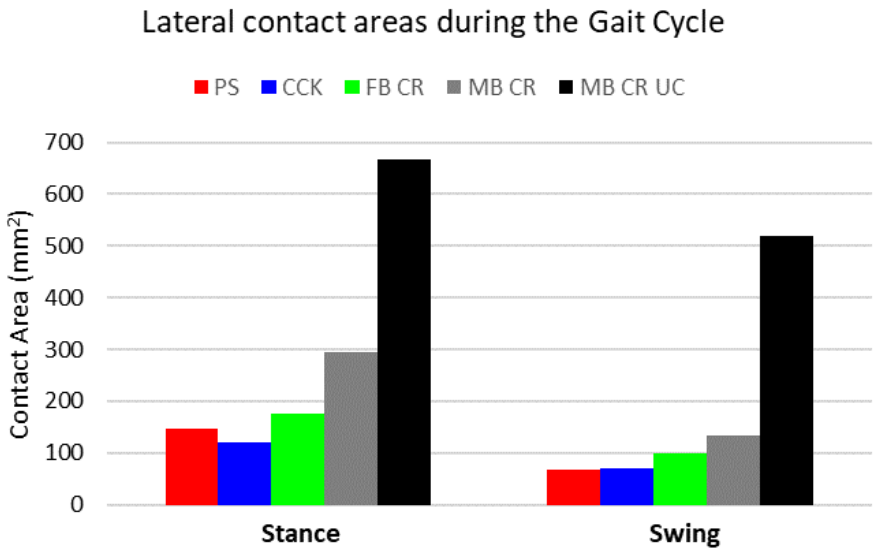

Figure 4.18. Lateral insert CA average during gait.

4.1.6.2 Middle surface

Just during stance there is contact of the middle part of the insert, but the CA values are always under 80mm2 (and vertical CF values under 800N), with higher values for MB CR UC, then MB CR and finally FB CR (Figure 4.19, Figure 4.20).

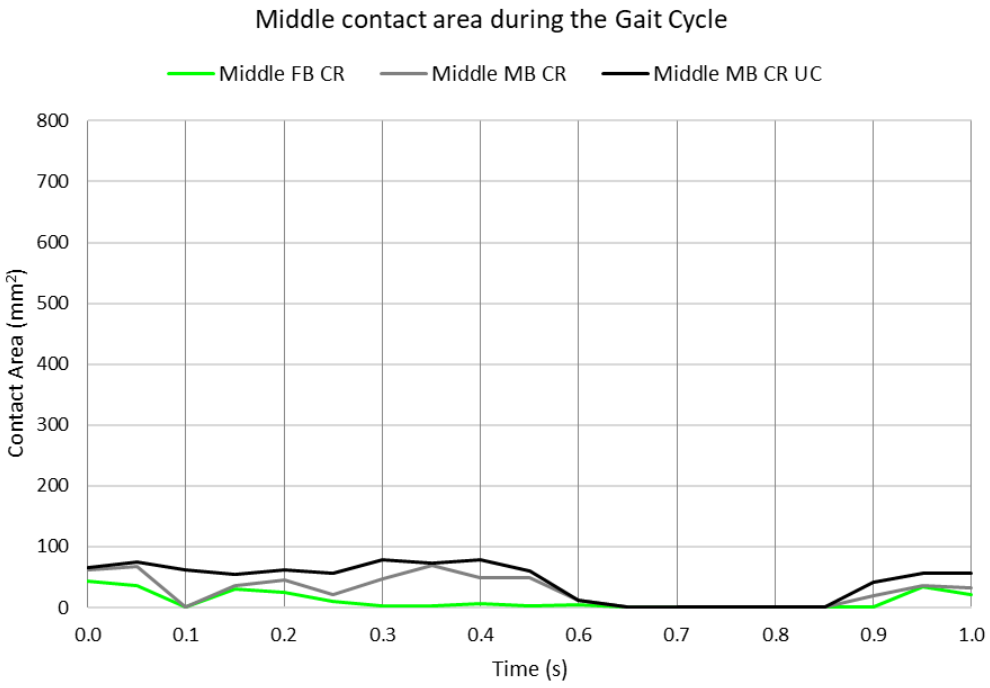

Figure 4.19. CA on the insert middle surface during gait.

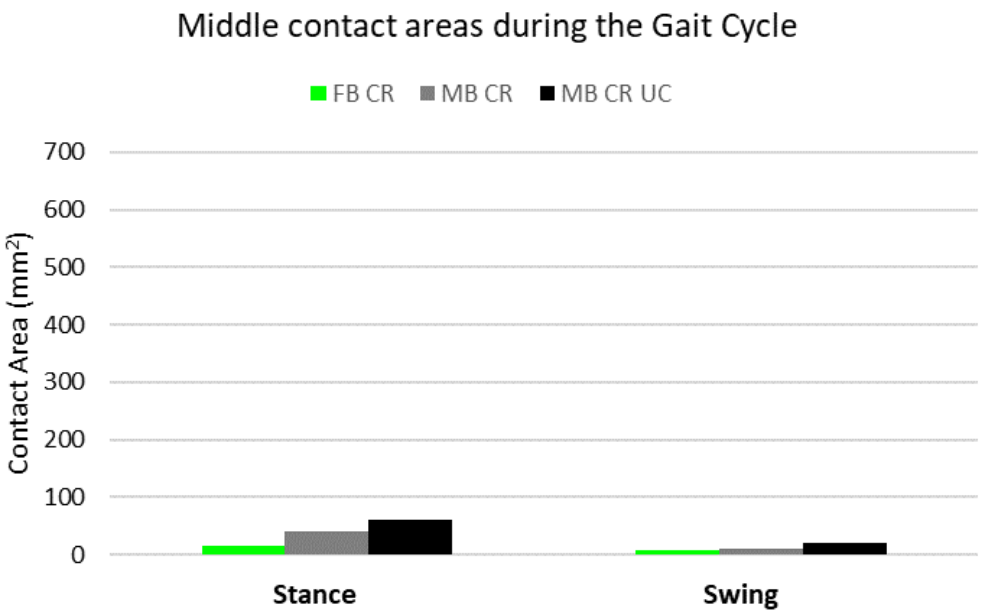

Figure 4.20. CA average on the insert middle surface during gait.

4.1.6.3 Post-cam surfaces

In PS the contact with the post-cam surfaces does not occur. In the CCK the M and L surfaces of the post-cam show similar values thus making the contact symmetric and more important at the end of the stance (Figure 4.21). The posterior surface presents a low CA at the end of the stance.

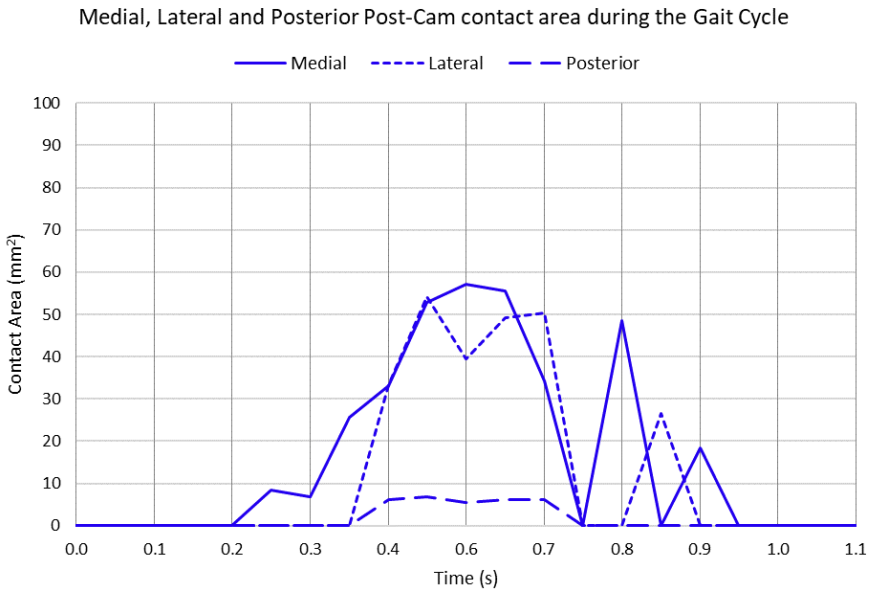

Figure 4.21. CA on CCK post-cam surfaces during gait.

4.1.7 Contact force on the insert

4.1.7.1 Medial and Lateral surfaces

Contact force (CF) trend along the vertical direction is similar between all models (Figure 4.22), being higher in M than in L, higher than 1000N during stance and lower than 1000N during swing. A difference can be found in MB CR UC which during swing decreases less with respect to the others, thus presenting higher average values of CF during all the cycle. FB CR has higher average values of force if compared to the MB CR (Figure 4.23, Figure 4.24).

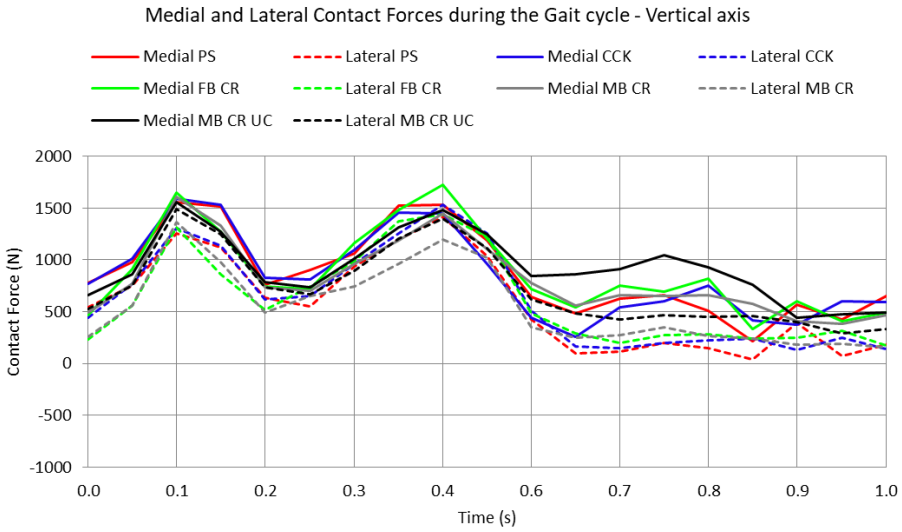

Figure 4.22. Contact force along the vertical axis on the insert during gait.

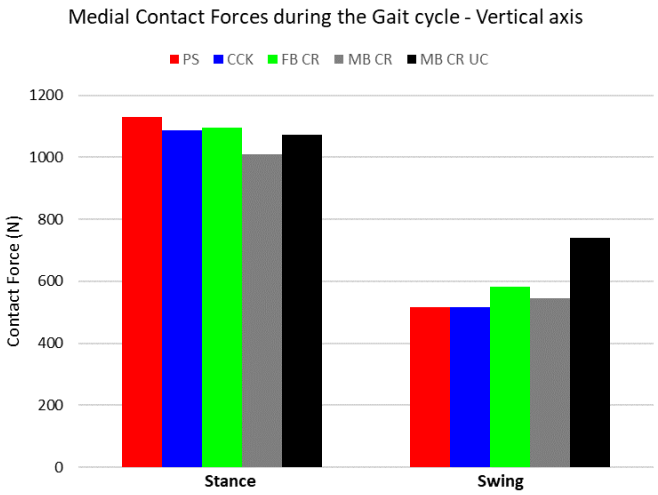

Figure 4.23. Average of Contact force along the vertical axis on the insert medial surface during gait

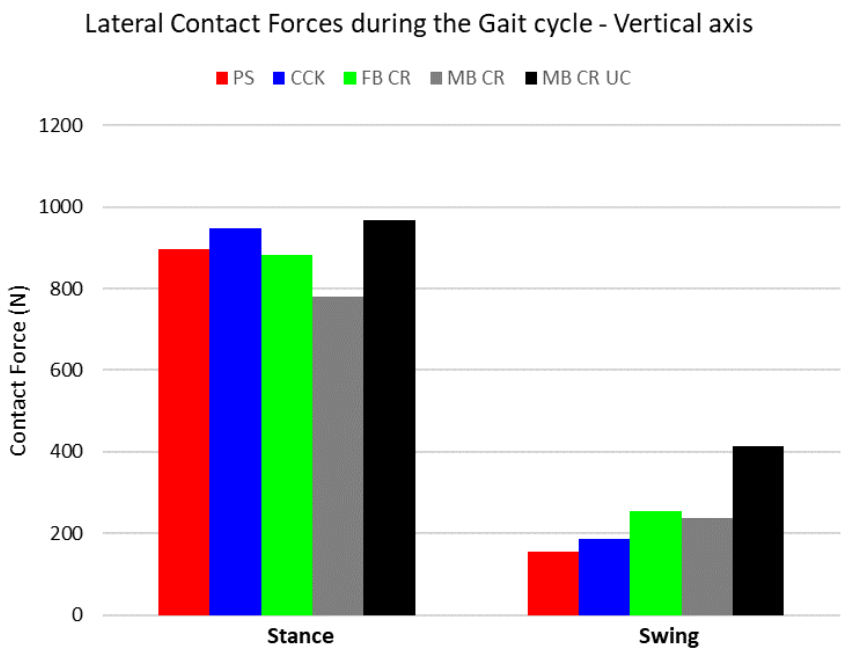

Figure 4.24. Average of Contact force along the vertical axis on the insert lateral surface during gait.

Values of CF along the sagittal direction are negligible with respect to the vertical one, but it can be noted in Figure 4.25 that the FB designs show a force peak towards the anterior direction during stance between 0.3-0.4s in M side (peak value higher than 500N for FB CR and lower than 300N for CCK and PS).

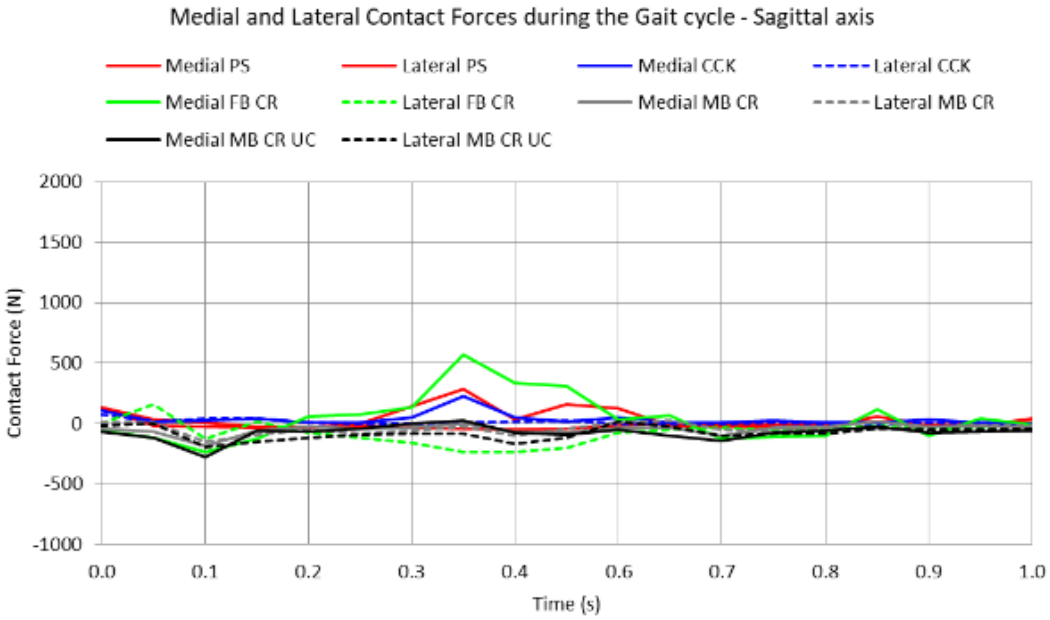

Figure 4.25. Contact force along the sagittal axis on the insert during gait.

Even CF values with respect to the horizontal axis (Figure 4.26, Figure 4.27), are negligible with respect to the vertical axis, but looking at MB CR in the L side in Figure 4.27, during stance exhibits force amplitudes directed towards the lateral direction with values around 300N. This laterally projecting force is not present in the FB prosthesis and could be due to the mobility of the insert, and in MB CR UC is restrained by the deep-dished shape. In the M side, FB CR and CCK show a peak around 0.4s.

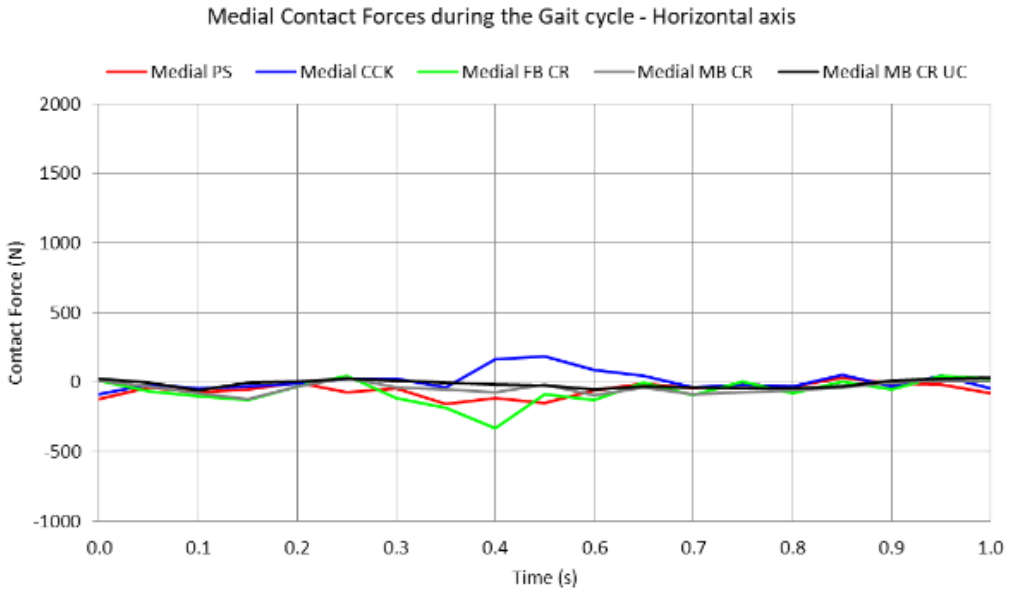

Figure 4.26. Contact force along the horizontal axis on the insert medial surface during gait.

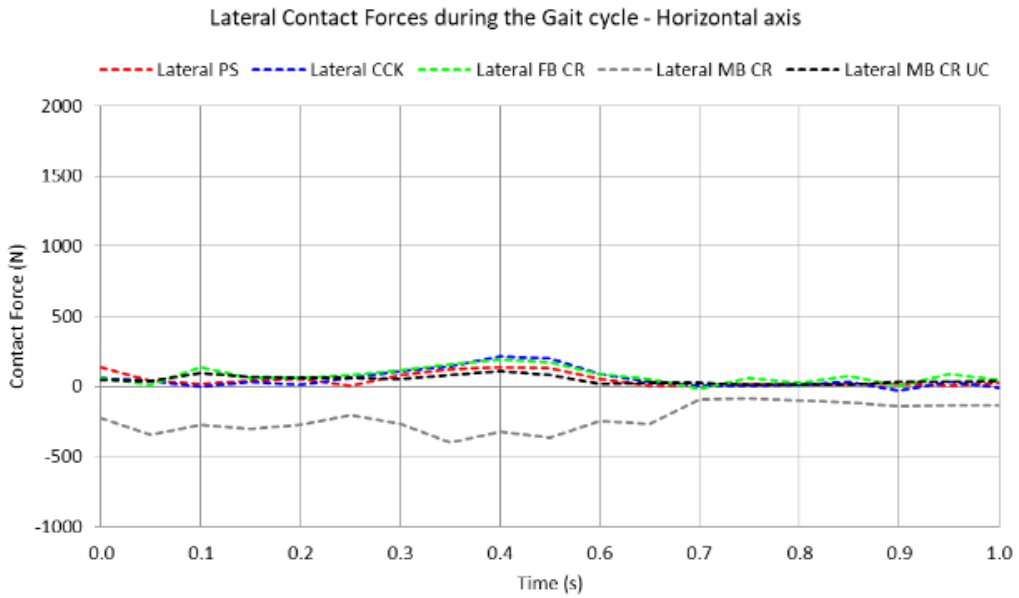

Figure 4.27. Contact force along the horizontal axis on the insert lateral surface during gait.

4.1.7.2 Post-cam surfaces

In the post-cam there are significant forces just in the horizontal direction in the M and L post-cam surfaces of the CCK design (Figure 4.28); in particular during stance, between 0.2-0.65s, there are force values pointing to the lateral direction in M side (peak value around 900N) and to the medial direction in L side (peak value around 600N), thus compressing the post.

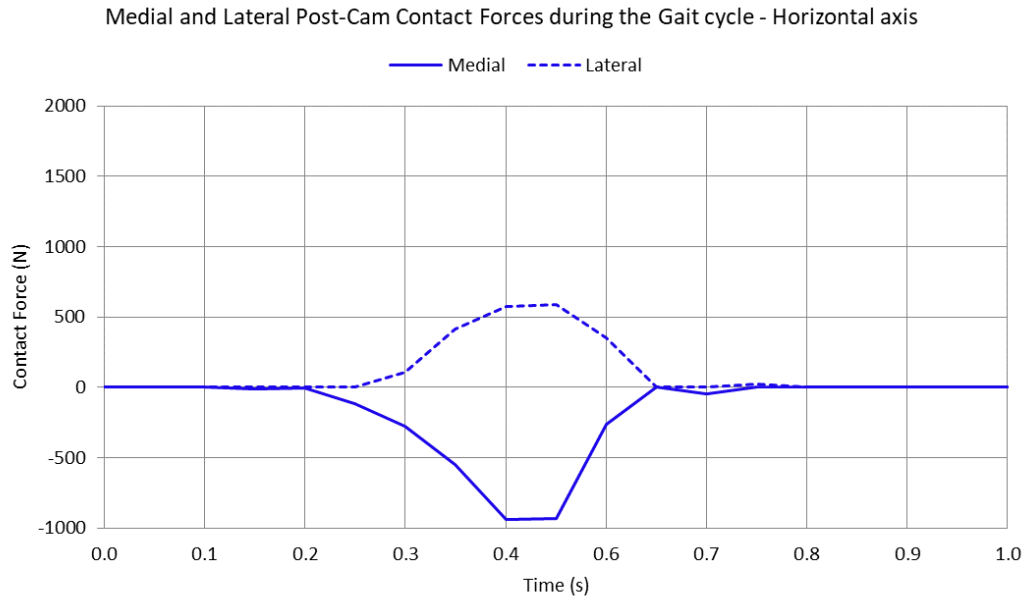

Figure 4.28. Contact force along the horizontal axis on CCK post-cam surfaces during gait.

4.1.8 Contact Pressure on the insert

4.1.8.1 Medial and Lateral parts

The trends of contact pressure on the insert are symmetrical among the models with higher values during stance and in the M part, as it can be seen in Figure 4.29. Even among M and L parts of each insert there is a symmetry in the trends, except to MB CR UC which presents lower values of pressure in the L side of the insert with respect to its M side along all the cycle. Thus, the congruency could determine a reduction of pressure in the L side, while in the M side during swing it has higher pressure with respect to all the other designs.

Both MB designs smooth the peak pressure values with respect to FB CR around 0.4s, where an increase in all pressure designs can be noted. PS model induces the highest-pressure peak in the M at the beginning of the stance, of more than 1MPa, increasing the risk of wear and implant failure.

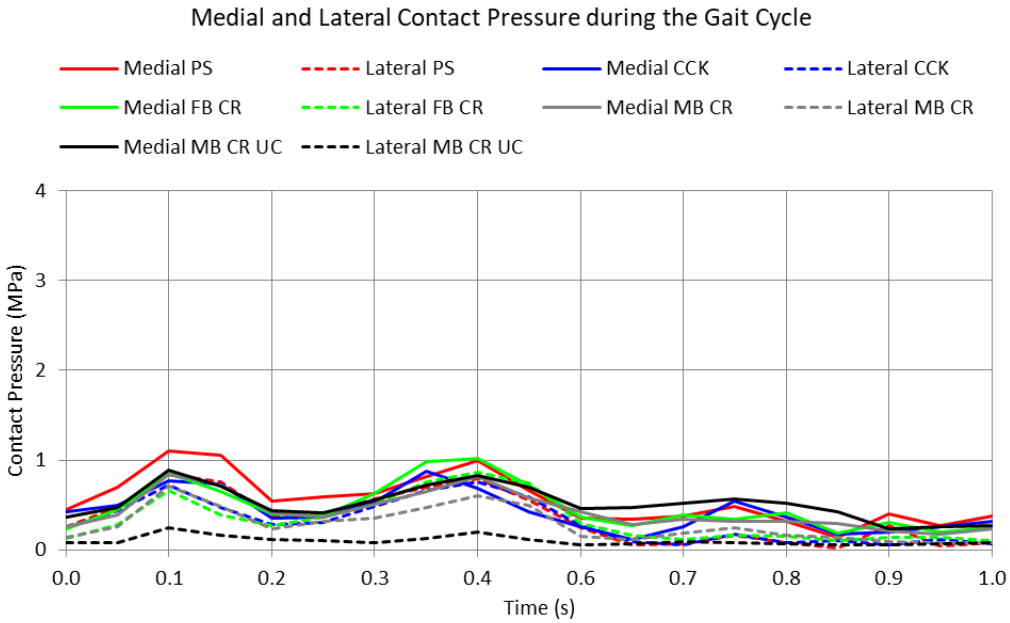

Figure 4.29. Contact pressure on the insert during gait.

4.1.8.2 Middle part

PS has almost no contact pressure in the middle part of the insert. The other models show contact pressure in the middle part just during the stance and at the end of the swing (Figure 4.30). In ascending order, from the lowest pressure values of PS (pressure close to null), then CCK (slight peak at 0.4s), FB CR, MB CR, to the highest values of MB CR UC. The ratio between FB CR, MB CR and MB CR UC pressure averages is about 1:2:3 during stance (Figure 4.31). Thus, the rotation freedom and the conformity of the insert can induce higher contact between femoral component and middle part of the insert, that in all the FB designs and in particular in presence of the post-cam systems, seems to be avoided.

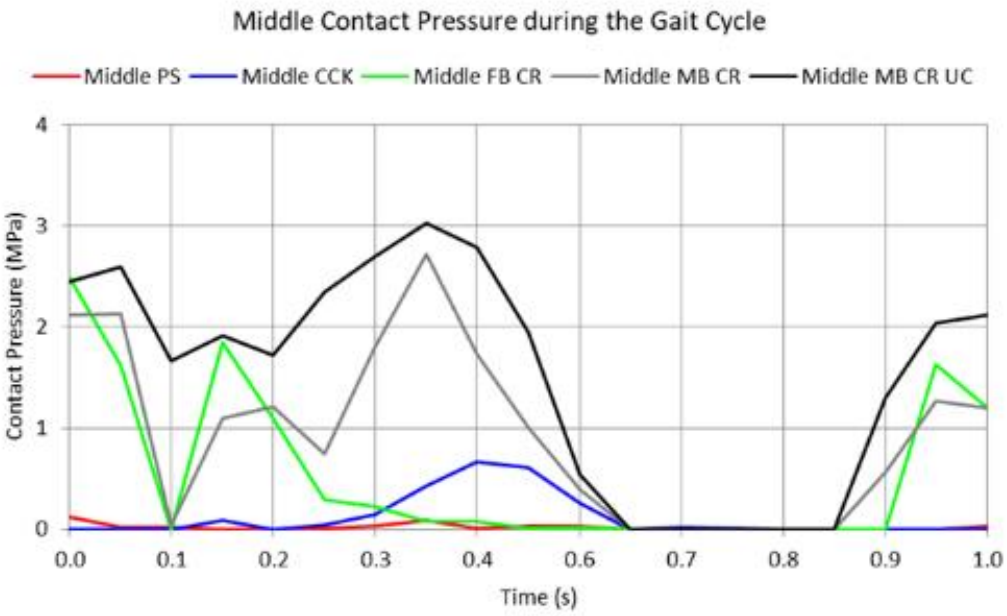

Figure 4.30. Contact pressure on the insert middle part during gait.

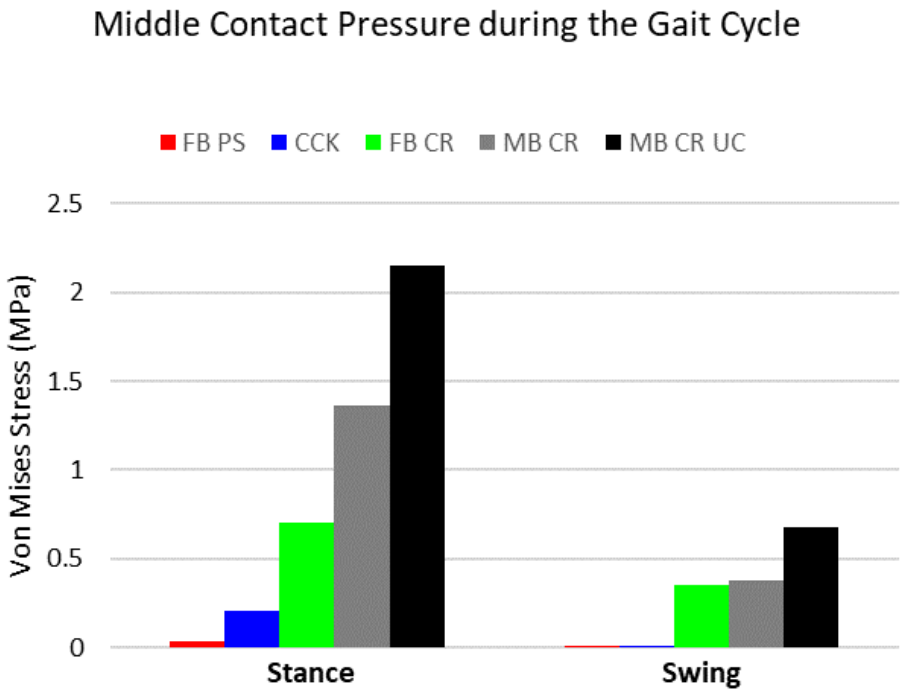

Figure 4.31. Contact pressure average on the insert middle part during gait.

4.1.8.3 Post-cam surfaces

CCK contact pressure displays a peak at 0.6s during stance in M (1.6MPa) and L (1.1MPa) of the post-cam, while is always null in the PS surface of post-cam. Contact pressure average on the insert middle part during gait.

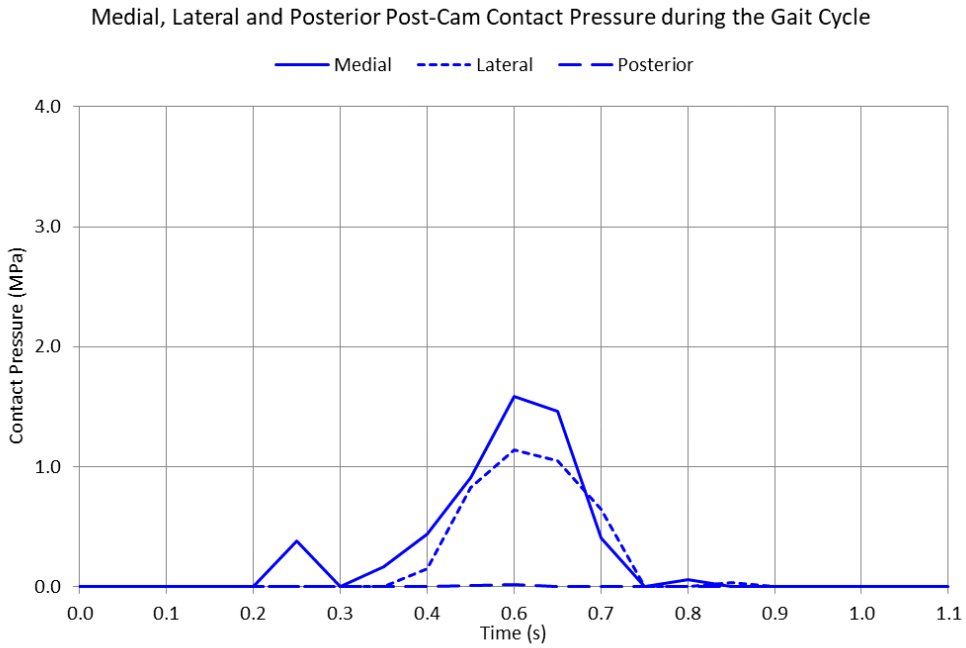

Figure 4.32. Contact pressure on CCK post-cam surfaces during gait.

PS and CCK presents high average CF values during stance but, differently from the CR designs and especially from the UC, these magnitudes are not compensated with larger CA, resulting in a narrower force distribution, hence they could induce high contact pressure and implant failure. This factor in fact represents one of the main causes of wear and stands as an important point in the kinetic comparison [5][21], [86]. From the results on M and L parts of the insert, PS has the major pressure peak among all, and in general FB designs have higher values than the MB ones. The lower pressure found in MB CR UC combined with the larger areas indicate a decreased risk of wear of the insert [76]. A criticism could emerge in the CR designs, from the fact that in the middle part the pressure values are high (even higher than in the M and L side), with small CAs.

4.1.9 Contact point displacement on the insert

PS and CCK contact point between femoral component and tibial insert show similar AP displacement trend on M and L insert surfaces, guiding the posterior roll-back (symmetry seen in both M and L sides) for which they have been conceived [93]. In addition, they have the widest ranges of motion than the rest of the implants, with an overall displacement range of 20mm anteriorly and posteriorly.

For all the designs, the contact point of the L part stays more in a still position during stance while the contact point of the M goes anteriorly (Figure 4.33). FB CR has similar sagittal displacement trend of the previous two but slightly limited and with a more stable L contact point.

MB prostheses, especially the UC one, significantly reduce the displacement of the contact point on the insert, almost halving the FB range values (Figure 4.34).

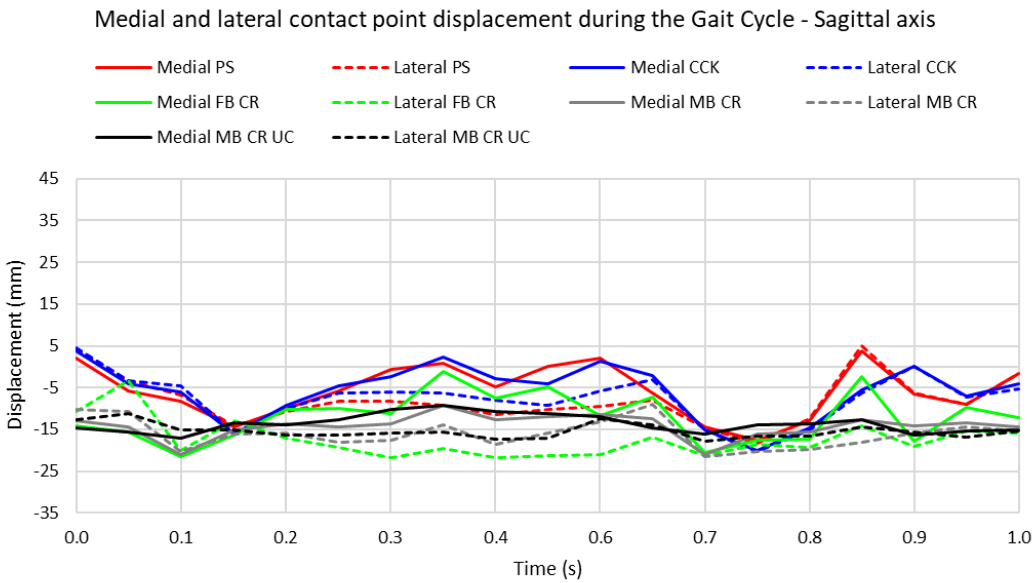

Figure 4.33. Contact point displacement along the sagittal axis on the insert surfaces during gait.

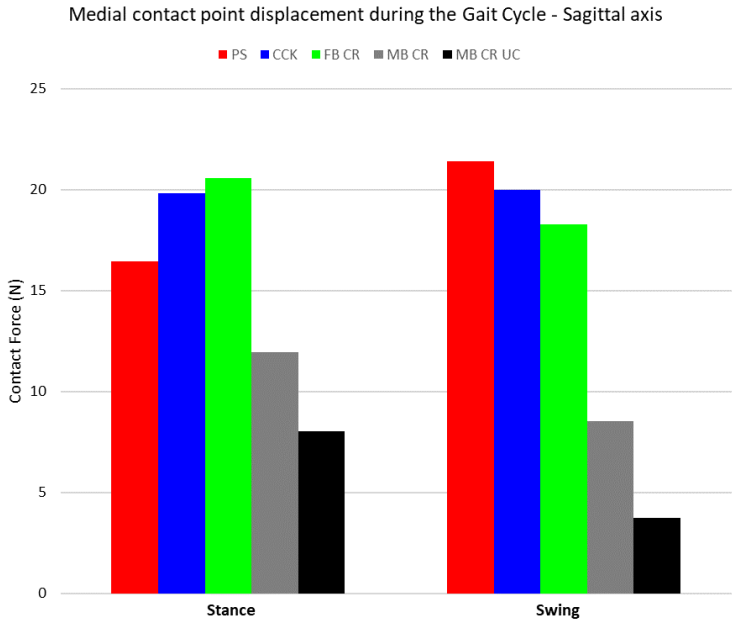

Figure 4.34. Contact point sagittal displacement range on the insert surfaces during gait.

Little oscillations (range from 5 to 13mm) in ML direction are detected for all the prostheses, with lower range for MB with respect to FB designs. In particular, the MB CR UC significantly lessen these fluctuations resulting in smoother trend along the entire cycle (Figure 4.35).

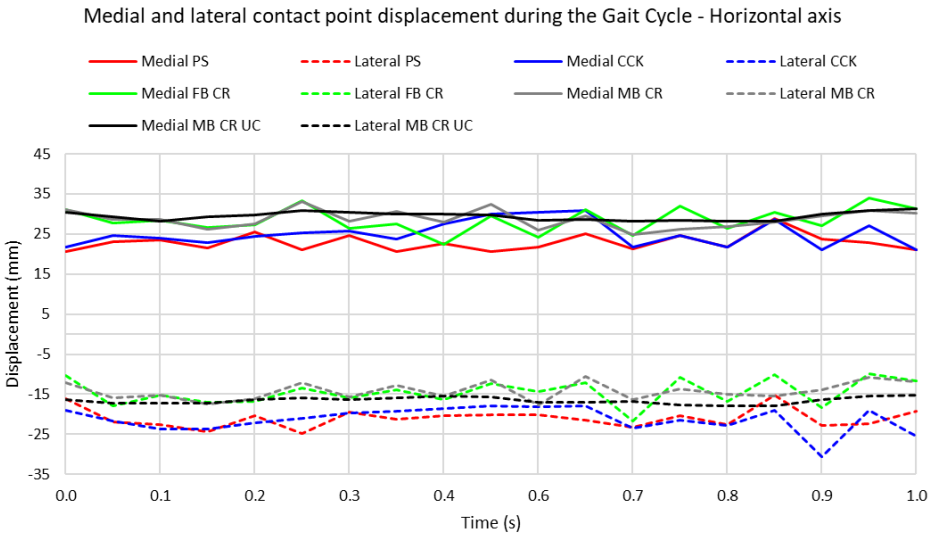

Figure 4.35. Contact point displacement along horizontal axis on the insert surfaces during gait.

4.2 Squat simulation results

The outcomes of the squat simulations are here reported and discussed. The graphs of the amplitudes that vary during the squatting activity and the average or maximum values histograms are displayed just for the initial part of the squat that is the flexion phase, since the relative symmetric trend of the extension phase.

4.2.1 Antero-Posterior displacement of the femur

AP displacement of all the TKA designs models returned to be similar to other prosthesis designs, with an initial anterior translation followed by a posterior displacement at increased flexion angles (Figure 4.36) that is in agreement with what reported in literature, reflecting the physiological behaviour of the roll-back [86], [58], [94], [28], [21], [74], [95]. The anterior sliding of the femur during flexion is called paradoxical motion since it is not present in the physiological knee [21], [96], [97], and it is related to the cruciate ligaments' resection. In particular in the PS and CCK, with the removal of both cruciate ligaments, the paradoxical motion is higher than in the CR implants, where PCL presence slightly limits this anterior displacement tendency.

PS and CCK designs show the same trend and range of AP displacement (a little higher for CCK [75]), spanning around 25mm and starting to go posteriorly in correspondence of the engagement angle (60°), where the post engages with the cam limiting the paradoxical motion and inducing a forced posterior roll-back [93]. FB CR and MB CR have almost equal trends and a range around 16mm (Figure 4.37) [21].

As it is observed in the gait, these results indicate that in PS and CCK the resection of the PCL causes higher femur anterior displacement [25], [1], but the post-cam mechanism is able to guarantee the roll-back, that is of eminent importance to provide enough space to allow deep knee flexion without posterior bone-implant impingement [19].

As in the gait, MB CR UC, with its lower AP range of around 5mm, limits femur AP displacement, thanks to the combination of the retention of the PCL and the inherent congruency of its design conformation [15], [1]. Furthermore, since UC does not exhibit paradoxical motion, it would not push the patella forward when implanted, thus avoiding the anterior knee pain.

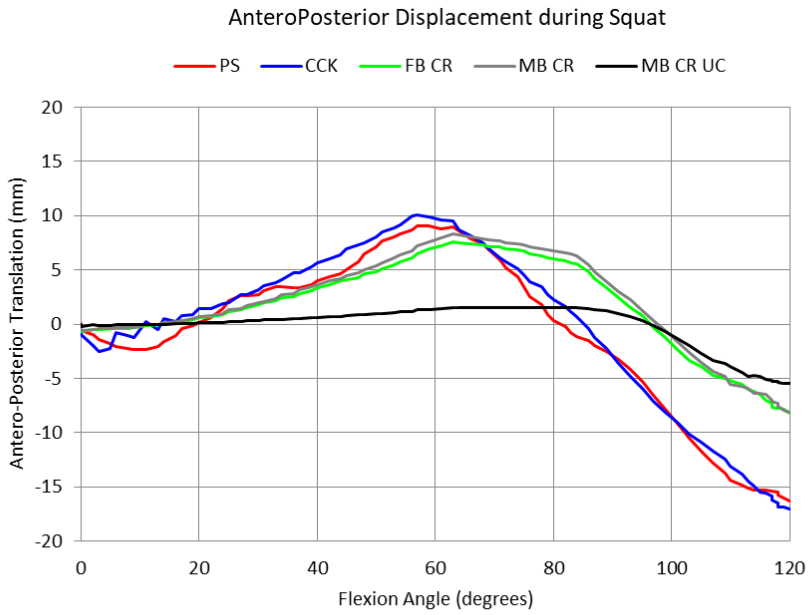

Figure 4.36 AP displacement of the femur during squat.

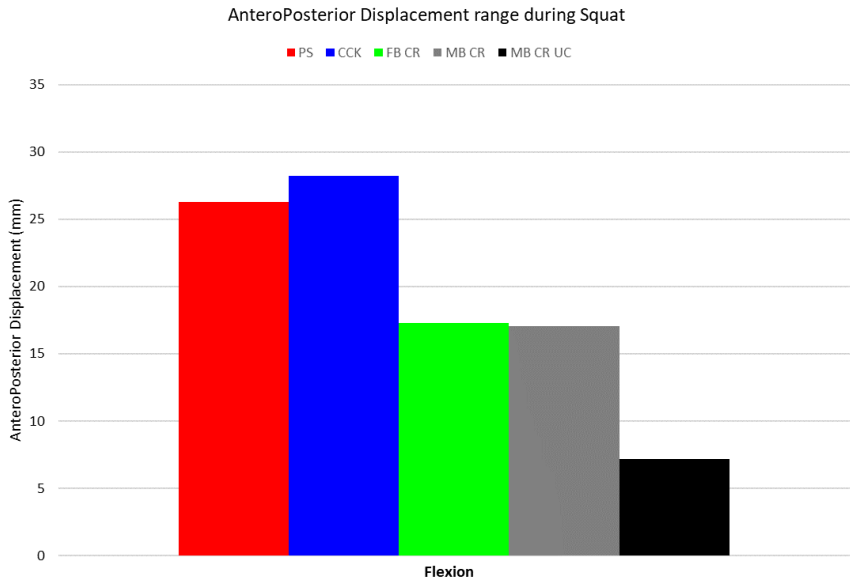

Figure 4.37. AP displacement range of the femur during squat.

4.2.2 Internal-External rotation of the femur

Starting from about 60° PS and CCK induce an external rotation (of 2° and less than 1° respectively), followed by internal rotation (of 3° and 1.5°) and at the end of flexion the femur results to be internally rotated of 1° for both models (Figure 4.38). This behaviour is found also in literature for other posterior-stabilized prostheses [86], [93], [28], [74].

CCK limits IE angles with respect to PS because of the geometry of the increased post with less rounded edges [5], [75]. The FB CR design is stable at low angles than from 60° it starts to have internal rotation that is more significant from 80° on and putting the femur in an internal rotation of more than 4° at maximum flexion.

The MB models present a slight external rotation then they rotate internally the femur from 80° of flexion. CR designs show an IE rotation closer to the physiological knee [97], [10] and the two MB reduce the range of angles with respect to FB CR which show the highest one (Figure 4.39).

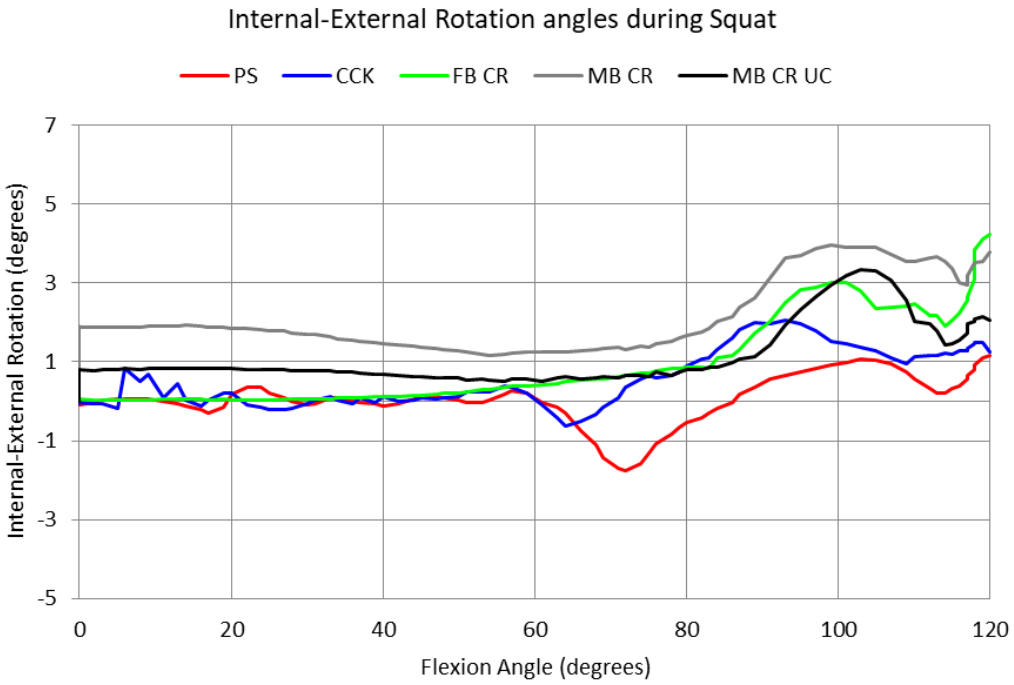

Figure 4.38. IE rotation angles of the femur during squat.

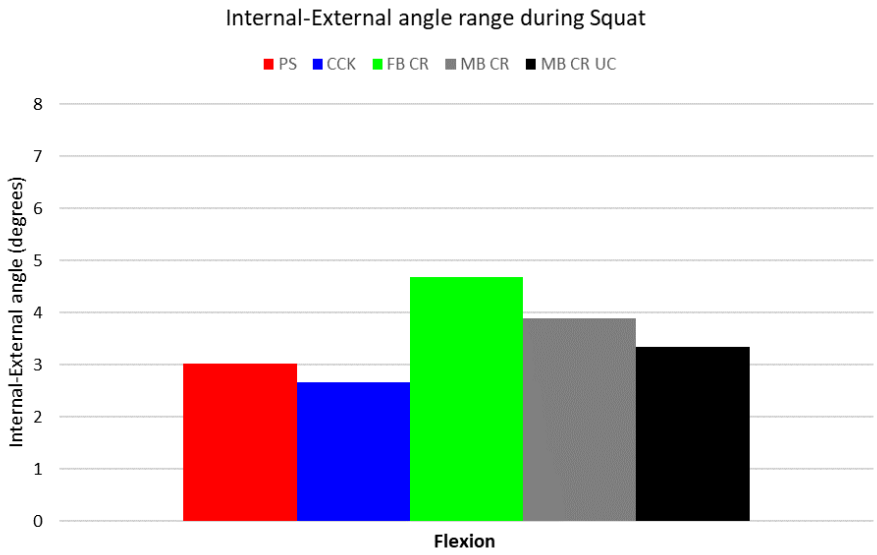

Figure 4.39. IE rotation angles range of the femur during squat.

4.2.3 Internal-External rotation of Mobile Bearing inserts

The MB designs follow at the beginning the femur slight external rotation; in particular it can be seen that the MB CR UC insert follows the femur angle until 80° of flexion, while MB CR begins to depart from the femur rotation before, at about 60° of flexion (Figure 4.40). Therefore, MB CR UC follows the femoral rotation until deeper angles of flexion.

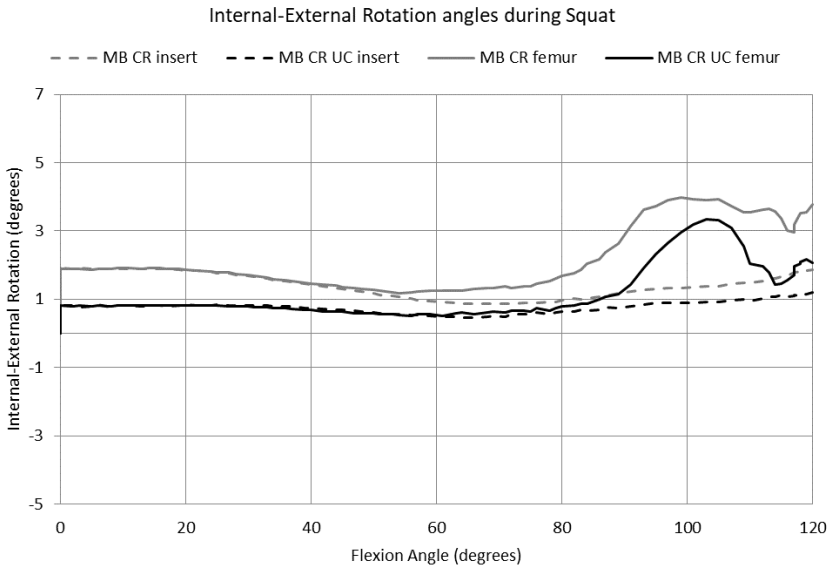

Figure 4.40. IE rotation angles of Mobile Bearing inserts (dashed lines) superimposed on femoral ones (solid lines) during squat.

4.2.4 Average von Mises Stress on the insert

4.2.4.1 Medial and lateral parts

For all the implants the greater stress values are found on the M side of the insert rather than on the L one. The stress rises with increasing angles until 60°, then it seems to stabilize producing a sort of plateau in the trends until maximum flexion, without further increase (Figure 4.41).

Among the FB designs, CR and CCK have almost the same values, while PS stress increases more at high angles in the M part, as happens for MB CR and UC. It follows that PS, differently from gait, together with the two MB options, has the highest average values (Figure 4.42, Figure 4.43).

Here it holds what have been found for gait about MB TKA designs, that is the fact that their higher conformity and mobility does not minimize the contact stress on the insert with respect to FB CR, but contrarily they seem to increase the stress on the M part of their inserts [20].

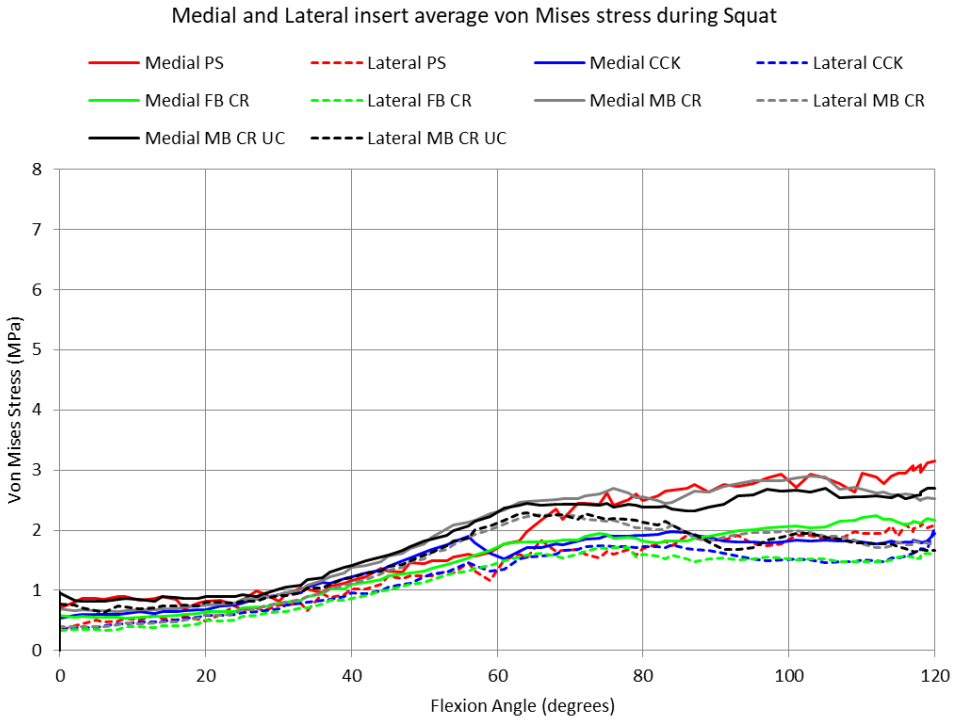

Figure 4.41. Average von Mises Stress on the insert during squat.

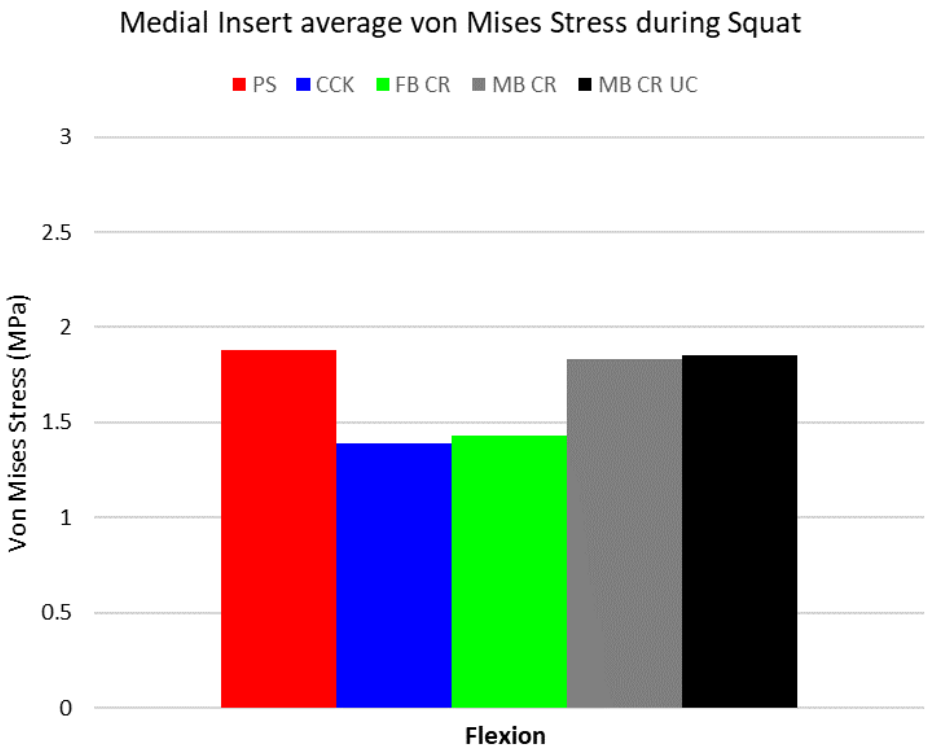

Figure 4.42. Average von Mises Stress range on the insert medial part during squat.

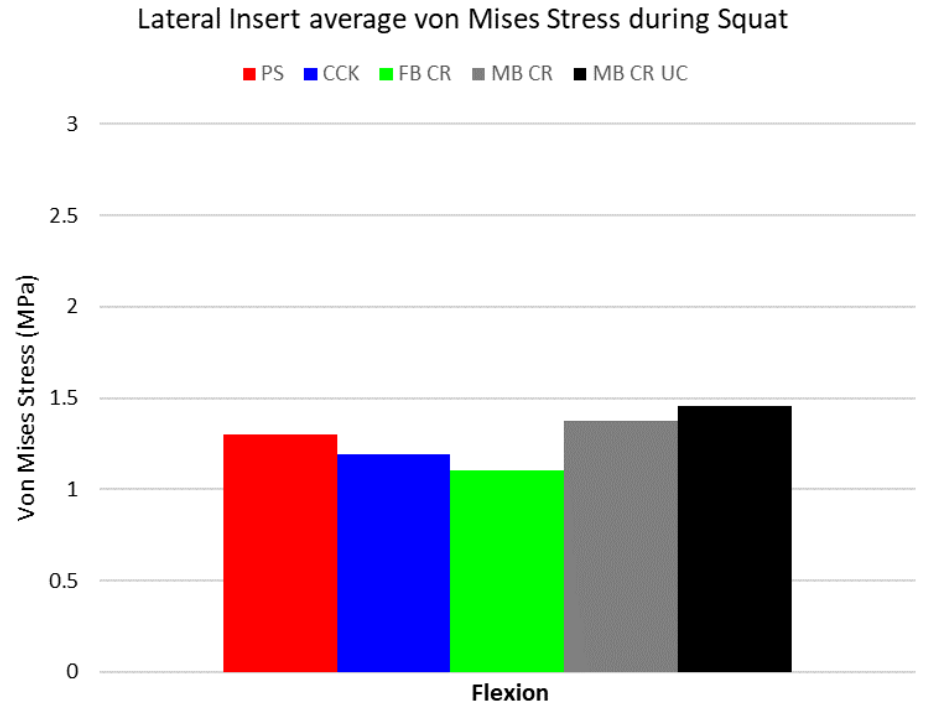

Figure 4.43. Average von Mises Stress range on the insert lateral part during squat.

4.2.4.2 Middle part

Concerning the middle part of the insert, FB CR has low and almost constant stress under 1Mpa until 100° of flexion, then it barely increases (Figure 4.44). The two MB designs provoke a rise in the stress with respect to FB CR, with close trends (slightly higher values for UC) where stress increases of about 4MPa until 60° of flexion, then slowly decreases until 2MPa at maximum flexion. PS and CCK generate a sudden rise of stress in correspondence of their engagement angles of the post-cam systems, which are around 60°; PS reaches the highest value of 7MPa then decreases until 3MPa at maximum flexion, while CCK stress increases until 3MPa, then stays still for 20° more of flexion and then decreases until 2MPa at the end of flexion.

In general, at high flexion, the congruency, mobility and the post-cam system are design factors that can rise the stress in the middle part of the insert (Figure 4.45), as manifested during gait; the additional observation that can be assessed during squat is that also the PS post-cam system comes into action, thus generating high stress in the middle zone, as soon as the engagement of the post with the cam occurs.

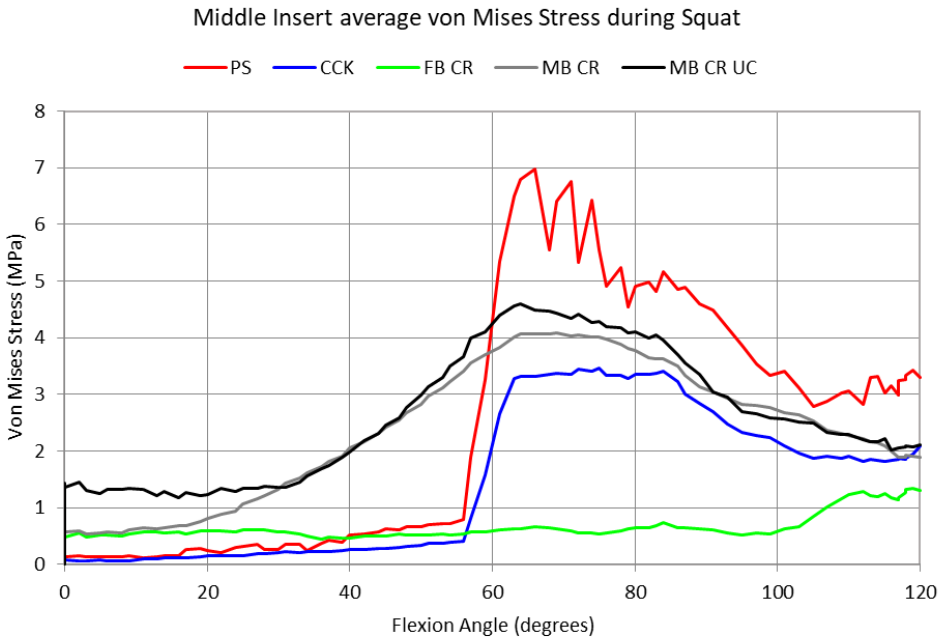

Figure 4.44. Average von Mises stress on the insert middle part during squat.

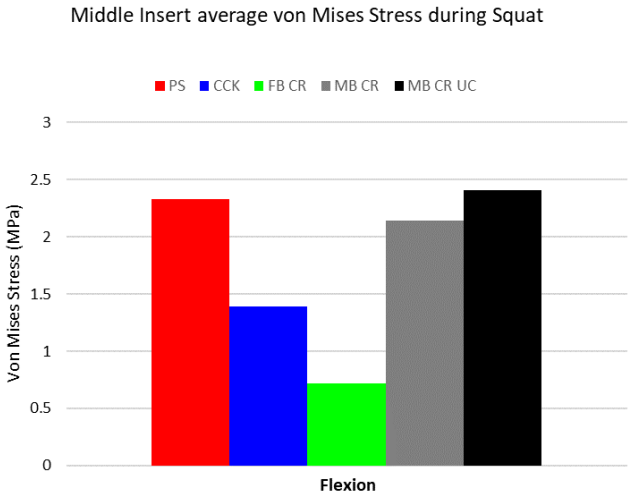

Figure 4.45. Average von Mises stress average on the insert middle part during squat.

AP displacement factor does not seem to be responsible for the increase of stress in the insert; in fact, for instance, even though CCK allows high femoral translation, it does not generate greater stress values than the other designs and in parallel MB CR UC has the tendency to limit the femoral displacement but not the stress, having indeed high stress values and average. Thus, AP displacement could be considered negligible as regards an eventual wear and failure of the implant due to stress with respect to other factors such as high force acting on narrow CAs [86].

4.2.5 Average von Mises Stress on the tibial bone

4.2.5.1 Proximal region of 5 mm

About the Von Mises stress on the tibial proximal ROI, there are similar trends for all the cases where stress increases up to 60° of flexion, then stabilizes in a sort of plateau with higher values in M than in L region (Figure 4.46). MB CR UC stress seems to increase more linearly and presents lower values with respect to FB CR, especially reducing stress in L side. FB CR on its side reaches the highest values before the plateau. MB CR stress barely decreases with respect to FB CR. PS and CCK display almost the same trend and present lower stress in the L part than FB CR. Therefore, post-cam and congruency seem to decrease the stress in the L proximal tibial ROI during squat with respect to FB CR.

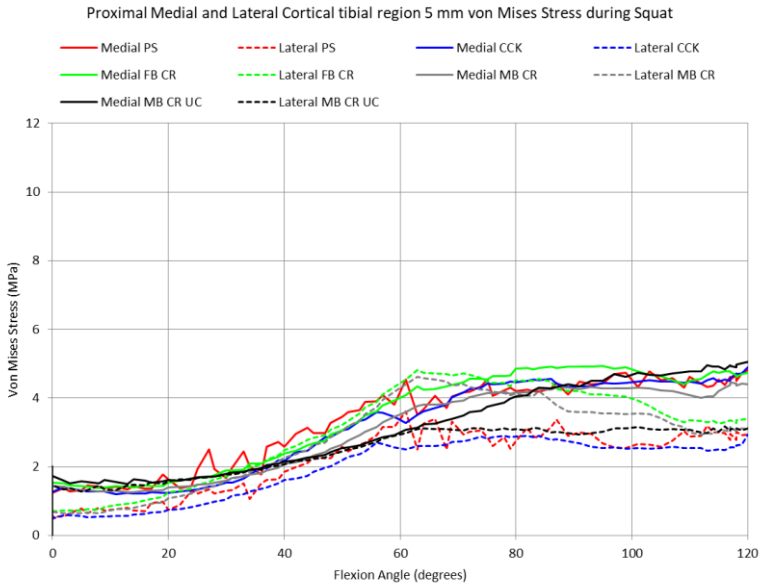

Figure 4.46. Average von Mises Stress on the proximal tibial bone during squat.

4.2.5.2 Distal region of 30mm

As in the 5mm zone, similar trends for all the cases with similar average and with higher values in M than in L (Figure 4.47). As in the gait, there are also similar trends to the 5mm ones, but the values are almost the double. FB and MB CR show almost coincident stress trends and very similar to the PS and CCK ones; differently to them, UC does not present a peak around 60° of flexion thus growing more linearly with the angle of flexion, and significantly lowers the stress in the L distal ROI.

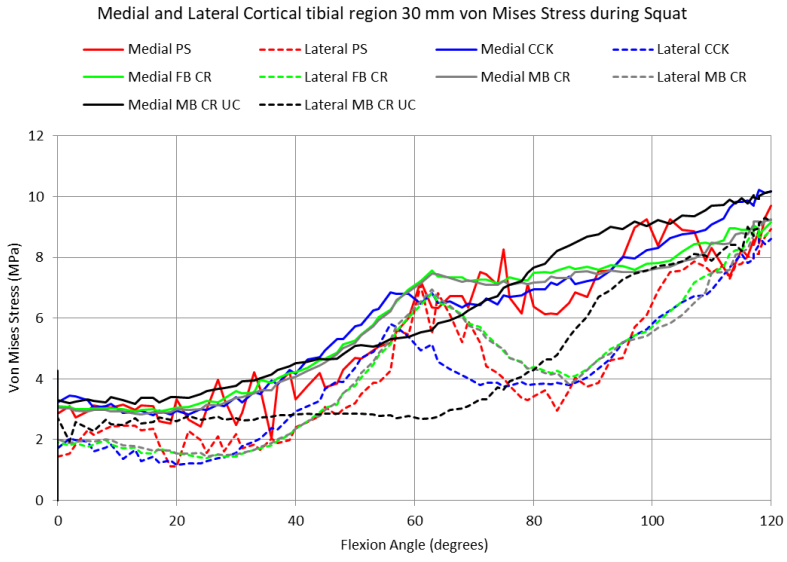

Figure 4.47. Average von Mises Stress on the distal tibial bone during squat.

Even here the consideration made for the gait holds: the distribution of the VM stress on the different zones of the tibia (proximal, distal) is relatively homogeneous between the models, but a different behaviour is observed in UC that, as in the gait, thanks to its higher congruency allows a more uniform distribution of stress, damping the peaks found in the other implants stress trends and in particular it significantly reduces the stress in the L tibial ROI both proximal than distal.

As during gait simulation, FB CR has lower values of stress on the insert, but reaches higher values on tibia regions. A difference found with respect to the gait is that MB CR does not significantly change the stress of FB CR, while UC, presenting more conformity, is able to reduce it [92], [6].

4.2.6 Contact Area on the insert

4.2.6.1 Medial and Lateral surfaces

CA values higher in M than in L for all the models. As in the gait, MB CR UC has always the highest CA values, reaching 800mm^2 around 30° of flexion (Figure 4.48).

As already noted in the gait, the surface of the UC insert is designed to have a maximal contact between the femoral component and the insert, and its CA averages are twice as high as FB or MB CR ones (Figure 4.49, Figure 4.50), that here result to be similar (instead during gait MB has shown higher values in the L part).

The trends of CA of the three CR decrease after 80° of flexion. PS and CCK are the designs which show lower values of CA than CR implants as in the gait [76], [6], increasing until the engagement angle up to almost 400mm^2 and then decreasing to 100mm^2 until 120°. The most symmetric design in terms of CA among M and L parts, seems to be CCK.

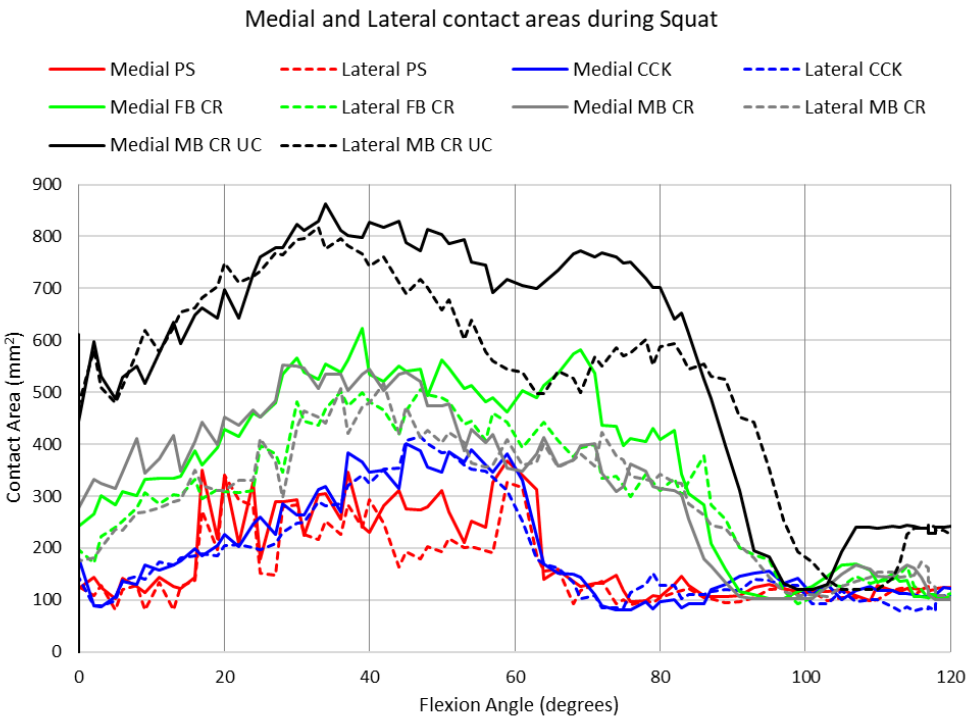

Figure 4.48. CA on the insert during squat.

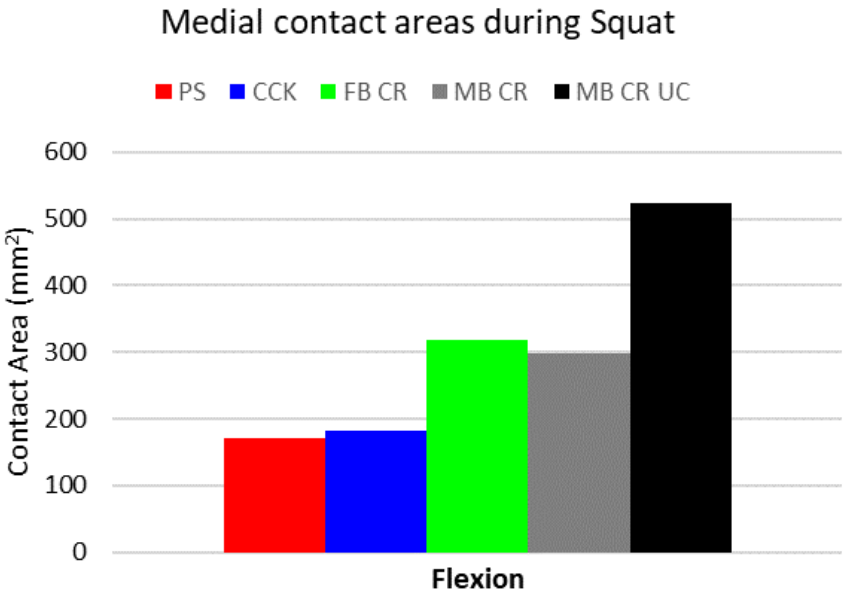

Figure 4.49. CA on the insert medial surface during squat.

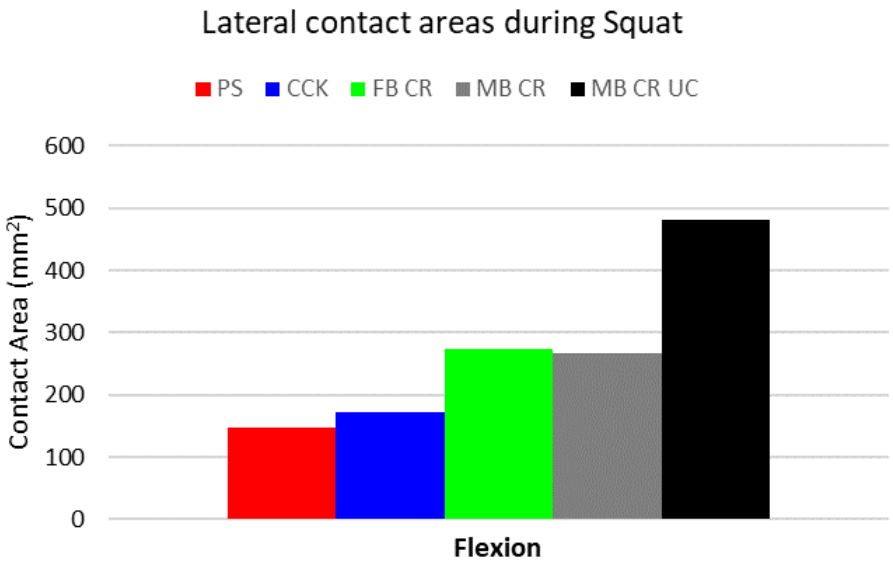

Figure 4.50. CA on the insert lateral surface during squat.

4.2.6.2 Middle surface of the insert

Just from 0 to 40° there is contact of the middle part of the insert, but the CA values are always under 70mm2 (and corresponding vertical CF values under 600N for UC, under 150N for FB and MB CR), with MB CR equal to FB CR and, as during gait, slightly higher values for UC (Figure 4.51).

Figure 4.51. CA on the insert middle surface during squat.

4.2.6.3 Post-cam surfaces

During squat both PS and CCK post-cam come in contact (Figure 4.52). Regarding the contact area and forces in the post-cam system, a parameter taken in consideration is the flexion angle corresponding to the contact between the two components, i.e., the engagement angle, at which contact area and force cease being zero [18]. Contact in the post-cam systems starts at the engagement angle that is slightly below 60° (consistent with the engagement angles found in literature in other prostheses [75], [86], [93], [18], [5], and comparable with the physiological cruciate activation angle [cruciate]) for both PS and CCK. Higher CAs are present in the posterior part of the post with respect to M and L and in particular are higher in the CCK. In the M surface of the post, CCK has CA values slightly greater than PS.

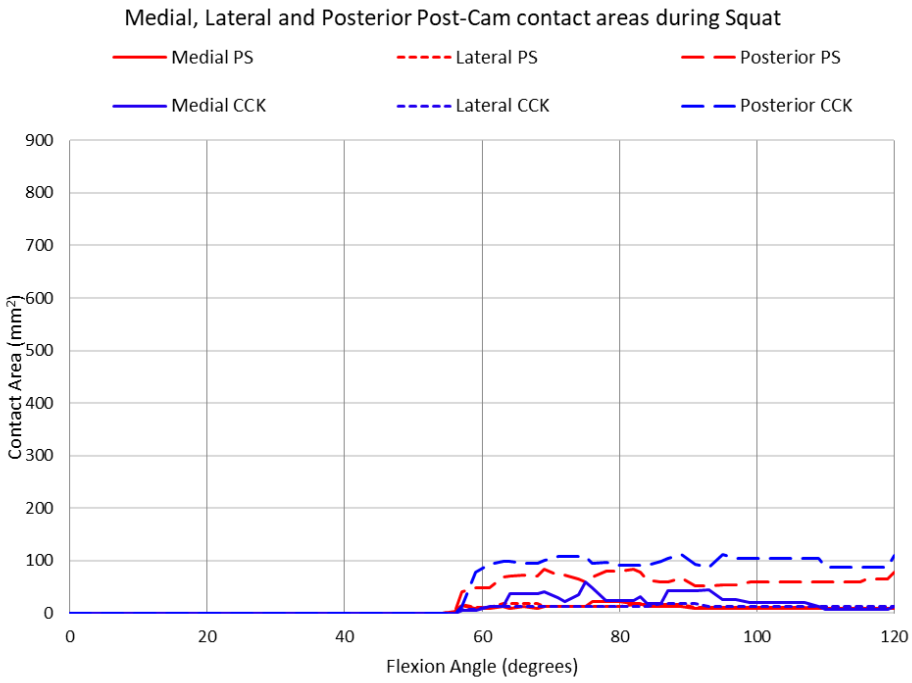

Figure 4.52. CA on PS and CCK post-cam surfaces during squat.

4.2.7 Contact force on the insert

4.2.7.1 Medial and Lateral surfaces

Vertical CF behaviour acting on the insert is similar between all models and higher in M than in L (M/L ratio is 3:2, consistent with literature [28], [73]), linearly increasing with the flexion angle, according to previous studies [86], [93], [18]. PS and CCK forces grow linearly with the angle as the others until the engagement angle, then are subjected to a dip at the engagement angle level and after that increase again.

MB CR UC has the highest force values; at 120° it exceeds 3000N in M and almost reaches 2000N in L (Figure 4.53). In second position there are FB and MB CR with coincident trends and averages and in the third one PS and CCK that also have quite the same trend and average (Figure 4.54, Figure 4.55). This order reflects the one seen in CA values.

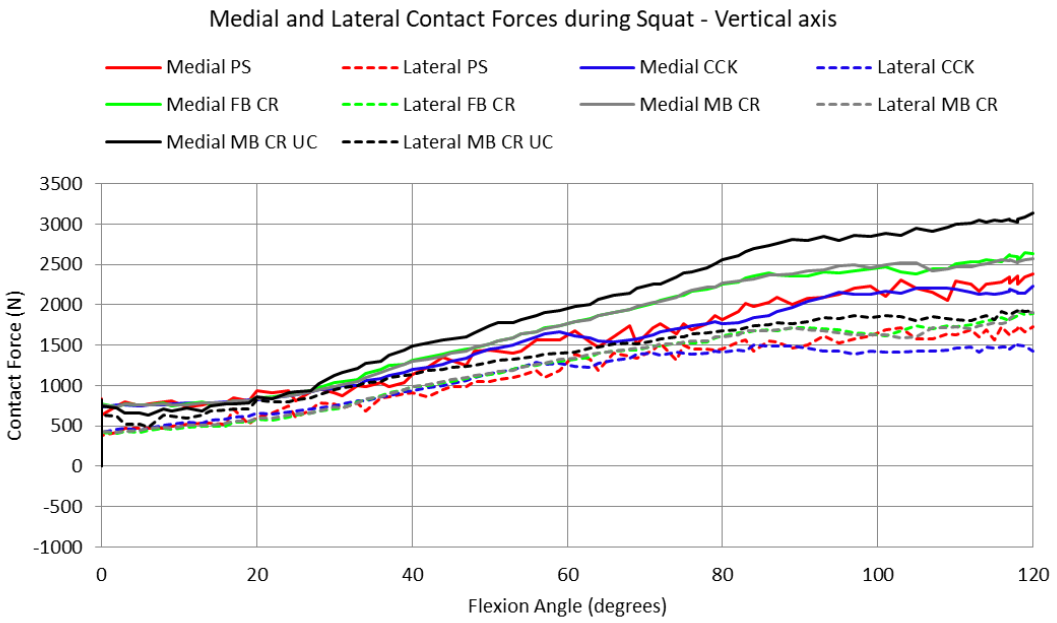

Figure 4.53. Vertical CF on the insert during squat.

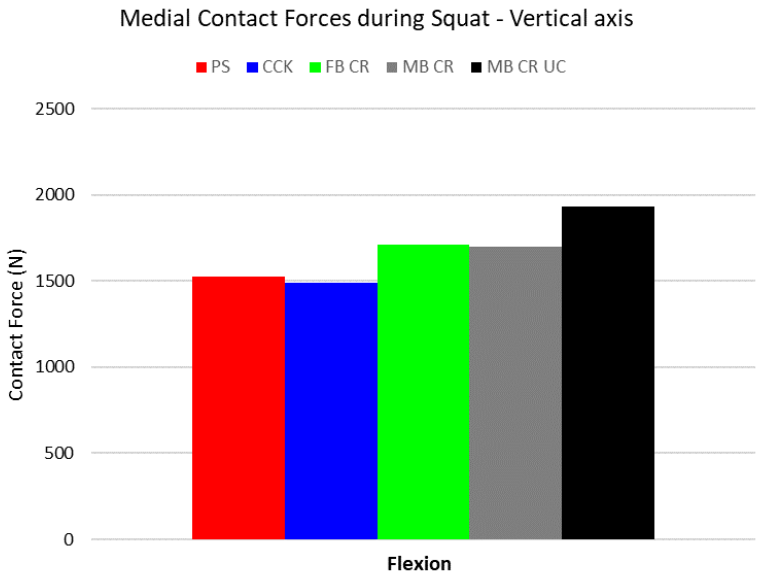

Figure 4.54. Vertical CF on the insert medial surface during squat.

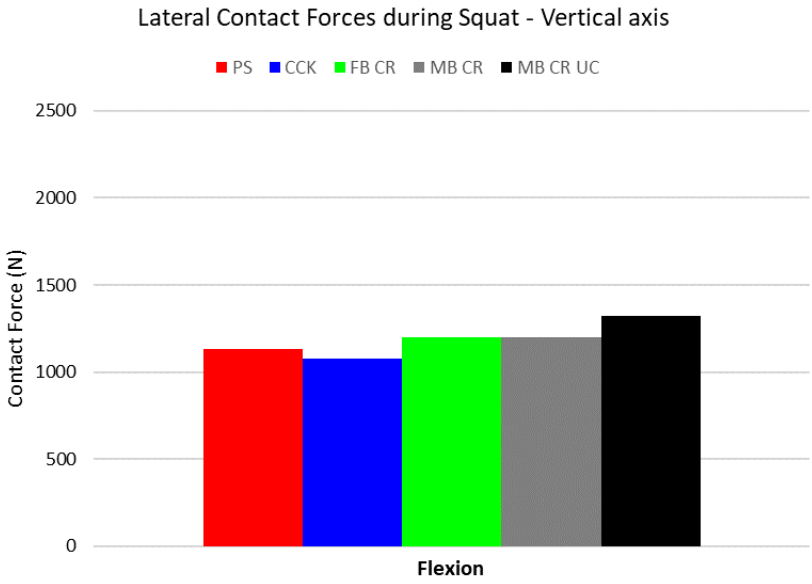

Figure 4.55. Vertical CF on the insert lateral surface during squat.

Values of sagittal CFs are negligible with respect to the vertical ones (lower than 600N), but it can be noted the similarity between M and L CF for all the prosthesis (Figure 4.56).

Among the models, there is resemblance between PS and CCK trends, and between the three CR trends. The first two designs present increase in force directed anteriorly but that reduce in magnitude starting from the engagement angle; this can confirm that the post-cam mechanism acts as a barrier for a further anterior displacement that would be provoked by the absence of the PCL. The CR implants CF increase until about 600N at 60° and then decrease.

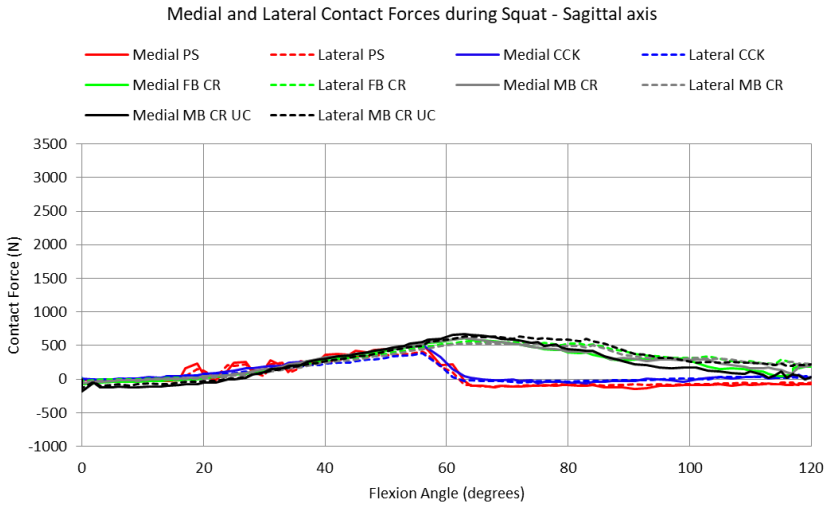

Figure 4.56. Sagittal CF on the insert during squat.

Also values of horizontal forces are negligible with respect to the vertical ones, but it can be noted that PS and CCK have the lower values (Figure 4.57, Figure 4.58, Figure 4.59).

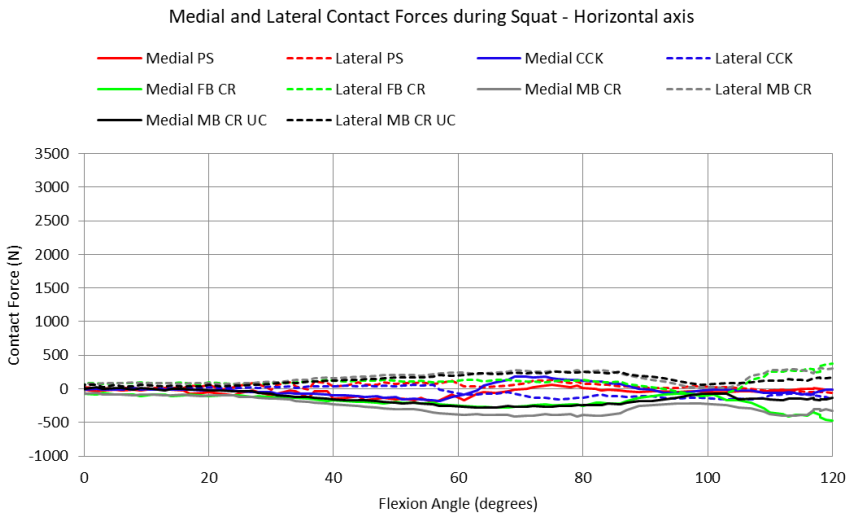

Figure 4.57. Horizontal CF on the insert during squat.

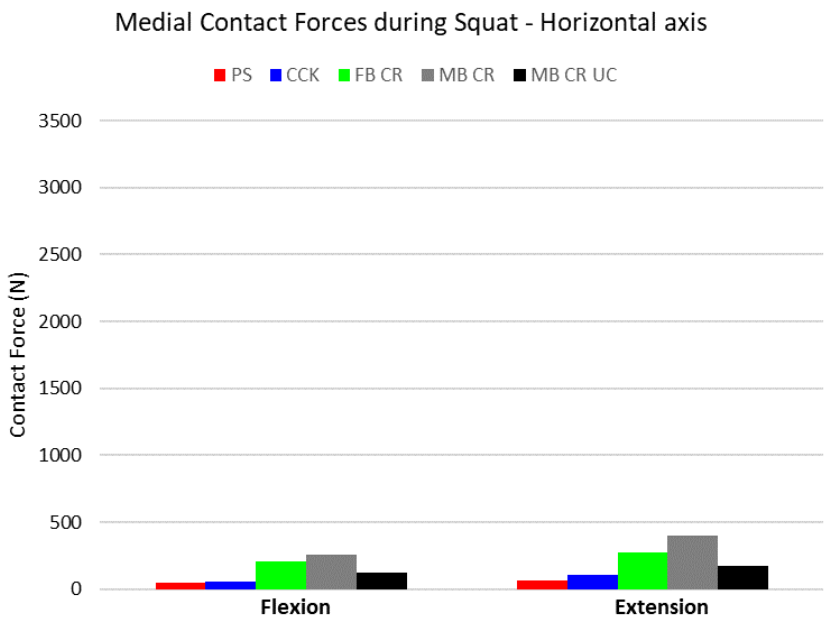

Figure 4.58. Horizontal CF on the insert medial surface during squat.

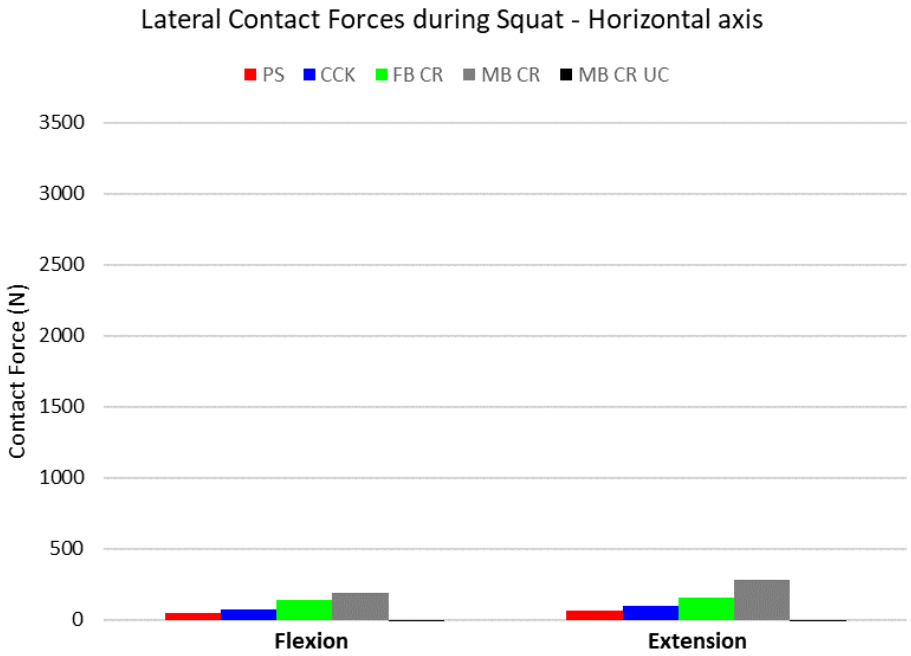

Figure 4.59. Horizontal CF on the insert lateral surface during squat.

4.2.7.2 Post-cam surfaces

Values of vertical CFs in the post-cam are visible starting from the engagement with the post [18], [93], [18], and, as in the CA, there are higher values in the posterior surface of the post (around 250N) for both CCK and PS (Figure 4.60).

In the M, L and posterior surfaces of PS post and starting from 80° of flexion, there are forces directed towards superior direction (in the figure the negative direction corresponds to the superior) and this could represent a potential risk of lift-off of the implant, that is the separation between femoral component and tibial insert [98].

Instead in the CCK the forces are exerted along a proximo-distal direction thus preventing lift-off of the insert [86].

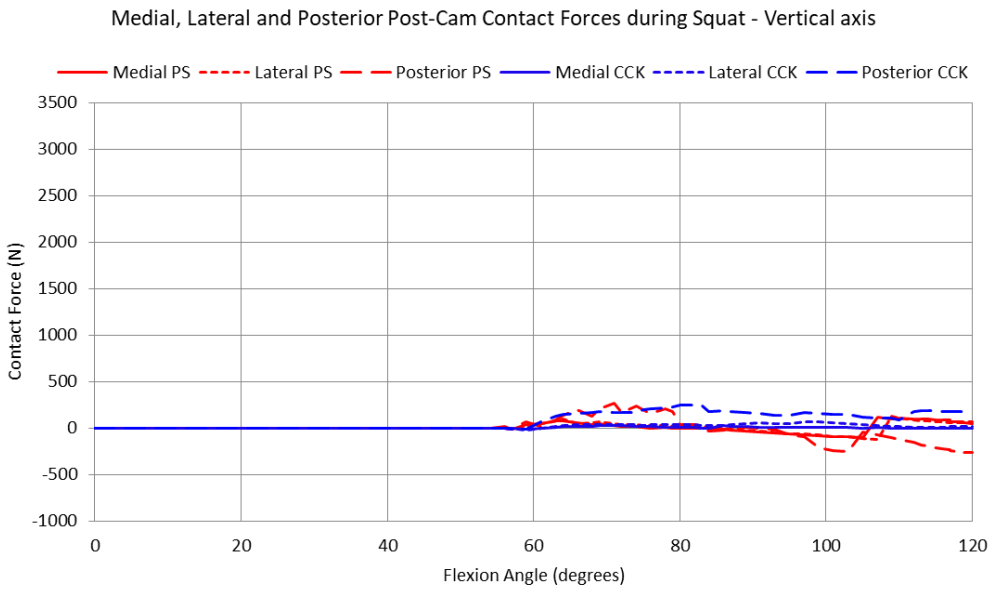

Figure 4.60. Vertical CF on PS and CCK post-cam surfaces during squat.

This study confirms that major force magnitudes in the post-cam systems are in the sagittal direction [99]. It is known that altered post-cam forces will increase polyethylene stresses that could lead to post-cam failure and consequently the need for a revision component. So, it is important to know what level of CF is generated at the post-cam interface [5].

As observed in the vertical forces, values of sagittal forces are present only starting from the engagement with the post and, as in the CA, there is continuous contact between post-cam components [86] and higher values in the posterior surface of the post (around 1500N for PS, 1300N for CCK) (Figure 4.61).

PS has higher values than CCK also in M and L, but three times lower than those found in the posterior surface. Thus, since increasing the flexion the force in sagittal direction is mainly concentrated between post and cam, this can induce local deformity and luxation of the post-cam system.

With respect to the post back, both designs achieve larger values of CFs during the squatting task compared to the gait task. That can be explained due to the larger range of flexion–extension angle which will facilitate the back side contact of the post with the cam of the femoral component [75].

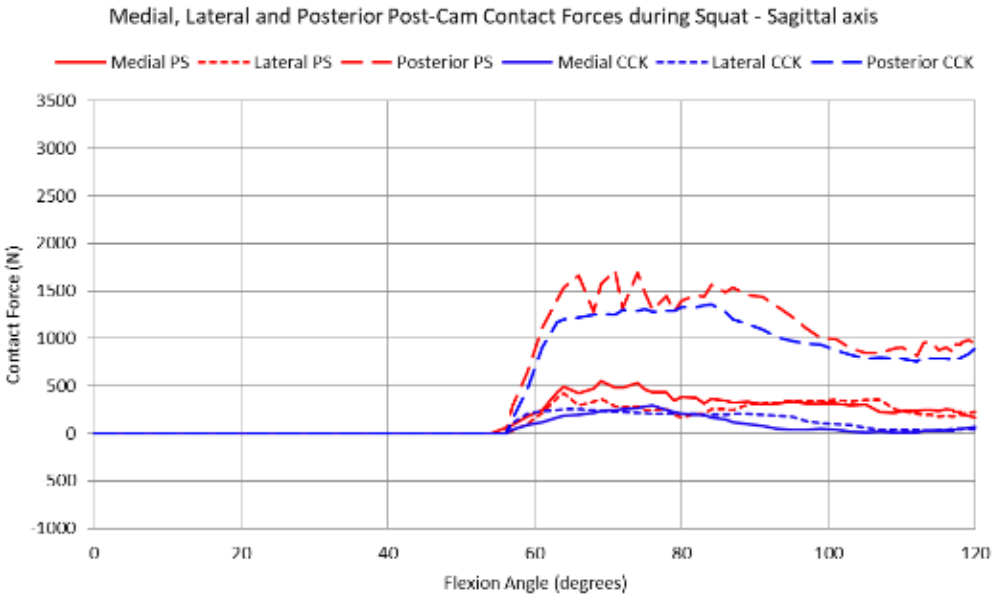

Figure 4.61. Sagittal CF on the insert during squat.

Values of horizontal forces are present only starting from the engagement with the post and, differently from the vertical and sagittal forces, higher values are detected in the M surface (towards the lateral direction) and L one (towards the medial direction), both lower than 500N and slightly higher in CCK with respect to the PS (Figure 4.62). As during gait, these forces result in a compression of the post.

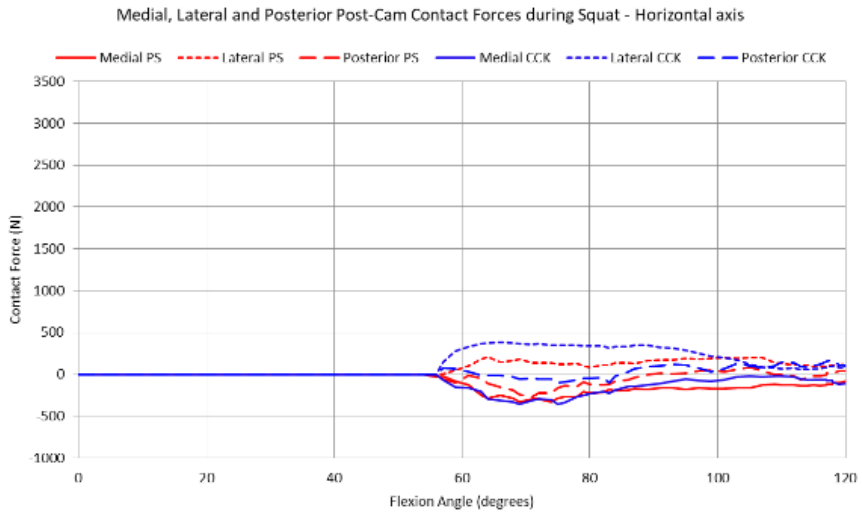

Figure 4.62. Horizontal CF on PS and CCK post-cam surfaces during squat.

4.2.8 Contact Pressure on the insert

4.2.8.1 Medial and Lateral surfaces

As in the gait, the trends of contact pressure are similar among the models and also among M and L parts of the inserts, with higher values in the M part (Figure 4.63). All the trends show increasing pressure with angle, from 0MPa to almost 2 MPa but CCK from the engagement angle starts to show lower values of pressure under 1MPa.

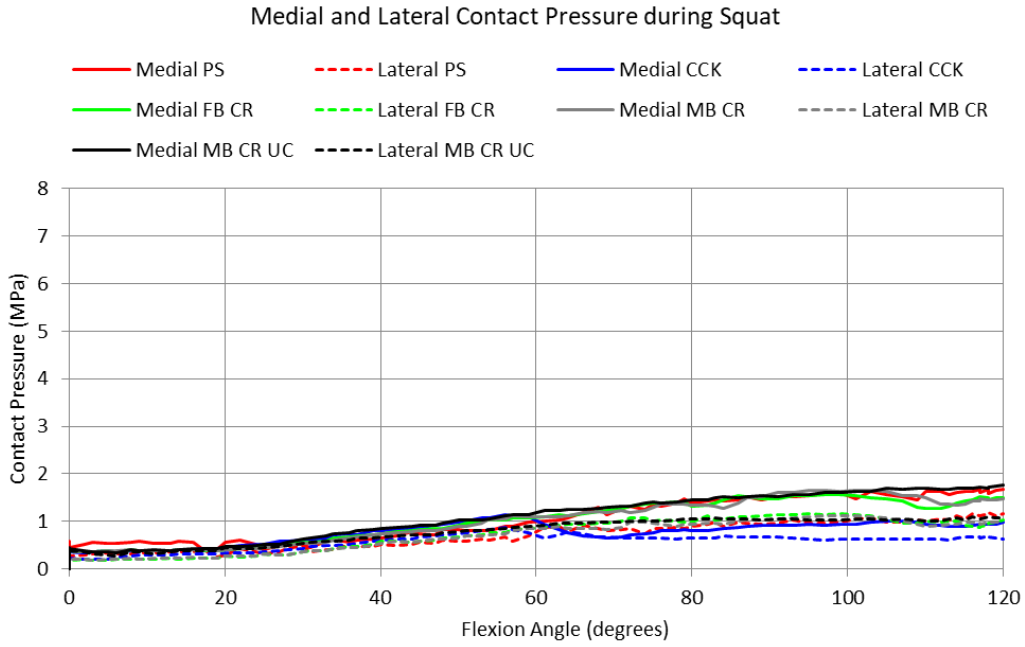

Figure 4.63. Contact pressure on the insert during squat.

4.2.8.2 Middle surface

The CR show decreasing values from 0 to 40°, with UC starting from 2MPa while FB and MB CR, with the same trend, start from a value lower than 1MPa.

PS and CCK have pressure values from the engagement angle on, with PS pressure higher that CCK one, but lower than MB CR UC (Figure 4.64).

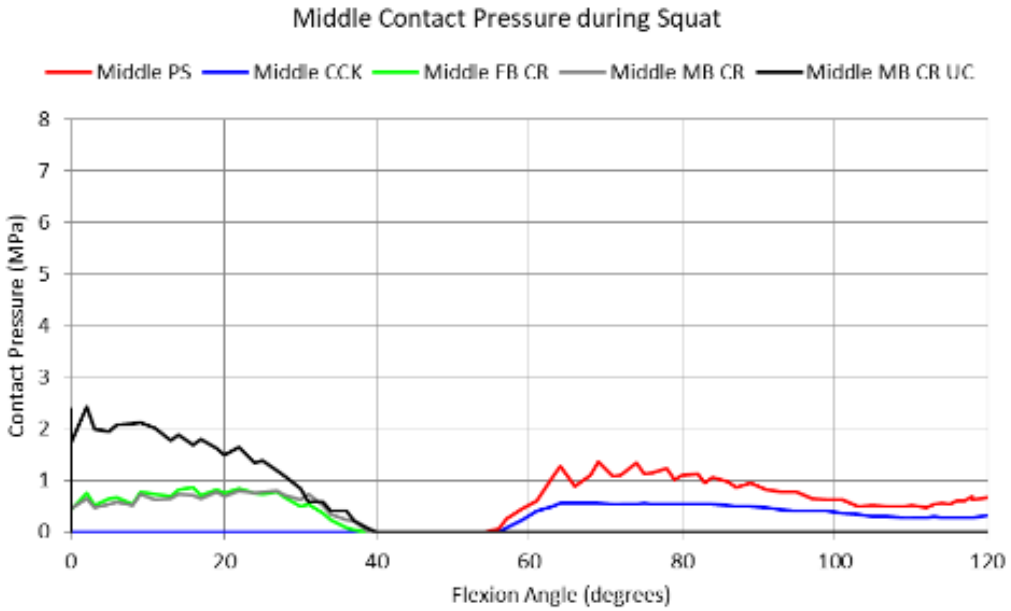

Figure 4.64. Contact pressure on the insert middle surface during squat.

4.2.8.3 Post-cam surfaces

The contact pressure behaviour is similar to the sagittal force one. Values of pressure are present only starting from the engagement with the post, then decreasing from 80°-90° of flexion.

Higher values are displayed in the posterior surface of the post (around 6MPa for PS, 3.5MPa for CCK). PS has higher values than CCK also in M and L, but three times lower than those found in the posterior surface (Figure 4.65).

The post of CCK is more congruent to the cam, thus the distribution of the forces in a wider area of contact diminishes the risk of post wear and failure.

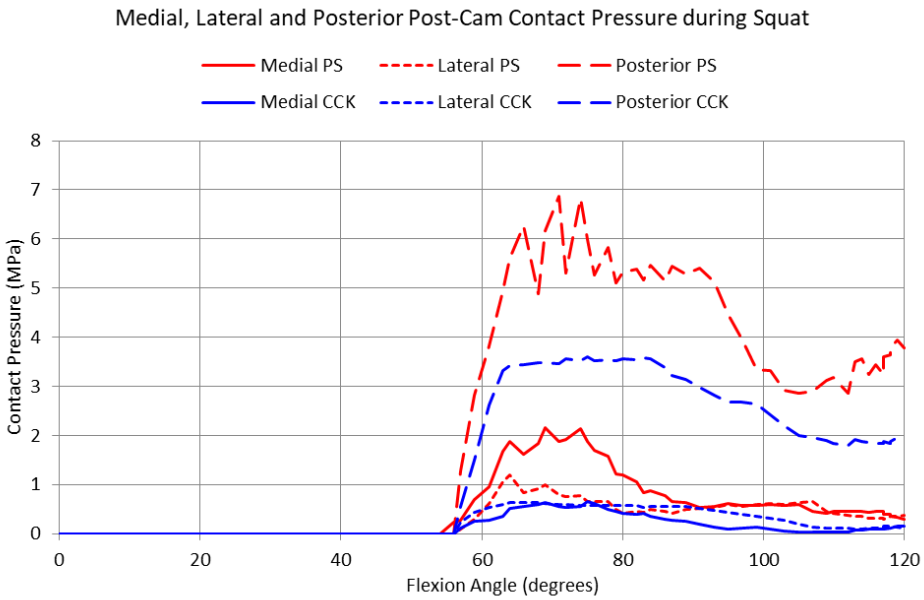

Figure 4.65. Contact pressure on PS and CCK post-cam surfaces during squat.

As in the gait, PS and CCK presents high average CF values but, differently from the CR designs and especially from the UC, these magnitudes are not compensated with larger CA, so the force distribution is narrower. In particular, in the posterior surface of the post CA is around 100mm² in PS and lower that 80mm² in CCK, while for both the sagittal CF in the is around 1000N-1500N. High forces acting on narrow areas lead to the high values of pressure. Indeed, from the contact pressure results, PS and CCK show a marked concentration of pressure in the posterior surface of the post where they reach from 3 to 6 MPa, while in the M and L surface of the insert their pressures remain under 2MPa.

With higher sagittal force values acting on the post, PS presents lower CA therefore higher contact pressure than CCK post (Pressure=Force/Surface).

This reduction in pressure resulting in CCK can be due to the augment of post dimension which, making the post more congruent to the cam, allows the distribution of the forces in a wider area of contact, diminishing the risk of post wear (which is linearly dependent to the contact pressure) and failure [5], [21], [86].

4.2.9 Contact point displacement on the insert

4.2.9.1 Medial and Lateral surfaces

As in the gait, PS and CCK contact points show almost identical AP displacement trends in M and L and have the widest ranges of motion than the rest of the implants, that is between 20-25mm (slightly higher for CCK). In detail, their contact points go anteriorly until the engagement angle and then rapidly go posteriorly of about 10mm and then continue to go posteriorly of other 10mm until 120° of flexion (Figure 4.66). This posterior roll-back can be seen also in Figure 4.67 and Figure 4.68, in which between the lines of 50° and 70° there is more distance in PS and CCK, while in the CR designs are closer; from these images it can be also noted that in the post-cam designs there isn't pivoting between the M and L contact, while a slight lateral pivoting seems to be present in the CR during the posterior translation thus being closer to natural kinematics [53], coherently with the internal rotation of the femur. The CR show the same trend which go anteriorly of about 20mm until 60° and then posteriorly of about 15mm according to literature [21].

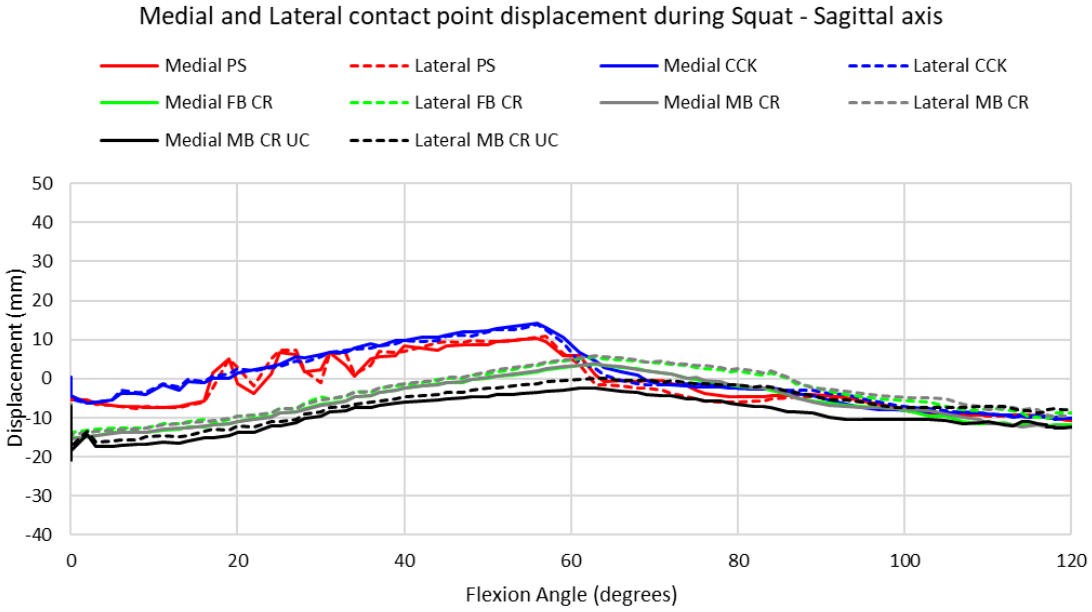

Figure 4.66. Contact point sagittal displacement on the insert during squat.

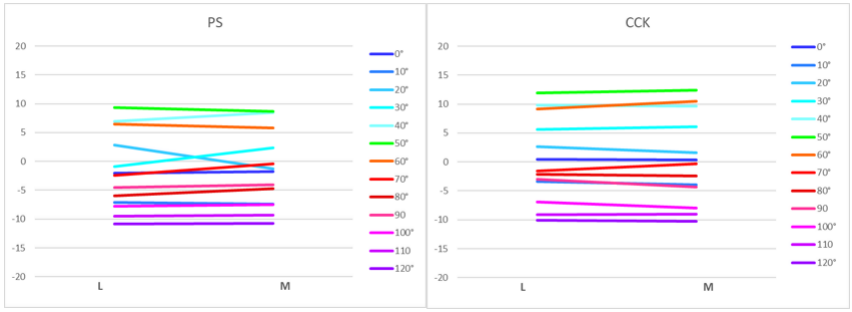

Figure 4.67. Contact point sagittal displacement on PS and CCK during squat.

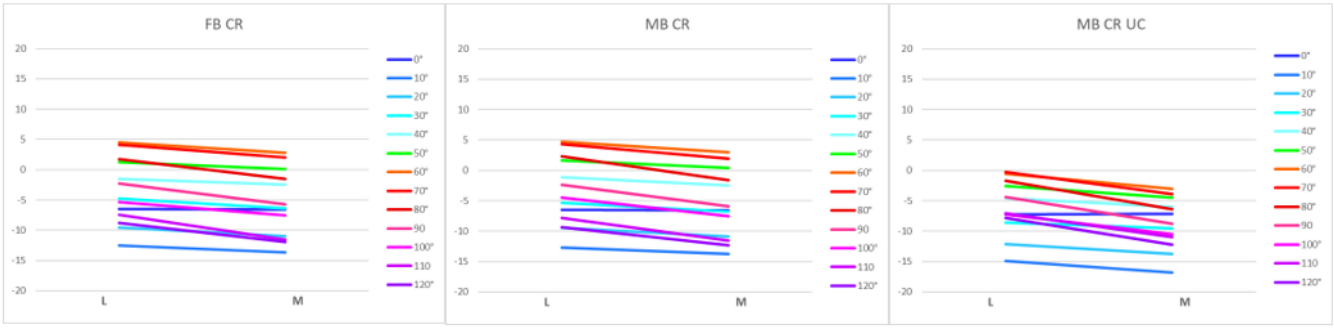

Figure 4.68. Contact point sagittal displacement on CR designs during squat.

In ML direction the contact displacement in all the insert surfaces is minimal and not noteworthy.

4.2.9.2 Post-cam surfaces

In the sagittal and vertical directions, the displacements of contact point in the M and L surfaces of the post undergo a rapid variation of 5-10mm towards posterior direction in CCK and superior direction in PS, in correspondence of the engagement angle (Figure 4.69, Figure 4.70).

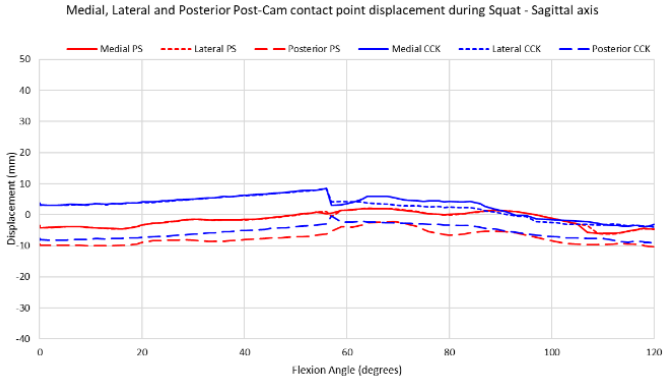

Figure 4.69. Contact point sagittal displacement on PS and CCK post-cam surfaces during squat.

Figure 4.70. Contact point vertical displacement on PS and CCK post-cam surfaces during squat.

4.2.10 Medio-Lateral displacement of the patella

In Figure 4.71 it is represented the patellar translation towards the medial direction that increases with the flexion angle [100] until about 100° then remain quite stable until maximum flexion. All the prostheses induce a translation of around 10mm, except MB CR UC which translates of 8mm, thus limiting the patellar displacement.

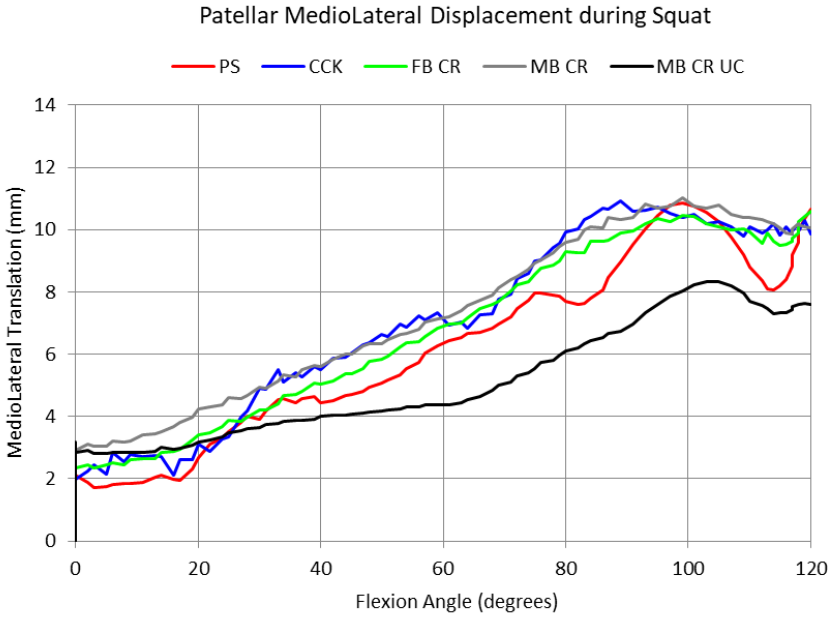

Figure 4.71. Patellar ML displacement during squat.

4.2.11 Patellar rotation around Medio-Lateral axis

Trends of patellar rotation around the ML axis are similar for all the designs (Figure 4.72); from 0° to 40° there is a linear increasement in rotation following the femur flexion, then from about 50° the curve change inclination and reaches overall 20° of rotation at maximum flexion for all the designs, reflecting a rotation behaviour in agreement with literature [101]. Post-cam designs and UC slightly limit the rotation (Figure 4.73).

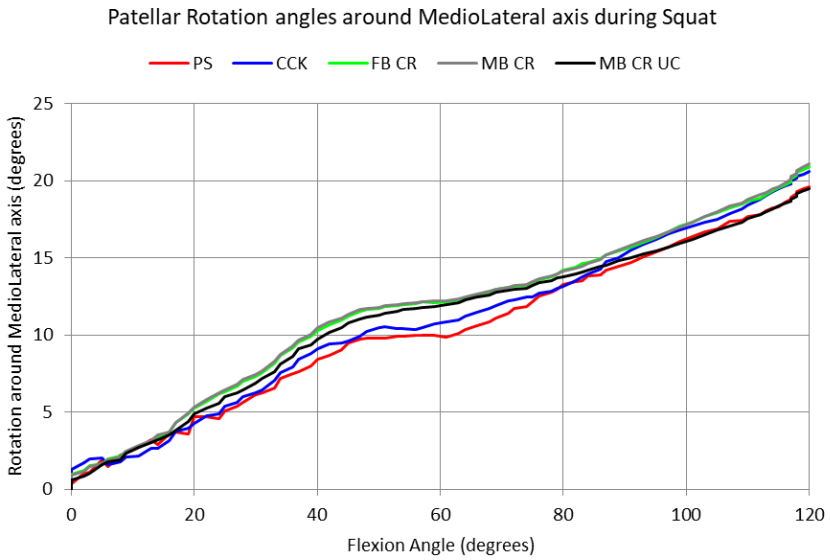

Figure 4.72. Patellar rotation angle around ML axis during squat.

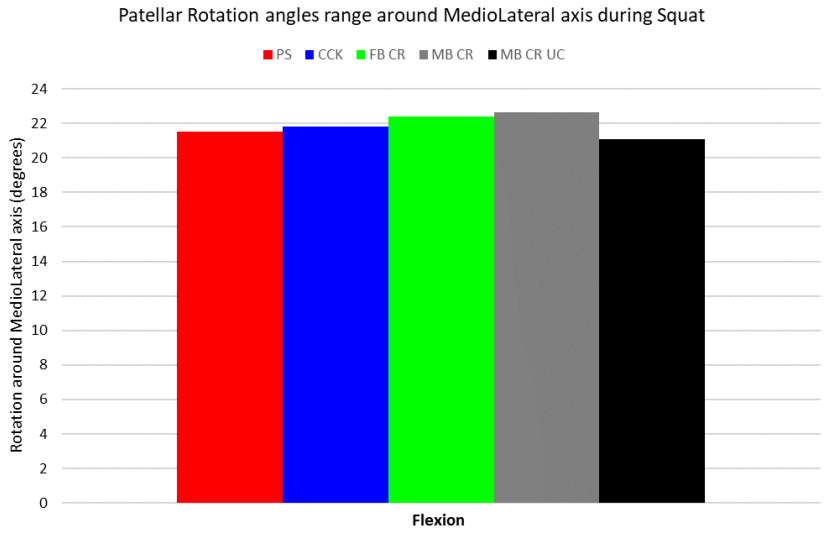

Figure 4.73. Patellar rotation angle range around ML axis during squat.

4.2.12 Patello-femoral contact area

Similar CA trends for the CR where the PF CA values grows with the flexion angle until around 50mm², with higher average for MB CR UC (Figure 4.74, Figure 4.75). PS and CCK have the same values at the beginning but from 60° on CCK CA trend decreases until 30mm² and at 120° increases until 50mm², resulting to show less compliance for the PF contact, that, at equal PF force of the other designs, induces narrower force distribution.

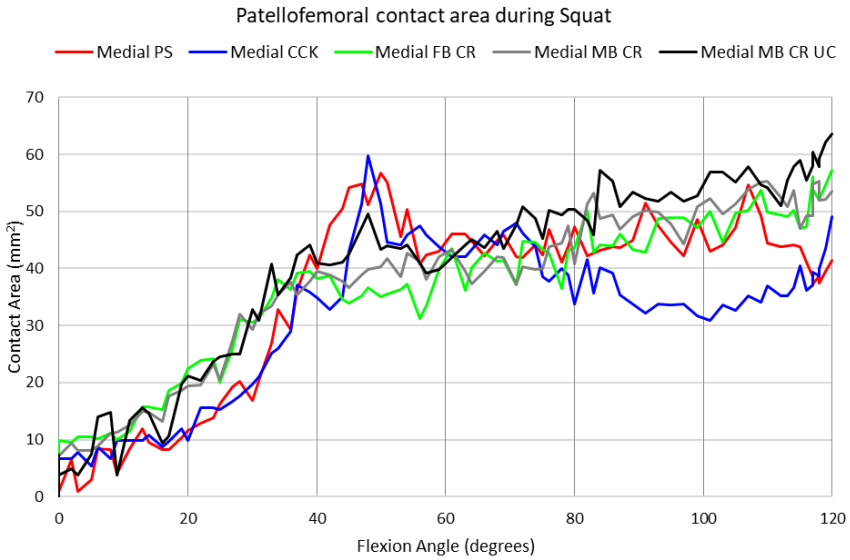

Figure 4.74. PF CA during squat.

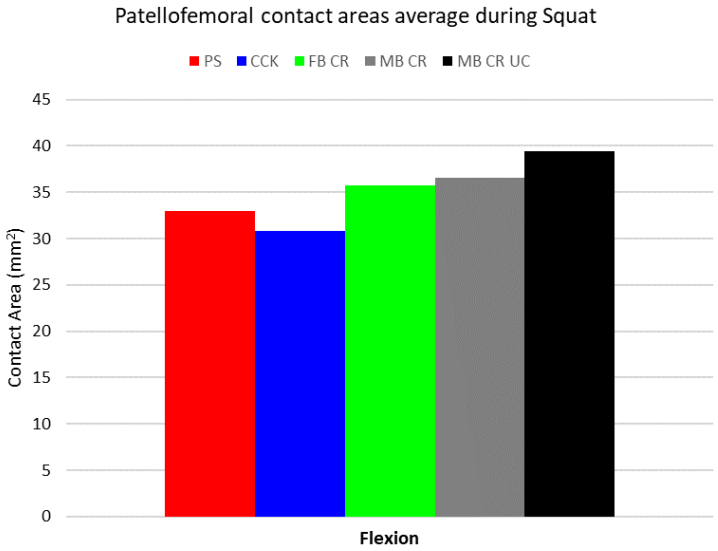

Figure 4.75. PF CA average during squat.

4.2.13 Patello-femoral contact force and quadriceps force

Symmetrical trends for all the prostheses PF forces that grow with the flexion angle and have comparable ranges in relation with literature findings [18], [101], [93], [102], [103], [39], [73]. In PF sagittal CF, close average values between all the models and agreement is found in the pattern as their outcomes show 80° of flexion as the ending of the increase of force and the starting of a plateau, that have been detected after 60° of flexion also in previous studies [18]. This AP force points anteriorly and reaches higher values for the CR at the end of flexion, especially in MB CR UC, thus they could provoke more anterior knee pain than post-cam prosthesis (Figure 4.76, Figure 4.77).

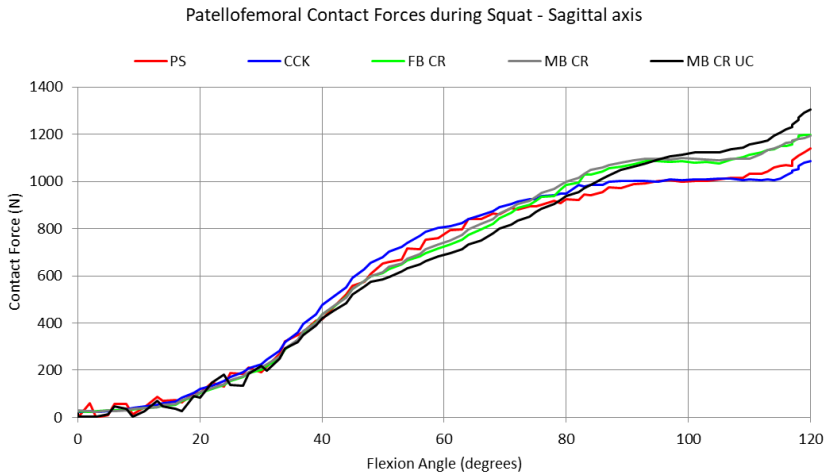

Figure 4.76. PF CF during squat.

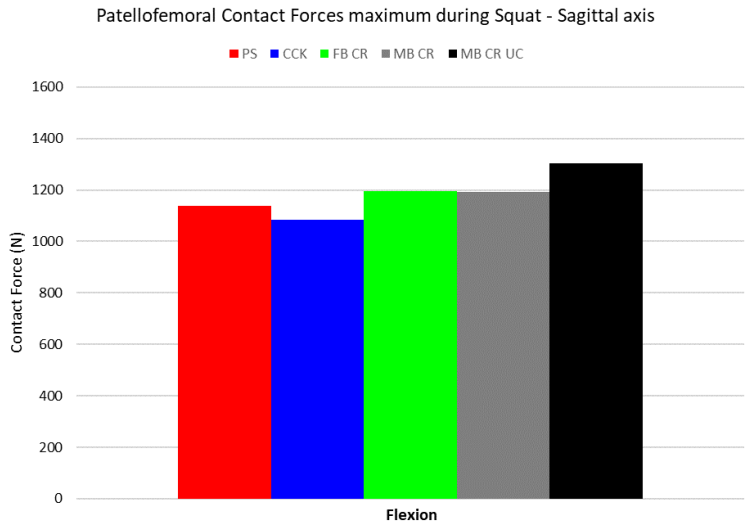

Figure 4.77. PF CF maximum during squat.

In the vertical force, which represents the quadriceps force resulting from the passive reaction of the soft tissues implemented [18], CR designs show higher values thus they require more force to efficiently flex the femur, especially MB CR which reaches almost 1400N at the end of flexion; MB CR UC shows lower amplitudes of quadriceps force with respect to FB CR and to the standard MB design (Figure 4.78, Figure 4.79).

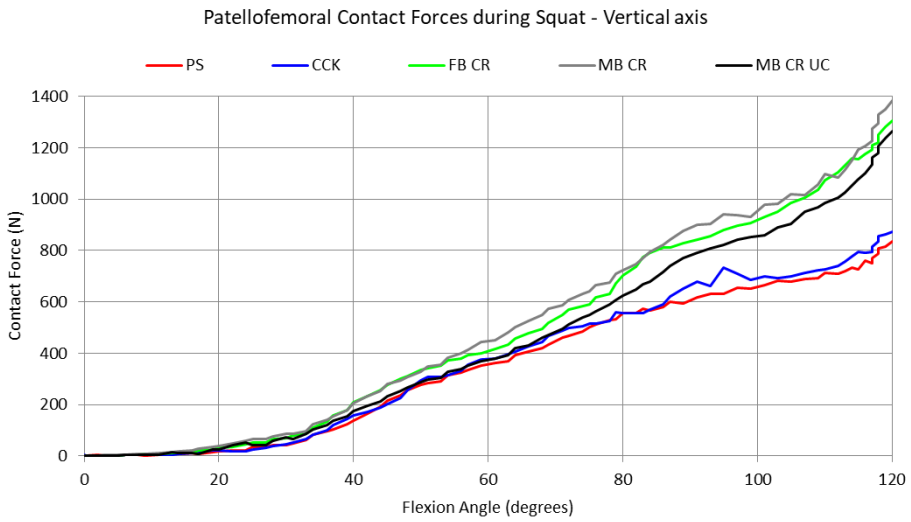

Figure 4.78. Quadriceps force during squat.

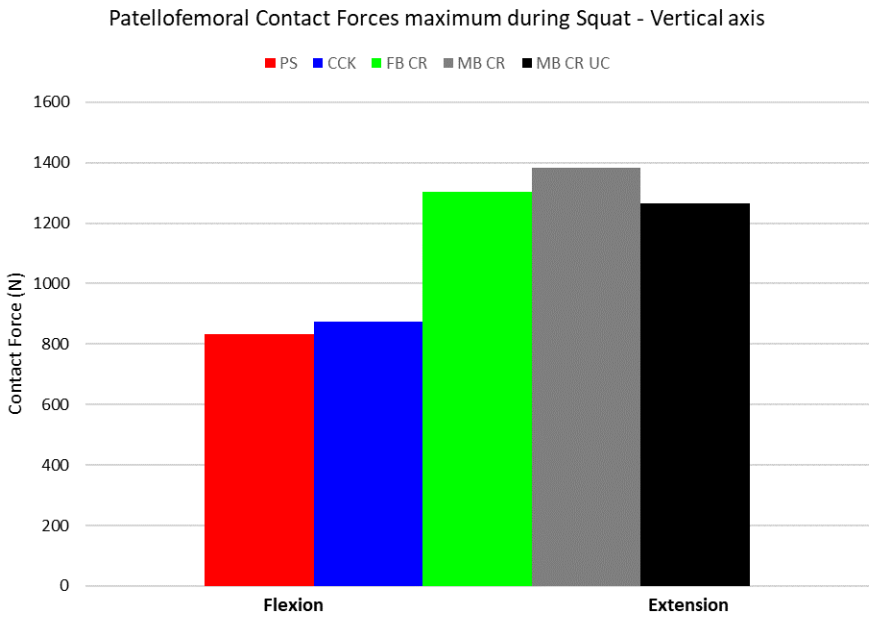

Figure 4.79. Quadriceps force maximum during squat.

5 Conclusions

The results of this study are comparable with literature [93], [18]. What it has been found is that the insert design differently affects the kinematics and the kinetics of the knee joint.

For what concerns the TF kinematics, it emerged that PCL and congruency improve the stability both in gait and squat. Indeed, MB CR UC limits almost completely femur AP displacement, thanks to the combination of the retention of the PCL and the inherent congruency of its design conformation that through a high anterior wall and a deep-dished plate guarantees a good stability during the walking cycle.

Moreover, during the simulation of squat UC does not exhibit paradoxical motion, thus it would not push the patella forward when implanted, avoiding the anterior knee pain.

Instead, in both activities simulated, post-cam systems induce more femoral AP displacement, indicating that the resection of the PCL, which is noted to have a stabilizing function in terms of posterior translation, causes higher femur displacement [25], [1], but the post-cam mechanism enable the posterior roll-back. In detail, CCK increases the femoral displacement with respect to PS, as previously observed in literature [75].

About the femoral IE angles, CR designs show an IE rotation and also a lateral pivoting during squat closer to physiological kinematics [53], [97], [10]. During both activities the MB CR UC insert faithfully follows the IE rotation of the femur until deeper angles of flexion, while MB CR, being less constrained, at some point deviates.

Regarding PF kinematics, MB CR UC limits the patellar displacement of 2mm at 120° of flexion with respect to the other implants, thus restraining an eventual patellar dislocation.

In the TF kinetics, a side effect of MB designs and of congruency seems to be the increase in VM stress on the insert: during gait MB CR UC has the highest average stress not only during stance but also during swing. During squat the two MB show higher stress at deep flexion in the M part on the insert with respect to FB CR. Thus, even though from some previous studies it was thought that MB TKA designs with their increased conformity could have minimized the contact stress on the insert [53], it is not observed here, as in previous research [20].

Both during walking and squatting, the congruency, mobility and the post-cam system resulted to be design factors that can rise the stress in the middle part of the insert; since during squat also the PS post-cam system comes into action, the additional observation that can be assessed during squat with respect to gait is that PS generates the highest stress peak in the middle zone of the insert, as soon as the engagement of the post with the cam occurs.

Furthermore, the distribution of the VM stress on the different considered regions of the tibia is relatively homogeneous between the models, but a different behaviour is observed in UC that, thanks to its higher congruency, allows a more uniform distribution of stress, damping the peaks found in the other implants stress trends and in particular it significantly reduces the stress in the lateral tibial ROI both proximal than lateral.

The FB CR has lower values of stress on the insert but reaches higher values on tibia regions. A difference found with respect to the gait is that, among the CR implants, MB CR does not significantly change the stress of FB CR on the tibia, while UC, presenting more conformity, is able to reduce it [92], [6].

During gait and squat MB CR UC always presents the highest CA values. Indeed, the surface of the UC insert is designed to have a maximal contact between the femoral component and the insert.

Instead, PS and CCK are the designs which show lower values of CA than CR implants in both gait and squat [6], [76], thus inducing narrower force distribution so high pressure with respect to the CR.

In the post-cam contact that occurs during squat, higher contact areas and contact forces are concentrated in the posterior part of the post with respect to M and L and this can induce local deformity and luxation of the post-cam system. The CA are higher in the CCK with respect to the PS, thus the higher level of constraint in the post improves the force distribution.

For what concerns the squat contact forces on the insert, in general CR designs are subjected to higher forces than post-cam prostheses, with the highest loads in MB CR UC; during gait MB CR and MB CR UC reduce the sagittal forces present in FB CR.

In both PS and CCK post-cam there are forces acting a compression in M and L parts of the post. During squat, in PS a potential risk of lift-off tuned out (there are forces in the post-cam surfaces directed towards superior direction), instead in the CCK the forces are exerted along a proximo-distal direction thus preventing lift-off of the insert [86]. Still in PS, higher sagittal forces in the posterior surface are present thus, having lower CA and higher forces, it generates narrower force distribution and higher contact pressure than CCK. This reduction in pressure resulting in CCK is due to the augment of post dimension which, making the post more congruent to the cam, allows the distribution of the forces in a wider area of contact, diminishing the risk of post wear (which is linearly dependent to the contact pressure) and failure [5], [21], [86].

It has been observed that contact in the post-cam systems starts at the engagement angle that is slightly below 60° (consistent with the engagement angles found in literature in other prostheses [86], [75], [93], [18], [5] and comparable with the physiological cruciate activation angle [104]) for both PS and CCK. In correspondence of this angle, the sagittal forces acting towards the anterior direction are decreased, thus this study can confirm that the post-cam mechanism acts as a barrier for a further anterior displacement that would be provoked by the absence of the PCL.

Focusing on the PF joint, higher CA average values are always found for MB CR UC. CCK shows less compliance for the PF contact at higher flexion angles, that, giving the similar PF force range of the other designs, can induce narrower force distribution.

PF force is higher in the CR designs and above all UC shows the maximum value at end of flexion, but it is compensated by higher PF CA.

With respect to the post-cam implants, FB CR designs require more quadriceps force to efficiently flex the femur, but while the less constrained MB CR worsen this situation, the congruency of UC appears to decrease the forces values.

To summarize, two mainly important aspects turned out from this TKA comparison. Firstly, that the stress in the TF contact changes with the difference in design constraint. Indeed, the mobility of two designs increases the stress on the insert, but as already explained the congruency of the UC provide a more homogeneously distributed stress in a wider area of contact. At high flexion, the congruency, mobility and the post-cam system are design factors that can rise the stress in the middle part of the insert. Furthermore, between the two post-cam designs, the addition of constraint in CCK can reduce the stress, that in PS resulted to be the greatest on all insert surfaces. This leads to deduce that the higher the constraint level, the lower the stress on the insert.

Secondly, the other important findings deriving from the output analysis of both simulations regard the UC design, which shows the best kinematics and kinetics performance with respect to the other implants. In terms of kinematics, it resulted in limiting the femoral displacement (paradoxical motion is not present) and patellar displacement, the rotation of its mobile platform follows better the femoral rotation with respect to the standard insert. About the TF kinetics, even though it increases the stress on the insert, this is compensated by the largest contact area allowing more homogeneous stress distribution. An enhanced uniformity in stress distribution is also visible along the tibia, damping the stress peaks and also significantly reducing the loads in the lateral part of the bone with respect to the fixed version. Finally, also in the PF joint there are improvements in larger contact area and also in reduction of quadriceps force.

Therefore, this study confirms that UC improves kinetics [6], but also kinematics, with the potential to avoid anterior knee pain and patellar dislocation, thus it could be an optimal choice for those patients which have the appropriate soft tissue needed to guarantee the success of this TKA implantation.

On the contrary, in case of ligament loosening the surgeon should opt for a post-cam design and could choose the CCK, which, with respect to PS, allows better force distribution and lower risk of implant lift-off, but taking into consideration that it could jeopardize the PF kinetics at high-demanding activities.

5.1.1 Limitations and future developments

In this study, during the implementation of the FE models, some assumptions have been made. First, not all the soft tissues that are comprised in the knee joint have been modelled in the various geometries, such as the quadriceps muscles and MPFL, but their action have been considered by means of the applied loads system [21].

Another assumption regards the PT and collateral ligaments that have been simplified as beams, but this is a common approach, and it can be found in existing validated models in literature [53], [86], [79], [6].

The PCL has been defined as a three-dimensional body either, but an axial connector has been used; however, this PCL model follows the force-strain behaviour of ligaments found in literature [82], thus it should not compromise the validity of this study.

The material models related to the bones and soft tissues have been assumed to be homogeneous and linear elastic, even though in the reality the cortical and cancellous bones are characterized by spatial inhomogeneity. Nonetheless, this approximation has been considered acceptable in similar FEA studies [21].

Another assumption has been to consider the UHMWPE as linear elastic, ignoring the plastic behaviour region, leading to an overestimation of the local value of stress; this in turn allowed to obtain the eventual worst-case scenario and in the obtained results the critical stress values have not been reached.

It is worth pointing out that since the purpose of this study was to compare different models through the same method, it is not compromising for the study validity to have established the abovementioned assumptions for all the models.

Another factor that could represent a limitation is related to the ideal approach by which the models' geometries did not consider any deformities, variations in anatomy or ligament loosening that could affect the TKA outcomes, but this approach is commonly used for FEA in the biomechanical field [105], [86], [79].

Besides, another limit is that just one manufacturer has been taken into account, thus this study is not representative of all the available TKA designs in the orthopaedic market. Nevertheless, this choice is thought to be reasonable in order to exclude eventual additional feature variations between different orthopaedic companies' products.

Furthermore, the PF joint was considered in the squat but not included in the gait models, and this decision relies on the fact that during the walking activity negligible forces are involved in PF joint with respect to the TF joint.

Finally, the possible postoperative misalignments occurring during TKA surgeries have not been considered, but this is not an issue for the purpose of the comparison [6].

From this study it has been observed that through the squat simulation it is possible to offer a better overview of the TKA performance with respect to gait, especially for what concerns the post-cam engagement and the stress deriving from high-demanding activity. In conclusion, future developments could integrate this analysis considering other available TKA designs such as hinged prostheses and also other families of products, modelling eventual patient-specific variations, anatomy deformities and simulating other high-demanding activities.

6 References

[1] A. I. Mirulla, L. Bragonzoni, S. Zaffagnini, T. Ingrassia, R. Zinno, and B. Innocenti, "Assessment of paradoxical anterior translation in a CR total knee prosthesis coupling dynamic RSA and FE techniques," *J Exp Orthop*, vol. 8, no. 1, Dec. 2021, doi: 10.1186/s40634-021-00361-y.

[2] G. Castellarin, E. Bori, and B. Innocenti, "Experimental and clinical analysis of the use of asymmetric vs symmetric polyethylene inserts in a mobile bearing total knee arthroplasty," *J Orthop*, vol. 23, pp. 25–30, Jan. 2021, doi: 10.1016/j.jor.2020.12.031.

[3] B. Innocenti, S. Pianigiani, L. Labey, J. Victor, and J. Bellemans, "Contact forces in several TKA designs during squatting: A numerical sensitivity analysis," *J Biomech*, vol. 44, no. 8, pp. 1573–1581, May 2011, doi: 10.1016/j.jbiomech.2011.02.081.

[4] A. E. M. Eltorai, C. P. Eberson, and A. H. Daniels, *Essential Orthopedic Review Questions and Answers for Senior Medical Students*. 2018.

[5] S. Pianigiani, L. Scheys, L. Labey, W. Pascale, and B. Innocenti, "Biomechanical analysis of the post-cam mechanism in a TKA: Comparison between conventional and semi-constrained insert designs," *Int Biomech*, vol. 2, no. 1, pp. 22–28, 2015, doi: 10.1080/23335432.2015.1014849.

[6] G. Castellarin, E. Bori, L. Rapallo, S. Pianigiani, and B. Innocenti, "Biomechanical analysis of different levels of constraint in TKA during daily activities," *Arthroplasty*, vol. 5, no. 1, Dec. 2023, doi: 10.1186/s42836-022-00157-0.

[7] C. Dall'oca *et al.*, "Evolution of TKA design," *Acta Biomed*, vol. 88, pp. 17–31, 2017, doi: 10.23750/abm.v88i2.

[8] S. E. Hohler, "Total Knee Arthroplasty: Past Successes and Current Improvements," 2008. [Online]. Available: http://www.aornjournal.org.

[9] H. Hsu and R. M. Siwiec, *Knee Arthroplasty*. 2022. [Online]. Available: https://www.ncbi.nlm.nih.gov/books/NBK507914/#_NBK507914_pubdet_

[10] S. Pianigiani, L. Labey, W. Pascale, and B. Innocenti, "Knee kinetics and kinematics: What are the effects of TKA malconfigurations?," *Knee Surgery, Sports Traumatology, Arthroscopy*, vol. 24, no. 8, pp. 2415–2421, Aug. 2016, doi: 10.1007/s00167-015-3514-y.

[11] H. A. Gray, S. Guan, T. J. Young, M. M. Dowsey, P. F. Choong, and M. G. Pandy, "Comparison of posterior-stabilized, cruciate-retaining, and medial-stabilized knee implant motion during gait," *Journal of Orthopaedic Research*, vol. 38, no. 8, pp. 1753–1768, Aug. 2020, doi: 10.1002/jor.24613.

[12] Y. G. Koh, J. A. Lee, P. K. Chung, and K. T. Kang, "Computational analysis of customized cruciate retaining total knee arthroplasty restoration of native knee joint biomechanics," *Artif Organs*, vol. 43, no. 5, pp. 504–514, May 2019, doi: 10.1111/aor.13382.

[13] J. Victor and J. Bellemans, "A COMPARATIVE STUDY ON THE BIOMECHANICS OF THE NATIVE HUMAN KNEE JOINT AND TOTAL KNEE ARTHROPLASTY."

[14] C. E. Bourdon *et al.*, "Comparison of long-term kinematics and wear of total knee arthroplasty implant designs," *J Mech Behav Biomed Mater*, vol. 124, Dec. 2021, doi: 10.1016/j.jmbbm.2021.104845.

[15] L. Mazzucchelli *et al.*, "Cruciate retaining and cruciate substituting ultra-congruent insert," *Annals of Translational Medicine*, vol. 4, no. 1. AME Publishing Company, Jan. 01, 2016. doi: 10.3978/j.issn.2305-5839.2015.12.52.

[16] B. Innocenti, "High congruency MB insert design: stabilizing knee joint even with PCL deficiency," *Knee Surgery, Sports Traumatology, Arthroscopy*, vol. 28, no. 9, pp. 3040–3047, Sep. 2020, doi: 10.1007/s00167-019-05764-0.

[17] M. M. Ardestani, M. Moazen, E. Maniei, and Z. Jin, "Posterior stabilized versus cruciate retaining total knee arthroplasty designs: Conformity affects the performance reliability of the

design over the patient population," *Med Eng Phys*, vol. 37, no. 4, pp. 350–360, Apr. 2015, doi: 10.1016/j.medengphy.2015.01.008.
[18] E. Bori and B. Innocenti, "Development and validation of an in-silico virtual testing rig for analyzing total knee arthroplasty performance during passive deep flexion: A feasibility study," *Med Eng Phys*, vol. 84, pp. 21–27, Oct. 2020, doi: 10.1016/j.medengphy.2020.07.020.
[19] J. Zelle, A. C. van der Zanden, M. de Waal Malefijt, and N. Verdonschot, "Biomechanical analysis of posterior cruciate ligament retaining high-flexion total knee arthroplasty," *Clinical Biomechanics*, vol. 24, no. 10, pp. 842–849, Dec. 2009, doi: 10.1016/j.clinbiomech.2009.08.004.
[20] G. R. Srinivas, A. Deb, and M. N. Kumar, "A study on polyethylene stresses in mobile-bearing and fixed-bearing total knee arthroplasty (TKA) using explicit finite element analysis," *J Long Term Eff Med Implants*, vol. 23, no. 4, pp. 275–283, 2013, doi: 10.1615/JLongTermEffMedImplants.2013008440.
[21] B. Innocenti, "High congruency MB insert design: stabilizing knee joint even with PCL deficiency," *Knee Surgery, Sports Traumatology, Arthroscopy*, vol. 28, no. 9, pp. 3040–3047, Sep. 2019, doi: 10.1007/s00167-019-05764-0.
[22] R. Popescu, E. G. Haritinian, and S. Cristea, "Relevance of finite element in total knee arthroplasty - Literature review," *Chirurgia (Romania)*, vol. 114, no. 4, pp. 437–442, 2019, doi: 10.21614/chirurgia.114.4.437.
[23] S. Saha and A. Roychowdhury, "Application of the Finite Element Method in Orthopedic Implant Design," 2009.
[24] J. G. Betts *et al.*, *Anatomy & physiology*. 2013.
[25] M. T. Hirschmann and W. Müller, "Complex function of the knee joint: the current understanding of the knee," *Knee Surgery, Sports Traumatology, Arthroscopy*, vol. 23, no. 10. Springer Verlag, pp. 2780–2788, Oct. 26, 2015. doi: 10.1007/s00167-015-3619-3.
[26] S. Affatato, "Biomechanics of the knee," in *Surgical Techniques in Total Knee Arthroplasty (TKA) and Alternative Procedures*, Elsevier Ltd, 2015, pp. 17–35. doi: 10.1533/9781782420385.1.17.
[27] Bozkur Murat and Acar Halil Ibrahim, *Clinical Anatomy of the Knee*. Springer International Publishing, 2021. doi: 10.1007/978-3-030-57578-6.
[28] B. Innocenti, E. Bori, and S. Piccolo, "Development and validation of a robust patellar reference coordinate system for biomechanical and clinical studies," *Knee*, vol. 27, no. 1, pp. 81–88, Jan. 2020, doi: 10.1016/j.knee.2019.09.007.
[29] A. J. S. Fox, A. Bedi, and S. A. Rodeo, "The Basic Science of Human Knee Menisci: Structure, Composition, and Function," *Sports Health*, vol. 4, no. 4, pp. 340–351, Jul. 2012, doi: 10.1177/1941738111429419.
[30] J. F. Abulhasan and M. J. Grey, "Anatomy and physiology of knee stability," *Journal of Functional Morphology and Kinesiology*, vol. 2, no. 4. MDPI Multidisciplinary Digital Publishing Institute, Dec. 01, 2017. doi: 10.3390/jfmk2040034.
[31] B. Innocenti, N. Verdonschot, H.-P. W. van Jonbergen, and L. Labey, "Periprosthetic stress shielding in patello-femoral arthroplasty: a numerical analysis Periprosthetic stress shielding in patello-femoral arthroplasty: a numerical analysis," 2011. [Online]. Available: https://www.researchgate.net/publication/265988192
[32] J. Victor, F. van Glabbeek, J. vander Sloten, P. M. Parizel, J. Somville, and J. Bellemans, "An experimental model for kinematic analysis of the knee," *Journal of Bone and Joint Surgery*, vol. 91, no. SUPPL. 6, pp. 150–163, Nov. 2009, doi: 10.2106/JBJS.I.00498.
[33] H. Yazdi *et al.*, "Anatomical axes of the proximal and distal halves of the femur in a normally aligned healthy population: Implications for surgery," *J Orthop Surg Res*, vol. 13, no. 1, Jan. 2018, doi: 10.1186/s13018-017-0710-0.
[34] S. D. Masouros, A. M. J. Bull, and A. A. Amis, "Biomechanics of the knee joint," *Orthop Trauma*, vol. 24, no. 2, pp. 84–91, Apr. 2010, doi: 10.1016/j.mporth.2010.03.005.
[35] P. Johal, A. Williams, P. Wragg, D. Hunt, and W. Gedroyc, "Tibio-femoral movement in the living knee. A study of weight bearing and non-weight bearing knee kinematics using

'interventional' MRI," *J Biomech*, vol. 38, no. 2, pp. 269–276, Feb. 2005, doi: 10.1016/j.jbiomech.2004.02.008.
[36] Rivière Charles and Vendittoli Pascal-André, *Personalized Hip and Knee Joint Replacement*. 2020.
[37] R. Marcolongo and B. Canesi, "REUMATOLOGIA PRATICA - PROBLEMATICHE CLINICHE OSTEO-ARTICOLARI," 2007. [Online]. Available: www.pacinimedicina.it
[38] J. S. Blackburne and T. E. Peel, "A new method of measuring patellar height," vol. 59-B, no. 2, 1977.
[39] T. Luyckx, K. Didden, H. Vandenneucker, L. Labey, and J. Bellemans, "Is there a biomechanical explanation for anterior knee pain in patients with patella alta? INFLUENCE OF PATELLAR HEIGHT ON PATELLOFEMORAL CONTACT FORCE, CONTACT AREA AND CONTACT PRESSURE," pp. 91–344, 2009, doi: 10.1302/0301-620X.91B3.
[40] D. Blalock, A. Miller, M. Tilley, and J. Wang, "Joint instability and osteoarthritis," *Clinical Medicine Insights: Arthritis and Musculoskeletal Disorders*, vol. 8. Libertas Academica Ltd., pp. 15–23, Feb. 19, 2015. doi: 10.4137/CMAMD.S22147.
[41] K. D. Brandt, P. Dieppe, and E. L. Radin, "Etiopathogenesis of Osteoarthritis," *Rheumatic Disease Clinics of North America*, vol. 34, no. 3. pp. 531–559, Aug. 2008. doi: 10.1016/j.rdc.2008.05.011.
[42] S. M. Kurtz *et al.*, "International survey of primary and revision total knee replacement," *Int Orthop*, vol. 35, no. 12, pp. 1783–1789, Dec. 2011, doi: 10.1007/s00264-011-1235-5.
[43] M. Hussain *et al.*, "Ultra-high-molecular-weight-polyethylene (UHMWPE) as a promising polymer material for biomedical applications: A concise review," *Polymers*, vol. 12, no. 2. MDPI AG, Feb. 01, 2020. doi: 10.3390/polym12020323.
[44] C. J. Vertullo, P. M. Grimbeek, S. E. Graves, and P. L. Lewis, "Surgeon's Preference in Total Knee Replacement: A Quantitative Examination of Attributes, Reasons for Alteration, and Barriers to Change," *Journal of Arthroplasty*, vol. 32, no. 10, pp. 2980–2989, Oct. 2017, doi: 10.1016/j.arth.2017.04.035.
[45] S. Babazadeh, "The relevance of ligament balancing in total knee arthroplasty: how important is it? A systematic review of the literature," *Orthop Rev (Pavia)*, vol. 1, no. 1, p. 26, Oct. 2009, doi: 10.4081/or.2009.e26.
[46] Z. X. Zhao, L. Wen, T. B. Qu, L. L. Hou, D. Xiang, and J. Bin, "Kinematic analysis of a posterior-stabilized knee prosthesis," *Chin Med J (Engl)*, vol. 128, no. 2, pp. 216–221, 2015, doi: 10.4103/0366-6999.149205.
[47] T. Watanabe, H. Koga, M. Horie, H. Katagiri, I. Sekiya, and T. Muneta, "Post-Cam Design and Contact Stress on Tibial Posts in Posterior-Stabilized Total Knee Prostheses: Comparison Between a Rounded and a Squared Design," *Journal of Arthroplasty*, vol. 32, no. 12, pp. 3757–3762, Dec. 2017, doi: 10.1016/j.arth.2017.07.010.
[48] A. A. Hofmann, T. K. Tkach, C. J. Evanich, and M. P. Camargo, "Posterior stabilization in total knee arthroplasty with use of an ultracongruent polyethylene insert," *Journal of Arthroplasty*, vol. 15, no. 5, pp. 576–583, 2000, doi: 10.1054/arth.2000.6633.
[49] L. Sabatini, S. Risitano, L. Rissolio, A. Bonani, F. Atzori, and A. Massè, "Condylar constrained system in primary total knee replacement: Our experience and literature review," *Ann Transl Med*, vol. 5, no. 6, Mar. 2017, doi: 10.21037/atm.2017.03.29.
[50] K. K. Athwal, L. Willinger, W. Manning, D. Deehan, and A. A. Amis, "A constrained-condylar fixed-bearing total knee arthroplasty is stabilised by the medial soft tissues," *Knee Surgery, Sports Traumatology, Arthroscopy*, vol. 29, no. 2, pp. 659–667, Feb. 2021, doi: 10.1007/s00167-020-05995-6.
[51] C.-W. Chang *et al.*, "Early mechanical complications of a multidirectional mobile-bearing total knee replacement," *J Bone Joint Surg [Br]*, vol. 93, no. 4, pp. 93–479, 2011, doi: 10.1302/0301-620X.93B4.
[52] R. M. Grzeskowiak, J. Schumacher, M. S. Dhar, D. P. Harper, P. Y. Mulon, and D. E. Anderson, "Bone and Cartilage Interfaces With Orthopedic Implants: A Literature Review," *Frontiers in Surgery*, vol. 7. Frontiers Media S.A., Dec. 21, 2020. doi: 10.3389/fsurg.2020.601244.
[53] G. Castellarin, S. Pianigiani, and B. Innocenti, "Asymmetric polyethylene inserts promote favorable kinematics and better clinical outcome compared to symmetric inserts in a mobile

bearing total knee arthroplasty," *Knee Surgery, Sports Traumatology, Arthroscopy*, vol. 27, no. 4, pp. 1096–1105, Apr. 2018, doi: 10.1007/s00167-018-5207-9.

[54] M. R. Perkins, C. M. Arnholt, D. W. MacDonald, S. M. Kurtz, and W. M. Mihalko, "Retrieval Analysis of Cruciate-Retaining and Posterior-Stabilized Total Knee Arthroplasty and Correlations to Laxity and Wear," *Journal of Arthroplasty*, vol. 35, no. 8, pp. 2249–2253, Aug. 2020, doi: 10.1016/j.arth.2020.03.027.

[55] Y. G. Koh, J. Son, O. R. Kwon, S. K. Kwon, and K. T. Kang, "Tibiofemoral conformity variation offers changed kinematics and wear performance of customized posterior-stabilized total knee arthroplasty," *Knee Surgery, Sports Traumatology, Arthroscopy*, vol. 27, no. 4, pp. 1213–1223, Apr. 2019, doi: 10.1007/s00167-018-5045-9.

[56] J. S. Broberg, S. Ndoja, S. J. MacDonald, B. A. Lanting, and M. G. Teeter, "Comparison of Contact Kinematics in Posterior-Stabilized and Cruciate-Retaining Total Knee Arthroplasty at Long-Term Follow-Up," *Journal of Arthroplasty*, vol. 35, no. 1, pp. 272–277, Jan. 2020, doi: 10.1016/j.arth.2019.07.046.

[57] M. R. Angerame, D. C. Holst, J. M. Jennings, R. D. Komistek, and D. A. Dennis, "Total Knee Arthroplasty Kinematics," *Journal of Arthroplasty*, vol. 34, no. 10. Churchill Livingstone Inc., pp. 2502–2510, Oct. 01, 2019. doi: 10.1016/j.arth.2019.05.037.

[58] N. Arnout *et al.*, "Post-cam mechanics and tibiofemoral kinematics: a dynamic in vitro analysis of eight posterior-stabilized total knee designs," *Knee Surgery, Sports Traumatology, Arthroscopy*, vol. 23, no. 11, pp. 3343–3353, Nov. 2015, doi: 10.1007/s00167-014-3167-2.

[59] C. Stukenborg-Colsman, S. Ostermeier, C. Hurschler, and C. J. Wirth, "Tibiofemoral contact stress after total knee arthroplasty," *Acta Orthop Scand*, vol. 73, no. 6, pp. 638–646, Dec. 2002, doi: 10.3109/17453670209178028.

[60] E. Most, S. Zayontz, G. Li, E. Otterberg, K. Sabbag, and H. E. Rubash, "Femoral rollback after cruciate-retaining and stabilizing total knee arthroplasty," in *Clinical Orthopaedics and Related Research*, May 2003, vol. 410, pp. 101–113. doi: 10.1097/01.blo.0000062380.79828.2e.

[61] J. Victor, S. Banks, J. Bellemans, " J Victor, " S Banks, and " J Bellemans, "Kinematics of posterior cruciate ligament-retaining and-substituting total knee arthroplasty A PROSPECTIVE RANDOMISED OUTCOME STUDY," *J Bone Joint Surg*, 2005, doi: 10.1302/0301-620X.87B5.

[62] A. Sharma, F. Leszko, R. D. Komistek, G. R. Scuderi, H. E. Cates, and F. Liu, "In vivo patellofemoral forces in high flexion total knee arthroplasty," *J Biomech*, vol. 41, no. 3, pp. 642–648, 2008, doi: 10.1016/j.jbiomech.2007.09.027.

[63] K. Harato, R. B. Bourne, J. Victor, M. Snyder, J. Hart, and M. D. Ries, "Midterm comparison of posterior cruciate-retaining versus -substituting total knee arthroplasty using the Genesis II prosthesis. A multicenter prospective randomized clinical trial," *Knee*, vol. 15, no. 3, pp. 217–221, Jun. 2008, doi: 10.1016/j.knee.2007.12.007.

[64] K. Shiramizu, F. Vizesi, W. Bruce, S. Herrmann, and W. R. Walsh, "Tibiofemoral contact areas and pressures in six high flexion knees," *Int Orthop*, vol. 33, no. 2, pp. 403–406, Apr. 2009, doi: 10.1007/s00264-007-0478-7.

[65] F. R. Kolisek, M. S. Mcgrath, and N. Jessup, "Posterior-stabilized versus posterior cruciate ligament-retaining total knee arthroplasty," 2009, [Online]. Available: https://www.researchgate.net/publication/26800406

[66] S. G. Urwin, D. F. Kader, N. Caplan, A. St Clair Gibson, and S. Stewart, "Gait analysis of fixed bearing and mobile bearing total knee prostheses during walking: Do mobile bearings offer functional advantages?," *Knee*, vol. 21, no. 2, pp. 391–395, 2014, doi: 10.1016/j.knee.2013.10.007.

[67] O. Riaz, A. Aqil, G. Sisodia, and G. Chakrabarty, "P.F.C Sigma® cruciate retaining fixed-bearing versus mobile-bearing knee arthroplasty: a prospective comparative study with minimum 10-year follow-up," *European Journal of Orthopaedic Surgery and Traumatology*, vol. 27, no. 8, pp. 1145–1149, Dec. 2017, doi: 10.1007/s00590-017-1920-1.

[68] K. L. Puah, H. C. Chong, L. S. S. Foo, N. N. Lo, and S. J. Yeo, "Clinical and Functional Outcomes: Primary Constrained Condylar Knee Arthroplasty Compared with Posterior

Stabilized Knee Arthroplasty," *J Am Acad Orthop Surg Glob Res Rev*, vol. 2, no. 2, Feb. 2018, doi: 10.5435/JAAOSGlobal-D-17-00084.
[69] S. S. Lee, J. Yeom, D. H. Lee, and Y. W. Moon, "Similar outcomes between ultracongruent and posterior-stabilized insert in total knee arthroplasty: A propensity score-matched analysis," *Journal of Orthopaedic Surgery*, vol. 28, no. 1, Jan. 2020, doi: 10.1177/2309499019893515.
[70] G. Castellarin, E. Bori, A. Menon, and B. Innocenti, "The effect of different insert design congruencies on the kinematics of a mobile bearing TKA: A cadaveric study," *J Orthop*, vol. 34, pp. 89–93, Nov. 2022, doi: 10.1016/j.jor.2022.07.018.
[71] B. PARCELLS, "TKA - PRIMARY DESIGN — Hip & Knee Book," 2017. https://hipandkneebook.com/tka-implants/2017/3/15/tka-primary-design (accessed Feb. 01, 2023).
[72] S. J. Song, C. H. Park, and D. K. Bae, "What to know for selecting cruciate-retaining or posterior-stabilized total knee arthroplasty," *CiOS Clinics in Orthopedic Surgery*, vol. 11, no. 2. Korean Orthopaedic Association, pp. 142–150, Jun. 01, 2019. doi: 10.4055/cios.2019.11.2.142.
[73] B. Innocenti, S. Pianigiani, L. Labey, J. Victor, and J. Bellemans, "Contact forces in several TKA designs during squatting: A numerical sensitivity analysis," *J Biomech*, vol. 44, no. 8, pp. 1573–1581, May 2011, doi: 10.1016/j.jbiomech.2011.02.081.
[74] S. Pianigiani, Y. Chevalier, L. Labey, V. Pascale, and B. Innocenti, "Tibio-femoral kinematics in different total knee arthroplasty designs during a loaded squat: A numerical sensitivity study," *J Biomech*, vol. 45, no. 13, pp. 2315–2323, Aug. 2012, doi: 10.1016/j.jbiomech.2012.06.014.
[75] S. Pianigiani, R. A. Bernabé, H. R. Yagüe, and B. Innocenti, "Investigation on the effects induced by TKA features on tibio-femoral mechanics part II: Tibial insert designs," in *Journal of Mechanics in Medicine and Biology*, Apr. 2015, vol. 15, no. 2. doi: 10.1142/S0219519415400357.
[76] L. Shu, T. Sato, X. Hua, and N. Sugita, "Comparison of Kinematics and Contact Mechanics in Normal Knee and Total Knee Replacements: A Computational Investigation," *Ann Biomed Eng*, vol. 49, no. 9, pp. 2491–2502, Sep. 2021, doi: 10.1007/s10439-021-02812-0.
[77] P. van der Voort *et al.*, "A systematic review and meta-regression of mobile-bearing versus fixed-bearing total knee replacement in 41 studies," *Bone Joint J*, pp. 95–1209, 2013, doi: 10.1302/0301-620X.95B9.
[78] N. Oehler, T. Schmidt, and A. Niemeier, "Total Joint Replacement and Return to Sports," *Sportverletzung-Sportschaden*, vol. 30, no. 4, pp. 195–203, Dec. 2016, doi: 10.1055/s-0042-119109.
[79] B. Innocenti, Ö. F. Bilgen, L. Labey, G. H. van Lenthe, J. vander Sloten, and F. Catani, "Load sharing and ligament strains in balanced, overstuffed and understuffed UKA. A validated finite element analysis," *Journal of Arthroplasty*, vol. 29, no. 7, pp. 1491–1498, 2014, doi: 10.1016/j.arth.2014.01.020.
[80] B. Innocenti, J. Bellemans, and F. Catani, "Deviations From Optimal Alignment in TKA: Is There a Biomechanical Difference Between Femoral or Tibial Component Alignment?," *Journal of Arthroplasty*, vol. 31, no. 1, pp. 295–301, Jan. 2016, doi: 10.1016/j.arth.2015.07.038.
[81] J. Victor, D. van Doninck, L. Labey, B. Innocenti, P. M. Parizel, and J. Bellemans, "How precise can bony landmarks be determined on a CT scan of the knee?," *Knee*, vol. 16, no. 5, pp. 358–365, Oct. 2009, doi: 10.1016/j.knee.2009.01.001.
[82] F. Galbusera *et al.*, "Material models and properties in the finite element analysis of knee ligaments: A literature review," *Frontiers in Bioengineering and Biotechnology*, vol. 2, no. NOV. Frontiers Media S.A., 2014. doi: 10.3389/fbioe.2014.00054.
[83] G. Seitlinger, G. Scheurecker, R. Högler, L. Labey, B. Innocenti, and S. Hofmann, "Tibial tubercle-posterior cruciate ligament distance: A new measurement to define the position of the

tibial tubercle in patients with patellar dislocation," *American Journal of Sports Medicine*, vol. 40, no. 5, pp. 1119–1125, May 2012, doi: 10.1177/0363546512438762.
[84] A. Race and A. A. Amis, "THE MECHANICAL PROPERTIES OF THE TWO BUNDLES OF THE HUMAN POSTERIOR CRUCIATE LIGAMENT," 1994.
[85] B. Innocenti, P. Salandra, W. Pascale, and S. Pianigiani, "How accurate and reproducible are the identification of cruciate and collateral ligament insertions using MRI?," *Knee*, vol. 23, no. 4, pp. 575–581, Aug. 2016, doi: 10.1016/j.knee.2015.07.015.
[86] B. Innocenti and E. Bori, "Change in knee biomechanics during squat and walking induced by a modification in TKA size," *J Orthop*, vol. 22, pp. 463–472, Nov. 2020, doi: 10.1016/j.jor.2020.10.006.
[87] S. Pianigiani, D. Croce, M. D. ' Aiuto, W. Pascale, and B. Innocenti, "Sensitivity analysis of the material properties of different soft-tissues: implications for a subject-specific knee arthroplasty," 2017.
[88] E. Bori, F. Armaroli, and B. Innocenti, "Biomechanical analysis of femoral stems in hinged total knee arthroplasty in physiological and osteoporotic bone," *Comput Methods Programs Biomed*, vol. 213, Jan. 2022, doi: 10.1016/j.cmpb.2021.106499.
[89] W. Bonfield and S. Saha, "Session 16 BONE MECHANICS FRACTURE MECHANICS OF CORTICAL BONE BENDING STRENGTH AND ASH CONTENT OF BONES DURING EMBRYONIC GROWTH," 1981.
[90] K. Smeets, J. Slane, L. Scheys, S. Claes, and J. Bellemans, "Mechanical Analysis of Extra-Articular Knee Ligaments. Part One: Native knee ligaments," *Knee*, vol. 24, no. 5, pp. 949–956, Oct. 2017, doi: 10.1016/j.knee.2017.07.013.
[91] S. Singh and A. P. Harsha, "Analysis of Femoral Components of Cemented Total Hip Arthroplasty," *Journal of The Institution of Engineers (India): Series D*, vol. 97, no. 2, pp. 113–120, Oct. 2016, doi: 10.1007/s40033-015-0096-2.
[92] S. Sathasivam and P. S. Walker, "Computer Model to Predict Subsurface Damage in Tibia1 Inserts of Total Knees," 1998.
[93] J. Victor and J. Bellemans, "A COMPARATIVE STUDY ON THE BIOMECHANICS OF THE NATIVE HUMAN KNEE JOINT AND TOTAL KNEE ARTHROPLASTY," 2009.
[94] P. S. Walker, J. M. Sussman-Fort, G. Yildirim, and J. Boyer, "Design Features of Total Knees for Achieving Normal Knee Motion Characteristics," *Journal of Arthroplasty*, vol. 24, no. 3, pp. 475–483, Apr. 2009, doi: 10.1016/j.arth.2007.11.002.
[95] Y. G. Koh, J. Son, O. R. Kwon, S. K. Kwon, and K. T. Kang, "Effect of post-cam design for normal knee joint kinematic, ligament, and quadriceps force in patient-specific posterior-

stabilized total knee arthroplasty by using finite element analysis," *Biomed Res Int*, vol. 2018, 2018, doi: 10.1155/2018/2438980.
[96] B. Innocenti, L. Labey, J. Victor, P. Wong, and J. Bellemans, "An in-vitro study of human knee kinematics: natural vs. replaced joint," 2008. [Online]. Available: www.springerlink.com
[97] J. Victor, L. Labey, P. Wong, B. Innocenti, and J. Bellemans, "The influence of muscle load on tibiofemoral knee kinematics," *Journal of Orthopaedic Research*, vol. 28, no. 4, pp. 419–428, Apr. 2010, doi: 10.1002/jor.21019.
[98] P. Randelli and P. Cabitza, "La protesi totale di ginocchio a piatto mobile," 2006.
[99] G. Li *et al.*, "Biomechanics of Posterior-Substituting Total Knee Arthroplasty: An In Vitro Study," *CLINICAL ORTHOPAEDICS AND RELATED RESEARCH Number*, vol. 404, pp. 214–225, 2002, doi: 10.1097/01.blo.0000030498.43495.db.
[100] C. H. Huang *et al.*, "Patellofemoral kinematics during deep knee flexion after total knee replacement: a computational simulation," *Knee Surgery, Sports Traumatology, Arthroscopy*, vol. 22, no. 12, pp. 3047–3053, Nov. 2014, doi: 10.1007/s00167-013-2819-y.
[101] C. K. Fitzpatrick, R. H. Kim, A. A. Ali, L. M. Smoger, and P. J. Rullkoetter, "Effects of resection thickness on mechanics of resurfaced patellae," *J Biomech*, vol. 46, no. 9, pp. 1568–1575, May 2013, doi: 10.1016/j.jbiomech.2013.03.016.
[102] K. Didden, T. Luyckx, J. Bellemans, L. Labey, and H. Vandenneucker, "Anteroposterior positioning of the tibial component and its effect on the mechanics of patellofemoral contact," *Br]*, pp. 92–1466, 2010, doi: 10.1302/0301-620X.92B10.
[103] J. B. Kowalczewski, L. Labey, Y. Chevalier, T. Okon, B. Innocenti, and J. Bellemans, "Does joint line elevation after revision knee arthroplasty affect tibio-femoral kinematics, contact pressure or collateral ligament lengths? An in vitro analysis," *Archives of Medical Science*, vol. 11, no. 2, pp. 311–318, 2015, doi: 10.5114/aoms.2014.46078.
[104] D. E. Toutoungi, T. W. Lu, A. Leardini, F. Catani, and J. J. Oõconnor, "Cruciate ligament forces in the human knee during rehabilitation exercises," 2000. [Online]. Available: www.elsevier.com/locate/clinbiomech
[105] B. Innocenti, E. Truyens, L. Labey, P. Wong, J. Victor, and J. Bellemans, "Can medio-lateral baseplate position and load sharing induce asymptomatic local bone resorption of the proximal tibia? A finite element study," *J Orthop Surg Res*, vol. 4, no. 1, 2009, doi: 10.1186/1749-799X-4-26.